A SENSITIVITY STUDY FOR PROBABILISTIC SEISMIC HAZARD ASSESSMENT OF SINOP NUCLEAR POWER PLANT SITE

A THESIS SUBMITTED TO
THE GRADUATE SCHOOL OF NATURAL AND APPLIED SCIENCES OF
MIDDLE EAST TECHNICAL UNIVERSITY

BY

ERKAN YILAR

IN PARTIAL FULFILLMENT OF THE REQUIREMENTS
FOR
THE DEGREE OF THE MASTER OF SCIENCE
IN
EARTHQUAKE STUDIES

MAY 2014

Approval of the thesis:

A SENSITIVITY STUDY for PROBABILISTIC SEISMIC HAZARD ASSESSMENT of SINOP NUCLEAR POWER PLANT SITE

Submitted by **ERKAN YILAR** in partial fulfillment of the requirements for the degree of **Master of Science in Earthquake Studies Department, Middle East Technical University** by,

Prof. Dr. Canan Özgen
Dean, Graduate School of **Natural and Applied Science** _____

Prof. Dr. Melih Ersoy
Head of Department, **Earthquake Studies Dept.** _____

Doç. Dr. Zeynep Gülerce
Supervisor, **Earthquake Studies Dept., METU** _____

Prof. Dr. Nuretdin Kaymakçı
Co-Supervisor, **Geological Engineering Dept., METU** _____

Examining Committee Members:

Prof. Dr. M. Semih Yücemen
Earthquake Studies Dept., METU _____

Doç. Dr. Zeynep Gülerce
Earthquake Studies Dept., METU _____

Prof. Dr. Nuretdin Kaymakçı
Geological Engineering Dept., METU _____

Prof. Dr. Kemal Önder Çetin
Earthquake Studies Dept., METU _____

Dr. Mehmet Bulut
Electricity Generation Company of Turkey _____

DATE --/--/----

I hereby declare that all information in this document has been obtained and presented in accordance with academic rules and ethical conduct. I also declare that, as required by these rules and conduct, I have fully cited and referenced all material and results that are not original to this work.

Name, Last Name: Erkan Yılar

Signature :

ABSTRACT

A SENSITIVITY STUDY FOR PROBABILICTIC SEISMIC HAZARD ASSESSMENT OF SINOP NUCLEAR POWER PLANT SITE

Yılar, Erkan
M.Sc., Department of Earthquake Studies
Supervisor: Assoc. Prof. Dr. Zeynep Gülerce
Co-Supervisor: Prof. Dr. Nuretdin Kaymakçı
May 2014, 95 Pages

Based on the studies conducted for more than 40 years, Sinop is chosen as one of the three most convenient places in Turkey to construct a Nuclear Power Plant (NPP). The objective of this study is to evaluate the sensitivity of the design ground motions for Sinop NPP Site to the seismic source characterization and ground motion prediction models within the probabilistic seismic hazard assessment (PSHA) framework.

This study introduces significant improvements over the previous seismic hazard studies conducted for the Sinop NPP in terms of seismic source characterization models. Based on the regulations of Turkey, United States and International Atomic Authority, the seismic sources located within the 320 km radius around the Sinop NPP site; North Anatolian Fault (NAF) Tosya- Erbaa Segment (1942-1943 earthquakes rupture zone), Abant-Ilgaz Segment (1944 Rupture), Erzincan Segment (1939 Rupture), Esençay - Merzifon Fault Zone, Sungurlu Fault, Ekinveren Fault, Erikli Fault, Balıfakı Fault and Pontic Escarpment Zone were investigated. To develop the planar source characterization models, geometries of the fault segments (length, width, dip angle and segmentation points) were determined with the help of previously conducted site studies, new fault maps and previous studies in the literature. Fault segments, rupture sources, rupture scenarios and fault rupture models

were determined using the USGS Working Group (2003) terminology. To properly represent the characteristic behavior, planar fault segments were defined with composite magnitude distribution model and multi-segment ruptures were considered. The Pontic Escarpment Zone and Sungurlu Fault were modeled as areal sources using truncated exponential magnitude distribution model. The sensitivity of the hazard results to the parameters of seismic source models was analyzed for each source to illustrate the needs for further site studies for Sinop NPP.

This study makes the first attempt to characterize the ground motions and its variability for Sinop NPP site. Several local, global and regionalized candidate ground motion prediction models (GMPEs) were proposed and evaluated. After a detailed evaluation of median predictions and resulting hazard curves, four NGA models and two TR-adjusted NGA models were used for the ground motion characterization of the Sinop NPP site. Equal weights are assigned to the global and regionalized NGA models. Results of the study are presented in terms of a range of hazard curves for the peak ground acceleration since the site surveys and ground motion characterization efforts are not yet finalized. These results will be refined by the help of the newly obtained site data in the next few years.

Keywords: Sinop Nuclear Power Plant, Probabilistic Seismic Hazard Assessment, Pontic Escarpment Zone, TR-Adjusted NGA Models, North Anatolian Fault.

ÖZ

SİNOP NÜKLEER GÜÇ SANTRAL SAHASI İÇİN OLASILIKSAL SİSMİK TEHLİKE DEĞERLENDİRİLMESİNİN DUYARLILIK ÇALIŞMASI

Yılar, Erkan
Yüksek Lisans, Deprem Çalışmaları Bölümü
Tez Yöneticisi: Doç. Dr. Zeynep Gülerce
Yardımcı Danışman: Prof. Dr. Nuretdin Kaymakçı
Mayıs 2014, 95 Sayfa

40 yılı aşkın bir süredir devam eden çalışmalar sonucunda Sinop Türkiye'de Nükleer Güç Santrali (NGS) kurulması için en uygun 3 sahadan biri olarak belirlenmiştir. Bu çalışmanın temel amacı Sinop NGS Sahası için tasarım yer hareketinin sismik kaynak nitelendirmesi ve yer hareketi tahmin denklem modellerine olan duyarlılığının olasılıksal sismik tehlike değerlendirmesi yöntemiyle incelenmesidir.

Bu çalışma sismik kaynak nitelendirmesi açısından Sinop NGS için daha önce yapılmış olan sismik tehlike değerlendirmesi çalışmalarına göre önemli gelişmeler sağlamaktadır. Türk ve Amerikan Nükleer Enerji Düzenleme Kurumları ve Uluslararası Atom Enerjisi Ajansının düzenlemelerine göre 320 km yarıçap içindeki sismik kaynaklar; Kuzey Anadolu Fay Hattı (KAF) Tosya-Erbaa Bölümü (1942-1943 depremleri), Abant-Ilgaz Bölümü (1944 Kırığı), Erzincan Bölümü (1939 Kırığı), Esençay - Merzifon Fay Zonu, Sungurlu Fayı, Ekinveren Fayı, Erikli Fayı, Balıfakı Fayı ve Pontik Yamaç olarak belirlenmiştir. Çizgisel kaynak nitelendirmesini sağlamak için, fay segman geometrik özellikleri (uzunluk, genişlik, dip açısı ve segman noktaları) daha önce yapılmış saha çalışmaları, yeni fay haritaları ve literatürdeki daha önce yapılmış çalışmalar yardımıyla belirlenmiştir. Fay segmanları, kırılma kaynakları, kırılma senaryoları ve fay kırılma modeli USGS Çalışma Grubu (2003) terminolojisi kullanılarak belirlenmiştir. Fay karakteristik

davranışını doğru bir biçimde yansıtmak için çizgisel kaynaklar için birleşik büyüklük dağılım modeli ve çoklu segman kırıkları kullanılmıştır. Pontik Yamaç ve Sungurlu Fayı budanmış üstel büyüklük dağılım modeli ile alan kaynak olarak modellenmiştir. Tehlike analizi sonuçlarının sismik kaynak model parametrelerine olan duyarlılığı, daha sonra yapılacak olan saha çalışmalarına olan ihtiyaca ışık tutması açısından her kaynak için incelenmiştir.

Bu çalışma Sinop NGS sahası için yer hareketi nitelendirmesi ve değişkenliğinin belirlenmesi için gerekli ilk adımı atmaktadır. Pek çok yerel, global ve bölgesel aday yer hareketi tahmin denklemi önerilmiş ve değerlendirilmiştir. Medyan tahmin sonuçlarının detaylı olarak incelenmesi sonucunda dört Yeni Nesil Tahmin modeli ve iki Türkiye'ye uyarlanmış Yeni Nesil Tahmin modeli Sinop Sahası yer hareketi nitelendirmesi için kullanılmıştır. Global ve yerel modellere eşit ağırlıklar verilmiştir. Saha çalışmaları ve yer hareketi nitelendirmesinin henüz tamamlanmaması nedeniyle, çalışmanın sonuçları en büyük yer ivmesi için bir dizi tehlike eğrisi olarak sunulmuştur. Bu sonuçlar elde edilecek yeni veriler ışığında önümüzdeki birkaç yıl içinde yeniden incelenecektir.

Anahtar Kelimeler: Sinop Nükleer Güç Santrali, Olasılıksal Sismik Tehlike Değerlendirmesi, Pontik Yamaç, TR-Uyarlı NGA Modelleri, Kuzey Anadolu Fayı.

To My Beloved Family

ACKNOWLEDGEMENTS

First of all, I would like to express my sincere thanks and gratitude to my advisor, Assoc. Prof. Dr. Zeynep Gülerce for her guidance, patience and support throughout the preparation of this thesis.

I am grateful to my co-advisor Prof. Dr. Nuretdin Kaymakçı for his suggestions, guidance and understanding during the preparation of seismic source models.

I would also like to thank Dr. Norman Abrahamson, for his invaluable guidance in seismic source characterization and for providing the hazard code.

I would like to thank to Assoc. Prof. Dr. Ayşegül Askan Gündoğan for her understanding and patience during the advisor assignment procedures and being my advisor for that period.

I would like to thank to EUAS Nuclear Power Plant Department Head Dr. Mehmet Bulut and Site Works Manager Erhan İslamoğlu for their understanding throughout the preparation of this thesis.

Special thanks go to my ex-manager Ziya Erdemir for encouraging me to start the program and for his understanding and tolerance throughout taking the graduate courses.

Finally, I would like to give my thanks to my wife for her invaluable support during this long period.

TABLE OF CONTENTS

LIST OF TABLES

LIST OF FIGURES

CHAPTER 1

1. INTRODUCTION

After the Second World War and the abuse of nuclear power in Nagasaki and Hiroshima attacks, countries decided to have this new technology not just as nuclear weapons but also for peaceful aims, such as producing energy. In 1954, the first commercial Nuclear Power Plant (NPP), Obninsk NPP, started to produce electricity in USSR. In between 1954 and 1986 until the Chernobyl accident, there has been a tremendous increase in the number of NPPs. After 1986, there had been a stop in the rate of increase of the NPPs approximately for 15 years. Owing to the increasing energy prices and demand for energy resources, especially the developing countries have started to construct tens of new NPPs since the beginning of 2000s. Even though some of the European countries (especially Germany and Italy) have announced that they will not follow this nuclear power track anymore after the 2011 Fukushima accident, worldwide medium and long term plans indicate that this new era, the "nuclear renaissance", will go on for a long while.

In parallel with the economic and political changes in the world, Turkey's nuclear adventure started in early seventies. Lots of site screening studies were conducted to find suitable sites to construct NPPs. Among around 40 possible sites, Mersin Akkuyu, Sinop Yalancı Gerne, and Kırklareli İğneada sites were selected as the first three candidate NPP sites in Turkey. After signing the inter-governmental power purchase agreement with Russian Federation to construct a NPP in Mersin Akkuyu in 2010, Turkish Government announced that the Sinop İnceburun region is the second candidate NPP project site.

Although Turkey is one of the most earthquake-prone countries in the world, the fact that Sinop NPP site is located in a historically low-seismicity region is the one of the key factors for choosing Sinop İnceburun as the candidate site for a NPP. In the context of the feasibility studies for the plant, the proper calculation of the design ground motions is an important task since the failure/partial damage of the NPP can be disastrous for both the environment and in terms of economy. The Fukushima

Accident took place in Japan showed the importance of correct estimation of site related parameters not only for just life and environmental security but also for billions of dollars of effect on the economy. Since the nuclear power plants are generally constructed based on a standard design and design alterations made on the standard design require billions of dollars of investment with long time delays, the accurate estimations of design ground motions are indispensable.

1.1 Research Statement

The primary objective of this study is to evaluate the effect of the current knowledge on the seismic sources and ground motions context to be able to determine the design ground motions for the Sinop Nuclear Power Plant site accurately by the probabilistic seismic hazard assessment (PSHA) methodology. A large number of site survey studies were conducted in the region to determine the site parameters since the beginning of mid-seventies. Previously published reports (Doyuran, 1983, Barka et. al. 1985) and the latest site studies performed in the region between years 2005 and 2008 (Emre et. al. 2008, Kaymakçı, 2009) show that there are some tectonically active structures that may affect the design ground motion levels. Within the context of this study, seismic source characterization models for the tectonic structures defined in these reports are constructed and integrated into the PSHA framework in a consistent manner with the national and international regulations for NPP sites. The effect of the nearby seismic sources defined in the previous reports (as active or not) on the design ground motion levels for Sinop NPP is evaluated in a systematic manner to illustrate the needs for further research. Although previously conducted site studies accumulated a huge amount of data, there is still the need to have additional (especially off-shore) site studies in the Black Sea side to define the seismo-tectonics accurately.

The epistemic uncertainty in the rock ground motion is usually the largest contributor to the uncertainty in the hazard. Therefore, ground motion characterization for NPP sites has been evolving rapidly along with the lessons learned from the large-scaled NPP projects. This study makes the first attempt to characterize the ground motions and its variability for Sinop NPP site. Several candidate ground motion prediction models (GMPEs) were proposed and evaluated; the effect of GMPE standard deviations on the hazard outcome is discussed. Results of the study are presented in terms of a range of hazard curves for the peak ground acceleration since the site

surveys and ground motion characterization efforts are not yet finalized. These results will be refined by the help of the newly obtained site data in the next few years.

1.2 Problem Significance and Limitations of Previous Studies

Significance of proper estimation of the design ground motions for NPPs has been discussed among the community of earthquake professionals for the last 10 years. According to World Nuclear Association (WNA, 2012), 20% of nuclear reactors are operating in the areas of significant seismic activity and earthquakes have previously occurred in the vicinity of a number of Japanese and other power reactors without any adverse effect. For instance, approximately one year before the Great Tohoku Earthquake, an earthquake registering 6.2 on the Richter scale had occurred on offshore Fukushima in northern Japan and the nearest nuclear power plants, Fukushima I & II and Onagawa, were remained fortunately unaffected (WNA, 2012). However, less than one year later on 11 March 2011, the Great Tohoku Earthquake with 9.0 moment magnitude hit a very large region including Fukushima Daiichi Power Plant by strong ground shaking and tsunami (WNA, 2012). It is reported that the design basis ground acceleration level was upgraded to 441-489 gal in 2008 for Fukushima Daiichi NPP but the maximum acceleration recorded in the foundation of Unit 2 during the Tohoku Earthquake was 550 Gal. Units 2, 3 and 5 were reported to exceed their maximum response acceleration design basis values by approximately 20%. There are other documented cases where the effects of earthquakes were felt but the nuclear power plants in the close vicinity were continued to their normal operation as a result of previous plan (e.g. San Onofre 2 and 3, Diablo Canyon 1 and 2, in 6.6 magnitude earthquake in January 1994) (WNA, 2012). As demonstrated by Fukushima Daiichi case and others, failures/damages due to earthquakes caused many times more economic loss than a better design requires.

Sinop İnceburun site was selected in mid-seventies as the second nuclear power plant site due to the relatively lower seismic activity in the region. A large number of site surveying studies were conducted in the region and based on these reports, two (unpublished) seismic hazard assessment studies were conducted: a report was submitted to Turkish Electricity Institution (TEK) by Erdik and co-authors in 1990 (Erdik et al., 1990), and another more recent report was prepared for Turkish Atomic Energy Agency (TAEK) by Gülkan and Kalkan (2010). In the last 23 years since the

Erdik et al. (1990) report was prepared, improvements over the previous seismic hazard assessment practices were accomplished both on the seismic source and ground motion characterization round the world. Limitations of these previous attempts were discussed in Chapter 2 in detail. Significant improvements over the previous seismic hazard assessment reports are accomplished with the construction of advanced seismic source models in terms of source geometry and reoccurrence relations and use of improved global ground motion prediction models to represent the ground motion variability in this study.

1.3 Scope

The scope of this thesis can be summarized as follows:

In the first chapter general information about the concepts reviewed in this study are revisited.

In Chapter 2, the previous probabilistic seismic hazard studies performed for Sinop NPP are introduced. A brief summary of the reports mainly focusing on the seismic source and ground motion characterization are presented.

In the third chapter, source characterization models for the seismic sources in the region is provided and the effect of the seismic sources on the design ground motion levels for Sinop NPP is evaluated.

Chapter 4 is devoted to the initial attempt of ground motion characterization. Candidate ground motion prediction equations are reviewed and their applicability to Sinop NPP is questioned.

In the final chapter, a range of hazard curves are provided for the Sinop NPP site. Results of the analysis are discussed and suggestions to improve the results of this study are given.

CHAPTER 2

2. PREVIOUS SEISMIC HAZARD ASSESSMENT STUDIES FOR THE SINOP NUCLEAR POWER PLANT SITE

The study area comprises a part of Sinop Peninsula which has been the candidate site for Nuclear Power Plant (NPP) for over 35 years; therefore numerous site reports have been prepared until this date by various government agencies and universities. Most of the reports are related to the site investigation efforts to evaluate the active seismo-tectonic characteristics of the site. Based on these unpublished geological and seismo-tectonic reports, two seismic hazard assessment studies were conducted: a report was submitted to Turkish Electricity Authority (TEK) by Erdik et al. (1990), and another more recent report was prepared for Turkish Atomic Energy Agency (TAEK) by Gülkan and Kalkan (2010, herein GK10 for brevity). These two reports were accessed with the permission of Electricity Generation Company of Turkey (EUAS) for comparison. A brief summary of the reports mainly focusing on the seismic source and ground motion characterization are presented in this chapter.

2.1 Sinop Nuclear Power Plant Design Basis Ground Motion Report by Erdik et al. (1990)

The tectonic background and seismic source characterization of the seismic hazard assessment study by Erdik et al. (1990) was largely based on the report of Doyuran and Erdik (1983). The seismic sources in the region were separated into two distinct groups: the seismic sources on-land (Areas 1 and 3 in Figure 2.1) and the seismic sources off-shore (Area 2 in Figure 2.1). The seismic sources within the first rectangle on the land include the North Anatolian Fault (NAF) Zone and Ekinveren, Erikli, Ayancık, and Balıfakı Faults which were defined as thrust faults formed as a result of continuous N-S shortening during the late Eocene to late Miocene (approximately between 40-11 Ma). The tectonic structures on the south of the NAF Zone were not taken into consideration since they are far away from the candidate

NPP site. The authors stated that the site investigations conducted in the region until the submission date of the report did not reveal any evidence for the late Quaternary activity associated with Ekinveren, Erikli, Ayancık, and Balıfakı Faults. Therefore, they concluded that the NAF is the only active tectonic structure located in Area 1 that should be included in the seismic hazard analysis. The offshore region to the north of the site (Area 3 in Figure 2.1) is a rather complex tectonic region: considerable seismic activity and faulting due to convergence between the Arabian and Eurasian plates which gave way to the uplift of the Eastern Anatolia, Lesser Caucasus, Greater Caucasian and Crimean regions along the eastern and northern periphery of the Black Sea is observed while the N-S convergence is largely taken up by westwards escape of Anatolian Block along the North Anatolian Fault. Although, recent tectonic activity was recorded in the northern and north eastern coast of the Black Sea, these seismic sources would be insignificant in the seismic hazard analysis due to far proximity to the NPP site. Therefore, this seismic source was ignored in the deterministic seismic hazard analysis.

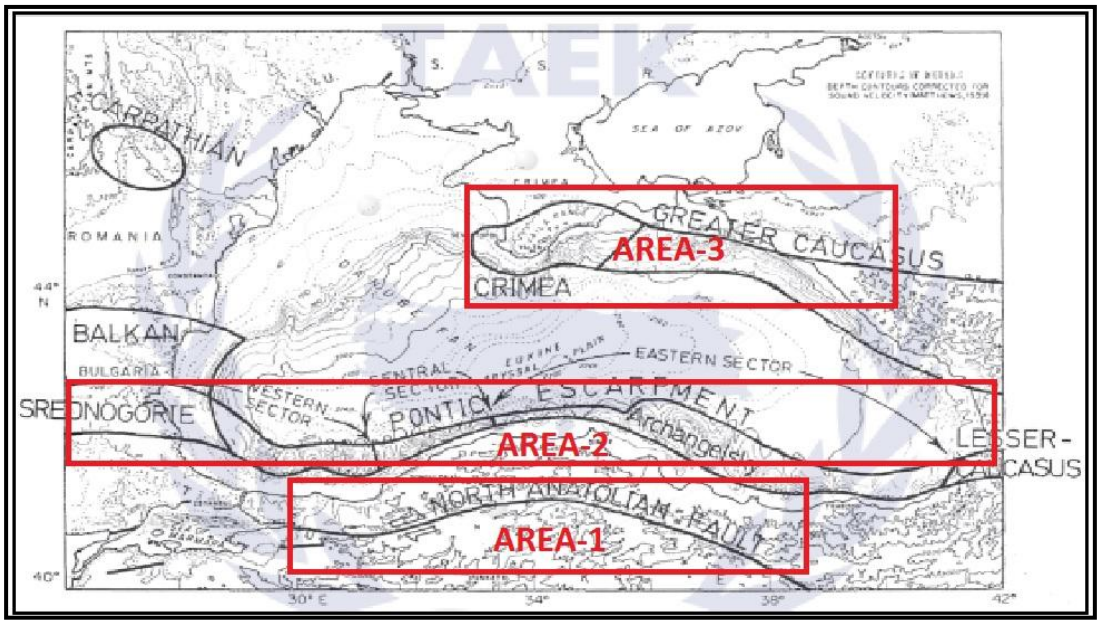

Figure 2.1: The Seismic Sources Included in Seismic Hazard Assessment Report by Erdik et al. (1990) (Modified After Erdik et al, 1990)

The Srednogorie - Pontic Escarpment- Lesser Caucasus seismic source zone (Area 2 in Figure 2.1) was evaluated in detail and the tectonic structures in the area were related to the Alpine Orogeny. Erdik et al. (1990) stated that the transverse faults and the Pontic Escarpment in the southern margin of the Black Sea cannot be defined as active tectonic structures due to the undisturbed southern basin apron and the

Abyssal Plain. The authors also argued that the seismic reflection surveys conducted by Texaco (1972) did not reveal any recent tectonic disturbance within the Black Sea sediments; therefore, the segments in between İnebolu and Samsun were assumed as inactive tectonic structures. Moreover, the earthquake epicenters located between Sinop and Ordu were associated with the Arkhangelsky Ridge.

However, the Bartın Earthquake (1968, Ms=6.8) was attributed to the Pontic Escarpment by Erdik et al. (1990) based on the fault mechanism solutions of Alptekin et al. (1986). The Pontic Escarpment, especially its eastern segment, was underlined as the most important tectonic structure in the report due to its close proximity to the site. The authors indicated that the tectonic structure has a significant role on the design basis earthquake ground motion for the Sinop NPP.

To estimate the ground motions and its variability, five candidate ground motion prediction equations (GMPEs) were considered by Erdik et al. (1990). The candidate GMPEs proposed by Campbell (1981), Joyner and Boore (1981), Fukushima et al. (1988), Kawashima et al. (1984), and Abrahamson and Litehiser (1989) were evaluated, however only two of them, Campbell (1981) and Joyner and Boore (1981) models were utilized in the seismic hazard analysis.

In the deterministic seismic hazard assessment (DSHA) part, one maximum credible earthquake was defined for each seismic source. For the NAF Zone, the location of the earthquake was selected to attain the closest distance to the Sinop NPP site (R_{rup}=110 km). Even if the largest earthquake attributed to NAF Zone in the earthquake catalog was an Ms=7.9 event, the magnitude of the maximum credible earthquake was selected as 8.3 (Ms) based on the recommendations by Siemmons (1977) and Bonilla et al. (1982). For the Eastern Pontic Escarpment Earthquake Source Zone, an earthquake scenario based on Ms= 6.5 thrust fault earthquake with a focal depth of 20 km and epicentral distance of 13 km was defined. The earthquake scenarios and corresponding peak ground acceleration (PGA) values are shown in Table 2.1.

The seismic sources used in the probabilistic seismic hazard analysis (PSHA) were: the North Anatolian Fault Zone, Eastern, Central and Western Pontic Escarpment Source Zones and Carpathian-Crimea-Greater Caucasus Seismic Source Zone. The truncated exponential magnitude distribution function was used for each zone and the

β-value was calculated by associating the earthquakes in the catalog with the seismic zones. At the same time, return periods of 10.000 years and 500 years are used to define the safe shut-down earthquake (SSDE) and the operation basis earthquake (OBE), respectively. Only one GMPE, the Campbell (1981) model, was utilized for the PSHA by: i) including the ground motion variability, and ii) by using the median values only. The truncation of the ground motion variability (number of standard deviations used in the analysis) was not clearly defined in the report. The PGA values for both hazard levels and both cases of ground motion variability are listed in Table 2.2.

Table 2.1: Earthquake Scenarios in DSHA Study and Corresponding PGA Values

Source	GMPE	Depth (km)	Closest Distance (km)	Median PGA (g)	Median + 1σ PGA (g)
NAF Zone	Campbell (1981)	20	110	0.12	0.17
NAF Zone	Joyner and Boore (1981)	20	110	0.06	0.11
Pontic Esc.	Campbell (1981)	20	13	0.18	0.27
Pontic Esc.	Joyner and Boore (1981)	20	13	0.24	0.44

Table 2.2: Earthquake Scenarios in PSHA Study and Corresponding PGA Values

GMPE	Annual Probability of Exceedance (0.002)- Median	Annual Probability of Exceedance (0.002)- Median + 1σ	Annual Probability of Exceedance (0.0001)- Median	Annual Probability of Exceedance (0.0001)- Median + 1σ
Campbell (1981)	0.07	0.09	0.12	0.17
Intensity Correlated	-	<0.32	-	<0.25

Erdik et al., (1990) argued that the peak ground acceleration for the SSDE level should be founded on the deterministic assessment using the expert judgment and median predictions among different attenuation relationships ought to be used. The final recommendations of Erdik et al. (1990) for the design basis ground motions

compatible with the United States Nuclear Regulatory Commission (US-NRC) and International Atomic Energy Agency (IAEA) specifications are given in Table 2.3.

Table 2.3: The Final Recommendations of Erdik et al. (1990) for the Design Basis Ground Motions

Hazard level	OBE-1	OBE-2	SSDE-1	SSDE-2
PGA (g)	0.07	0.18	0.14	0.35

2.2 An Assessment of Seismic Hazard for the Sinop Nuclear Technology Center – Report by Gülkan and Kalkan (2010)

TAEK conducted a large-scale research program for seismo-tectonic and geological evaluation of the candidate Sinop NPP site between years 2005 and 2008. During this time period, The General Directorate of Mineral Research and Exploration of Turkey (MTA) prepared a comprehensive site report on regional and site geology. Additionally, a detailed site report was prepared by a team of geological engineers from Middle East Technical University (METU) and a micro seismicity study was conducted using 12 broadband seismometers operated by Marmara Research Center of The Scientific and Technological Research Council of Turkey (TUBİTAK-MAM). Based on the accumulation of new geological and seismological data, the earlier seismic hazard assessment study was re-evaluated by Gülkan and Kalkan in 2010 (GK10) as an advisory attempt. It is stated in the GK10 report that the proposed seismic hazard assessment study can be considered as a preliminary attempt and should not be employed before further elaboration.

GK10 report handled the characterization of seismic sources differently for DSHA and PSHA phases. In the PSHA phase, the smoothed-gridded seismicity approach was used; therefore, distinct seismic sources were not defined. The smoothed-gridded seismicity model was based on the earthquake catalog for the events with magnitudes in between 4.0-7.0 and the b-value for the region was estimated as 0.8. In the DSHA study, only one earthquake source, the Tosya Segment of the NAF Zone that ruptured in 1943, was considered based on the geological site reports from MTA and METU. The magnitude of the maximum credible earthquake was selected as 8.0 and the closest distance to the rupture was calculated to be 120 km.

For ground motion characterization, global Next Generation Attenuation - (NGA) models of Campbell and Bozorgnia (2008), Boore and Atkinson (2008), Chiou and

Youngs (2008) and regional Kalkan and Gülkan (2004) GMPEs were employed. Equal weights (50%) were assigned to the regional and global model groups in the ground motion logic tree. Assuming that the Sinop Nuclear Power Plant would be constructed on a basaltic (rock) substratum, V_{S30} was taken as 760 m/s in the calculations. Preliminary findings of the report based on PSHA and DSHA approaches are summarized in Table 2.4 and 2.5, respectively.

Table 2.4: PSHA Results from Gülkan And Kalkan (2010) Preliminary Report.

Hazard level	%10 Prob. of Exceed. in 50 years	%2 Prob. of Exceed. in 50 years	%1 Prob. of Exceed. in 50 years	%0.5 Prob. of Exceed. in 50 years
PGA(g)	0.13	0.26	0.33	0.41

Table 2.5: DSHA Results from Gülkan and Kalkan (2010) Preliminary Report

GMPE	Kalkan and Gülkan (2004)	Boore and Atkinson (2008)	Campbell and Bozorgnia (2008)	Chiou and Youngs (2008)
PGA(g)	0.178	0.196	0.157	0.206

2.3 Limitations of the Previous Studies

PSHA methodology and the main components of the PSHA framework are rapidly evolving with the increasing number of special projects (such as nuclear power plants, bridges and high-rise structures) and awareness of earthquake risk assessment around the world. In the last 23 years since the Erdik et al. (1990) report was prepared, significant improvements over the previous seismic hazard assessment practices have been accomplished both on the seismic source and ground motion characterization.

Due to the lack of local predictive models, global GMPEs such as Campbell (1981) and Joyner and Boore (1981) were used by Erdik et al. (1990) for ground motion characterization. Today, all of these models are superseded by new and improved versions (NGA models) proposed by their developers. NGA GMPEs are improved in terms of additional prediction parameters (such as depth of the source, basin effects, magnitude dependent standard deviations, etc.), statistical approach, and a well-constrained global database when compared to the early stage GMPEs. Three of these new models (BA08, CB08 and CY08) were used by Gülkan and Kalkan (2010); however, selection of these three models among the other candidates and compatibility of the global models with the regional tectonic environment was not

discussed. Another unjustified but important feature of the GK10 report is the assignment of equal weights to the global models for the first 50% and weighing the regional GMPEs with the remaining 50%. Today, the epistemic uncertainty introduced to the PSHA framework due to the selected GMPEs and construction of the logic tree is a controversial issue that requires scientific justification and expert judgment. Finally, an important part of the PSHA methodology, the truncation of the ground motion variability (number of standard deviations used for the GMPE), was not clearly presented in both reports. However, GMPE standard deviation has a large impact on the final hazard curve (Bommer and Abrahamson, 2006) and should be implemented properly in the hazard equation. Discussion on the selection of GMPEs is provided in Chapter 4.

After the Erdik et al. (1990) report was submitted, a comprehensive site investigation program for geological and seismo-tectonic structures in the candidate Sinop NPP site was conducted. Important parameters such as fault geometry, fault displacement (off-set), slip rates, etc. are documented and can be implemented in the seismic source characterization models. Therefore, the seismic sources in the region may properly be modeled by planar features (especially the NAF Zone), by assigning appropriate magnitude distribution functions and balancing the accumulated seismic moment using the slip rates. Available seismo-tectonic information calls for an update in the source characterization approaches adopted by Erdik et al. (1990) (areal sources) and Gülkan and Kalkan (2010) (smoothed seismicity). Improvements in the seismic source characterization models and effect of this improvement on the hazard results are elaborated in Chapter 3.

Chapter 3

3. SEISMIC SOURCE CHARACTERIZATION FOR PSHA

Seismic source characterization is one of the key inputs of the PSHA framework that describes where the next earthquakes will occur, how big they will be and how often they will happen. Modelling the seismic sources for a moment-balanced PSHA framework involves; (i) definition of the planar source geometry (length, width, segmentation points, dip and strike angles) for the active faults or defining areal source zones, (ii) selection of the suitable magnitude recurrence model for each source and estimation of the necessary model parameters (mean characteristic magnitude, b-value, etc.), (iii) performing the source-to-epicenter matching analysis by overlying the available earthquake catalogues over the seismic sources, and iv) balancing the accumulated and released seismic moment for each source. Expertize on geology, tectonics, and seismology is essential for proper and accurate modelling of the seismic sources; therefore, a careful literature survey on the seismo-tectonic and geological characteristics of the Sinop NPP site and its surroundings was performed. These efforts, along with the details of the proposed seismic source models, will be described in Section 3.2. Before that, a summary of the equations employed in the seismic source characterization is provided in this section for future reference. National and international codes and regulations that define the seismic source characterization for NPP site are included where necessary.

Parameters of the seismic source models may have a great influence on the hazard potential depending on the sensitivity of the PSHA results and the location of the analyzed site with respect to the seismic source. Therefore, Section 3.3 is devoted to the analysis and discussion of the sensitivity of the final hazard outcome to the uncertainties involved in the source parameters. Analysis results presented in this chapter does not intend to discuss the activity of the seismic sources in the vicinity of Sinop NPP; such a task requires additional information and expertise on the field. The main objective is to present the effect of the nearby seismic sources listed in the

previous reports (as active or inactive) on the design ground motion levels for Sinop NPP.

3.1 Summary of the Seismic Source Characterization Methodology

Different statistical distributions and probability density functions are utilized in seismic source characterization procedures depending on the purpose. While uniform distribution is used for modeling the location of an earthquake on a finite fault, lognormal distribution is suitable for estimating the ground motion values for an earthquake scenario. In order to define the distribution of the different size earthquakes that a seismic source can produce, three alternative models can be employed. The first and the most common model that describes the magnitude distribution for a seismic source is the well-known Gutenberg and Richter relation;

$$\log_{10} N = a - bM \qquad 3.1$$

where M is the magnitude, N is the number of events greater than or equal to M and "a" and "b" are the regression parameters. The parameter "a" is the activity rate that provides a measure of the occurrence rate of earthquakes in the region. It can also be defined as intercept of minimum magnitude of engineering interest on the semi-log plot. The b-value is the slope of the line and it is controlled by the relative frequency of the different size magnitude events. In PSHA applications, the exponential distribution is generally truncated at both ends with a minimum magnitude of engineering interest (M_{min} in Equation 3.2) and the maximum magnitude event that the source can produce (M_{max} in Equation 3.2). The maximum magnitude is the largest historic magnitude in the source zone plus some additional value (generally half a magnitude unit). The truncated exponential model is given in Equation 3.2:

$$f_m^{TE}(m) = \frac{\beta \exp(-\beta(m - M_{\min})}{1 - \exp(-\beta(M_{\max} - M_{\min}))} \qquad 3.2$$

$$\text{Where } \beta = \ln 10 \times b \qquad 3.3$$

This magnitude distribution model is suitable for large regions or regions with multiple faults but in most cases does not work well for fault zones (Youngs and Coppersmith, 1985). Therefore, truncated exponential distribution is utilized for only areal sources in this study.

Another alternative magnitude distribution is the "characteristic model" proposed by Schwartz and Coppersmith (1984) based on the idea that during repeated rupture episodes occurring on the same fault, some characteristics, like fault geometry, source mechanism and seismic moment remain approximately constant over a large timescale. According to characteristic model, once a fault begins to rupture in a large earthquake, it will tend to rupture the entire fault segment and produces similar size earthquakes due to the geometry of the fault. However, the fully characteristic earthquake model does not acknowledge the small-to-moderate magnitude earthquakes that occur on the faults. Based on the combination of the truncated exponential model and the characteristic model, a composite model was proposed by Youngs and Coppersmith in 1985. The observational basis of the composite model relies on both geological and seismological data and the model combines a characteristic earthquake distribution for the large magnitude earthquakes and an exponential distribution for the smaller magnitude events. The key feature of this model is the relative sizes of released seismic moments for small-to-moderate and large magnitude events. Due to the constraints of the model, 94% of the accumulated seismic moment is released by characteristic events and the rest is released by small-to-moderate magnitude earthquakes on the exponential tail. The Youngs and Coppersmith (1985) composite magnitude distribution model is given by:

$$f_m^{YC}(m) = \begin{cases} \frac{1}{1+c_2}\frac{\beta \exp(-\beta(\overline{M}_{char} - M_{\min} - 1.25)}{1-\exp(-\beta(\overline{M}_{char} - M_{\min} - 0.25)} & for\ \overline{M}_{char} - 0.25 < M \le \overline{M}_{char} + 0.25 \\ \frac{1}{1+c_2}\frac{\beta \exp(-\beta(M - M_{\min})}{1-\exp(-\beta(\overline{M}_{char} - M_{\min} - 0.25)} & for\ M_{\min} \le M \le \overline{M}_{char} - 0.25 \end{cases} \quad 3.4$$

Where,

$$c_2 = \frac{0.5\beta \exp(-\beta(\overline{M}_{char} - M_{\min} - 1.25)}{1-\exp(-\beta(M_{char} - M_{\min} - 0.25)} \quad 3.5$$

and M_{Char} is the characteristic earthquake magnitude. For the seismic sources defined by planar faults, the composite magnitude distribution model is utilized in this study.

The magnitude distribution models defined above only represent the relative rate of different size earthquakes. To determine the absolute rate of events, activity rate should be incorporated. The activity rate $N(M_{min})$, is defined as the rate of earthquakes above the minimum magnitude. For areal sources, historical and

catalogue seismicity is used to calculate the activity rate, whereas annual slip rate should be employed for faults as given in Equations 3.6-3.8. The moment magnitude M_w and the seismic moment M_o is defined by Hanks and Kanamori (1979) as:

$$M_w = \frac{2}{3}\log_{10}(M_o) - 10.7 \qquad \textit{where} \qquad M_o = \mu AD \tag{3.6}$$

and μ is the shear modulus of the crust (in dyne/cm^2), A is the area of the fault rupture (in cm^2), D is the average displacement (slip) over the rupture surface (in cm). The annual slip rate is either estimated by the help of long-term geologic observations or calculated by the help of geodetic surveys. The seismic moment release in an earthquake is given by Equation 3.7 and the activity rate of a source is calculated by integrating the moment release per earthquake times the relative frequency of earthquakes as given in Equation 3.8:

$$\log_{10} M_o = 1.5M + 16.05 \tag{3.7}$$

$$N(M_{\min}) = \frac{\mu AS}{\int_{M_{\min}}^{M_{\max}} f_m(M_w) 10^{1.5M_w + 16.05} d_M} \tag{3.8}$$

Finally, the magnitude distribution and the activity rate are used to define the magnitude recurrence relation N(M) which describes the rate at which earthquakes with magnitudes greater than or equal to M occur on a source with following equation;

$$N(M) = N(M_{\min}) \int_{M_{\min}}^{M_{\max}} f_m(M_w) dm \tag{3.9}$$

3.2 Seismic Sources in and around Sinop NPP Site

The Turkish Nuclear Atomic Authority (TAEK) Guide (1989) on the requirements for granting the license and limited work permit for nuclear facilities regarding earthquakes is accepted as the technical framework of handling earthquake related hazards for nuclear power plants in Turkey. In this guide, an exact distance limitation to include the seismic sources in the seismic hazard analysis is not provided, but the required radius to check the historical seismicity is stated as several hundred kilometers. The United States Nuclear Regulatory Commission (US-NRC) regulatory guide (RG-1.208, in action since 2006) requires that all the active seismic sources within a radius of 320 km of the NPP site should be included in the PSHA analysis. SSG-9 Guide of the International Atomic Energy Agency (IAEA) advices that a

radius of hundreds of kilometers around the NPP site should be examined for the seismic sources.

One of the most important and disputable issues on the regulatory guides is the definition of the “active fault” or “capable fault”. The criteria in the TAEK Guide (1989) for “active fault” are:

- A movement that can be a precursor of future movements, occurred approximately within the last 500.000 years,
- Association with another active fault that can create surface rupture or rupture close to the surface.

Definition of “capable fault” by US-NRC is similar to the criteria of TAEK, but more detailed, as follows:

- Presence of surface or near-surface deformation of landforms or geologic deposits of a recurring nature within the last approximately 500.000 years or at least once in the last approximately 50.000 years,
- A reasonable association with one or more moderate to large earthquakes or sustained earthquake activity that are usually accompanied by significant surface deformation,
- A structural association with a capable tectonic source that has characteristics of either item 1 or 2 (above), such that movement on one could be reasonably expected to be accompanied by movement on the other

The provisions given in SSG-9 are similar to the regulations of TAEK and US-NRC. SSG-9 emphasizes that longer geological periods (e.g. Pliocene – Early Quaternary) may be investigated for the assessment of “capable faults” for regions where low seismic activity has been observed. In the Geological Investigations for the Sinop Nuclear Technology Center Final Report of MTA (Emre et al., 2008), a fault is defined as “capable fault” if surface rupture was developed between Late Quaternary (Holocene) and Recent (10.000 years). The activity based capability definition of Emre et al. (2008) falls short when compared with the first provisions of TAEK and US-NRC guidelines and also, it doesn’t have any constraints regarding the association with another capable source.

In this study, the active seismic sources within 320 km radius of Sinop NPP are included in the analysis based on the US-NRC approach. The seismic sources in the

region are defined using the latest Active Fault Map of General Directorate of Mineral Research and Exploration (MTA, 2012) and the findings of Emre et al. (2008). The lengths of the fault segments and the segmentation points are directly adopted from the new active fault map of MTA (2012), however other fault parameters such as fault width, dip and strikes of the fault planes etc. are either taken from the report by Emre et al. (2008) and other published resources or estimated from the magnitude-rupture area correlations.

The main seismic resources in the vicinity of the Sinop NPP are shown in Figure 3.1: East and Central segments of North Anatolian Fault (NAF) (including the rupture zones of 1939 Erzincan, 1942 Erbaa, 1943 Tosya and 1944 Bolu-Gerede Earthquakes), Ezinepazarı Fault, Merzifon-Esençay Fault, the Erikli, Balıfakı and Ekinveren Faults in the north, the offshore Pontic Escarpment, and the tectonic structures in the south of Merzifon Fault. Seismic source characterization models for the 1944 Bolu-Gerede Earthquake Rupture Zone and 1939 Erzincan Earthquake Rupture Zone are directly adopted from the recent studies by Vakilinezhad et al. (2013) and Vakilinezhad (2014). A brief summary on these models are added at the end of this chapter.

3.2.1 The North Anatolian Fault Zone

The North Anatolian Fault Zone (NAFZ) (Ketin, 1948) is an intra-continental strike-slip fault with a northwards convex arc-shaped geometry that forms the boundary between the Eurasian plate and Anatolian plate (Şengör and Yılmaz 1981). It is a widely accepted phenomenon that the neotectonic period in Anatolian plate started by the late Miocene (Şengör et al., 2005). It evolved from a previously very wide shear zone into a narrow fault belt where displacement is concentrated within a few master fault strands by the beginning of Pliocene (ca. 5 Ma years ago) (Barka, 1992). Currently, the width of the shear zone is not more than several kilometers in the Eastern segments (e.g. Kelkit and Yedisu valleys); however, it is as wide as 100 km in the central parts (Şengör et al., 2005). There is a strong correlation between the width of the NAF shear zone and the branching off from the main strand. NAF follows a straight course in the areas where the shear zone is narrow, mainly east of Niksar, but systematic offshoots can be observed in areas where the shear zone widens (Erturaç and Tüysüz, 2010). These wide zones of secondary fault splays are very distinct in Amasya Region; while the main strand of the NAF delimits the

northern boundary of the splay faults. Ezinepazarı and Sungurlu splays bound the southern margin and Esençay and Merzifon Faults lie in the center in between the other two fault segments (Erturaç and Tüysüz, 2010) as shown in Figure 3.1.

In the last century, nine big surface ruptures occurred along the NAF in a westwards migrating fashion of the earthquake epicenters starting from 1939 Erzincan earthquake in the east and 1942 Niksar - Erbaa, 1943 Tosya, 1944 Bolu - Gerede, 1951 Kurşunlu, 1957 Abant, 1967 Mudurnu Valley (Barka, 1992) and the 1999 İzmit and Düzce Earthquakes (Akyüz et al. 2002) sequentially westwards. During these 9 major events, 1100 km long surface faulting between Erzincan and the Sea of Marmara was observed (Barka et al, 2002). The closest segment of the NAF to the Sinop NPP site is the earthquake fault of the 1943 Tosya Earthquake. The 1943 earthquake rupture zone is approximately 110 km away from the Sinop NPP site; therefore, an extensive amount of site investigations was focused on this rupture zone. Emre et al. (2008) argued that the total length of the 1943 Tosya Earthquake (Mw=7.7) rupture is 290 km and estimated the recurrence interval for the characteristic event as 250-800 years based on paleoseismological investigations.

Emre et al. (2008) characterized the source geometry of 1943 Tosya earthquake rupture zone using geomorphologic and geological information and proposed a segmentation model with segment lengths varying between 7 and 57 km. To make the segmentation model more significant for the PSHA analysis, some segments are combined and 5 relatively longer segments are defined for 1943 Tosya Earthquake Rupture Zone in this study. The 1942 Niksar-Erbaa Earthquake (Mw=7.1) with a surface rupture of approximately 50 km is also added as a separate segment to this system to be able to create different rupture scenarios that combines the 1942-1943 events. The segment names, segment geometry, slip rates and characteristic magnitude values are provided in Table 3.1.

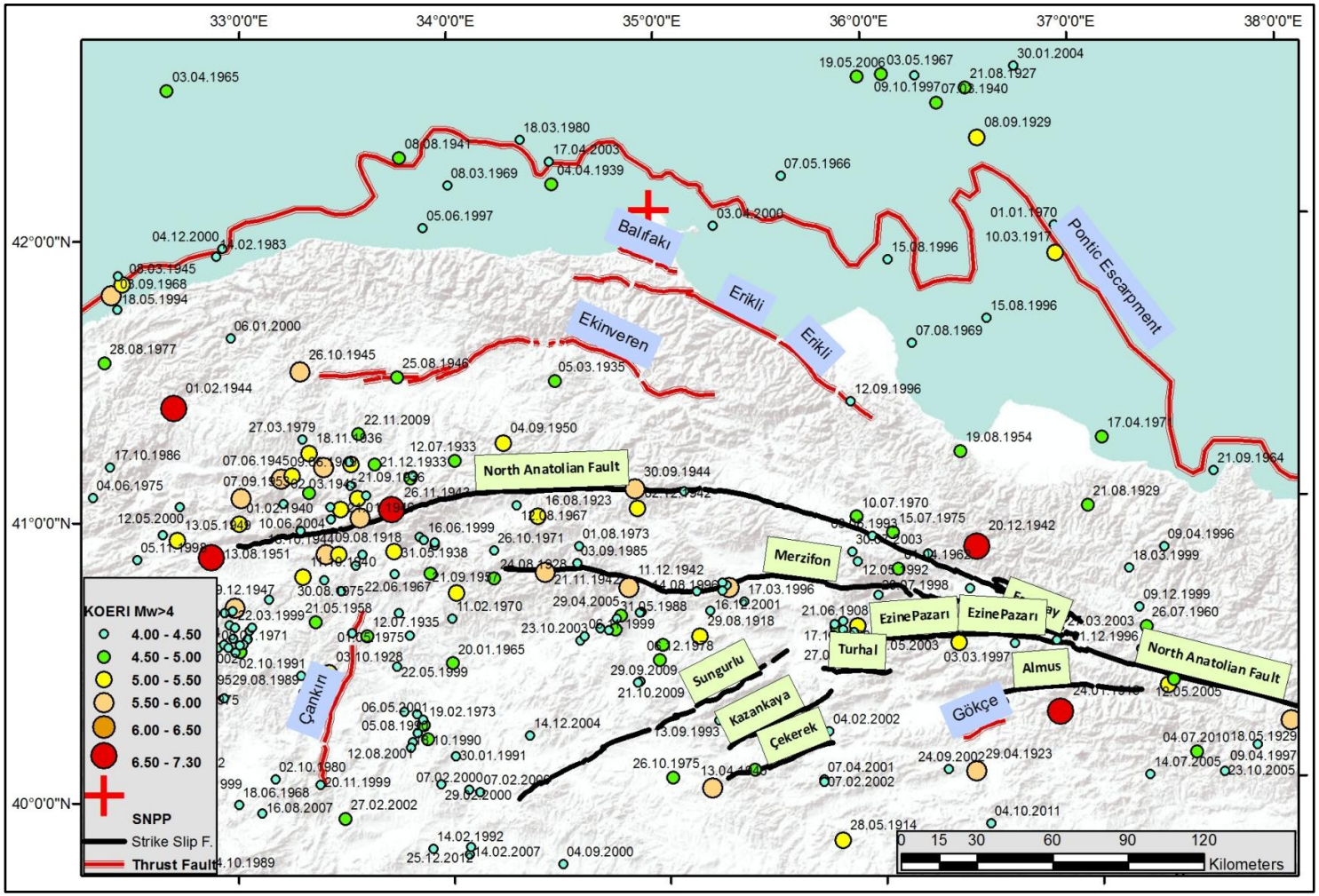

Figure 3.1: Seismic Sources within 320 Km Radius to the Sinop NPP Site and the Spatial Distribution of M>4 Catalogue Events

Table 3.1: Segments of NAF in 1943 and 1942 Earthquakes

ID	Segment Name	Length (km)	Width (km)	Slip Rate (mm/y)	M_{char} (M_w)
1	Ilgaz	57	16	21	7.1
2	Kargı	68	16	15	7.2
3	Kamil	36	16	15	6.9
4	Köprübaşı	69	16	15	7.2
5	Destek	41	16	7	7.0
6	1942 Rupture	46	16	7	7.0

The width of the rupture zone is back calculated by the area–magnitude relations proposed by Wells and Coppersmith (1994) (Eqn. 3.10) as 16 km. Then the characteristic earthquake magnitude for each segment is estimated using Equation 3.11 and listed in Table 3.1.

$$\log(RW) = -0.76 + 0.27 \times M \qquad 3.10$$

$$M_{char} = 3.98 + 1.02\log(RA)\,(\pm 0.23) \qquad 3.11$$

3.2.2 Splays from NAF: Esençay and Merzifon Faults

In the central segment of the NAF (Figure 3.1), the seismicity appears to be mainly distributed throughout the area bounded by the NAF-1943 Rupture Segment on the north and the Sungurlu Fault on the south (Peyret et al., 2012). Esençay and Merzifon fault segments lie in between NAF-1943 lineament and Ezinepazarı - Sungurlu Fault Zone. In some sources, this fault lineament was named as Uzunyazı Fault (Rojay and Koçyiğit, 2011) or Laçin Fault (Peyret et. al, 2012). When it is closely examined, especially the Merzifon Fault in the latest Active Fault Map of MTA (2012) coincides with Uzunyazı and Laçin Faults. Uzunyazı Fault is a dextral strike slip fault that runs parallel to the northern and southern bounding fault zones. According to Rojay and Koçyiğit (2011), the width (on plan) of the zone is 1 km and extends more than 150 km from Laçin in the west to Taşova in the east through Merzifon Suluova Basin. According to Peyret et al. (2012), the Mw=5.7 Salhan Çayı Earthquake (14.08.1996) occurred on one of the segments of the Laçin Fault at the south of the main lineament. Fault plane solutions of this event show a dextral strike slip mechanism solution (Rojay and Koçyiğit, 2011).

For this study, two distinct fault segments are defined for Merzifon-Esençay Fault Zone as shown in Table 3.2. Considering the far distance of the fault to the Sinop NPP site, a more detailed segmentation approach was not adopted. Since the magnitude of the characteristic event is unknown, the width of the fault zone is estimated as 8 km by considering the average depth of earthquakes associated with the Merzifon Fault after removing the outliers. The same width value is assigned to Esençay Fault to be consistent. The characteristic earthquake magnitude for each segment is estimated using Equation 3.11 and listed in Table 3.2.

Table 3.2: Segments and Characteristic Properties of Esençay Merzifon Faults

Segment	Length (km)	Width (km)	Slip Rate(mm/y)	Mchar (Mw)
Merzifon	164	8	6	7.2
Esençay	62	8	6	6.8

3.2.3 Ezinepazar Sungurlu Fault (EzSF)

Ezinepazar and Sungurlu Faults (EzSF) bound the southern margin of the NAF Shear Zone in Amasya Region. The EzSF is the first and the longest dextral off shoot (splay) of the NAF in the west of the Karlıova triple junction and forms the southern boundary of an active wedge shaped deformation zone (İşseven and Tüysüz, 2006). The morphology and geometry of this fault zone is not continuous; to the west its linear trend gradually becomes an en-echelon pattern, but later it branches into new faults (Erturaç and Tüysüz, 2010). Especially after the 1999 Düzce Earthquake that took place on one of the splays of NAF (Akyüz et al. 2002), the importance of the splay faults increased not only to understand the fault mechanism of the splay but also to understand the behavior of the main fault strand of the NAF. In general, while the width of the shear zone increases, the slip rates decreases, especially in the regions where big splays are observed (Yavaşoğlu et al. 2011, McClutsky et al. 2000). According to Erturaç and Tüysüz (2010), the recognition of EzSF dates back to 1939 Erzincan Earthquake. 65 km long eastern part of this fault zone is named as Ezinepazarı Fault and this segment was ruptured during 1939 Erzincan Earthquake with a co-seismic slip of 1.5-2 m. The Ezinepazarı segment is included in the 1939 Earthquake Rupture Zone model by Vakilinezhad (2014). Since the 1939 rupture

zone source model is directly adopted, Ezinepazarı segment is not modeled separately for this study.

In the west of Ezinepazarı segment, the Deliçay, Geldingen, Mecitözü and Sungurlu segments of the same fault zone were located by Erturaç and Tüysüz (2010). However, these strands do not have a complete match with the segments mapped in the latest active fault map of MTA (2012). Furthermore, the seismicity within the NAF shear zone is characterized by events up to M=6.0, usually occurring in a series of moderate-sized earthquakes on the active faults north of the EzSF (Erturaç and Tüysüz, 2010). Both in the west and the south of the EzSF, some other faults are mapped by MTA (Çankırı, Turhal, Kazankaya, Çekerek and Gökçe Faults) and these faults show different characteristics, some of them are strike slip in character and the rest are reverse faults.

The seismic sources on the south of Ezinepazarı Fault, including the splays of NAF Shear Zone (Deliçay, Geldingen, Mecitözü and Sungurlu) and the other small faults (Çankırı, Turhal, Kazankaya, Çekerek and Gökçe Faults) are modelled by a large areal source zone as shown in Figure 3.2. The areal source model is preferred since the slip rate for the Sungurlu splay is unknown and the sources are far away from the Sinop NPP site. For this areal seismic source, the truncated exponential magnitude distribution model was adopted with a maximum magnitude value of Mw=6.5. Geometry of the areal zone is bounded by the Merzifon – Esençay Fault Segment on the north and modified to contain all the seismicity within the 320 km radius around Sinop NPP in the south (Figure 3.2). The reverse fault mechanism was assigned to the source to be on the safe side. The b-value of the truncated exponential model is calculated by maximum likelihood methodology proposed by Weichart (1980) as 0.84 and given in Table 3.3.

Table 3.3: The "b" Value for Truncated Exponential Model for the Areal Source

Lower Bound	Upper Bound	Magnitude	# of events	Complete time intervals (years)	Rate	RxM
4.0	4.2	4.1	19	50	0.38	1.56
4.2	4.4	4.3	25	50	0.50	2.15
4.4	4.6	4.5	15	50	0.30	1.35
4.6	4.8	4.7	11	88	0.13	0.59
4.8	5.0	4.9	15	88	0.17	0.84
5.0	5.2	5.1	2	113	0.02	0.09
5.2	5.4	5.3	6	113	0.05	0.28
5.4	5.6	5.5	2	113	0.02	0.10
5.6	5.8	5.7	1	113	0.01	0.05
5.8	6.0	5.9	3	113	0.03	0.16
6.0	6.2	6.1	2	113	0.02	0.11
6.2	6.4	6.3	0	113	0.00	0.00
6.4	6.8	6.6	2	113	0.02	0.12
Σ		Total:	148	Total:	1.63	7.38
					$\overline{M}$ =4.52	
					'b" Value=0.84	

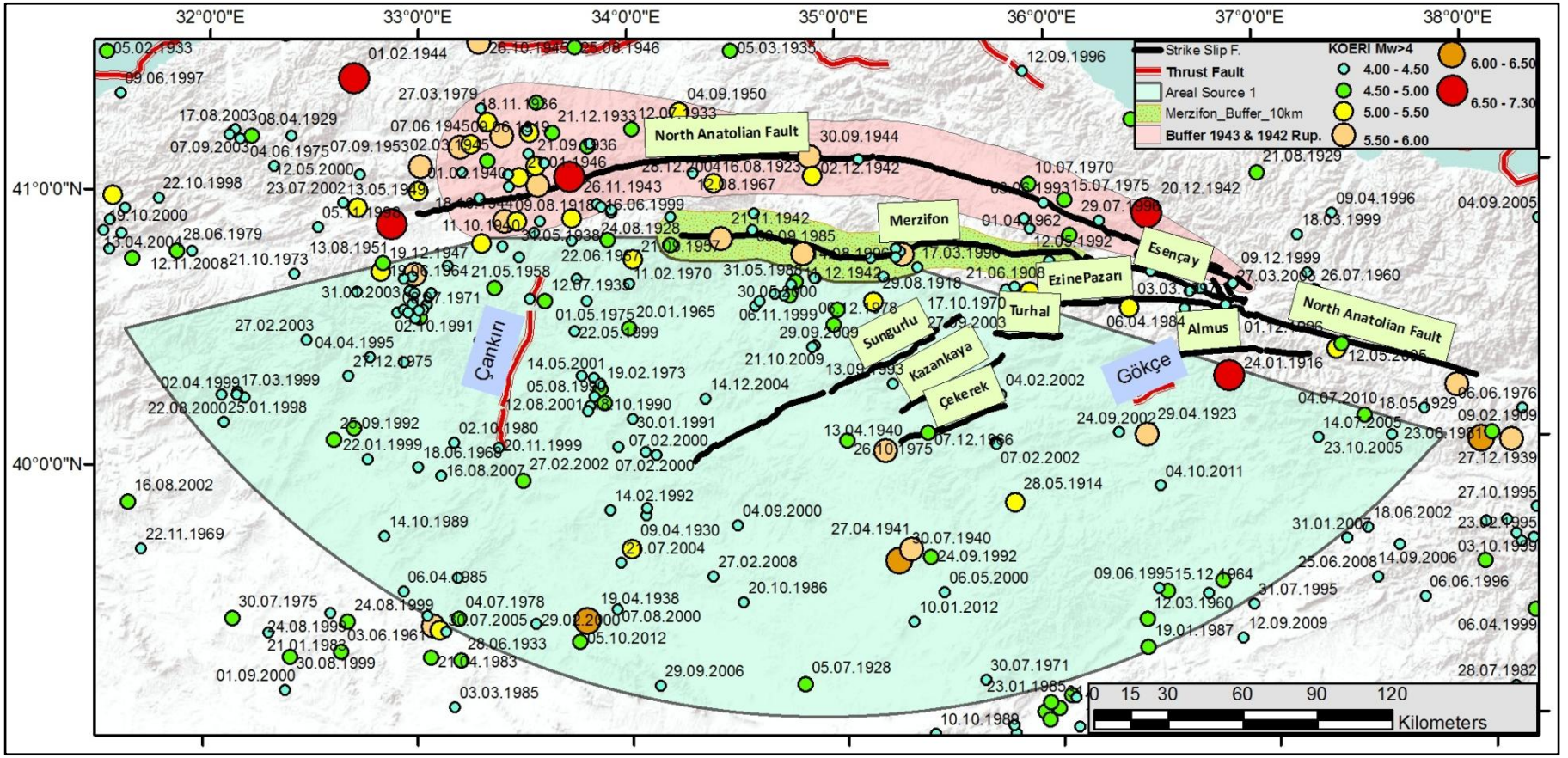

Figure 3.2: Areal Source and Seismicity in the Region

3.2.4 Slip Rate Partitioning between the NAF and the Other Parallel Faults

As shown in Section 3.1, the annual slip rate of the fault needs to be determined in order to balance the accumulated and balanced seismic moment and validate the magnitude recurrence model. Slip rate of the NAF system has been investigated by different researches in the last two decades and different values have been proposed based on different measurement techniques. The inter-seismic velocities of Global Positioning System (GPS) measurements performed by Yavaşoğlu et al. (2011), Reilinger et al. (2006) and McClutsky et al. (2000) result in a slip rate of 20 - 21 mm/y for totally unlocked regions around the longitudes bounding the Central NAF (Figure 3.3).

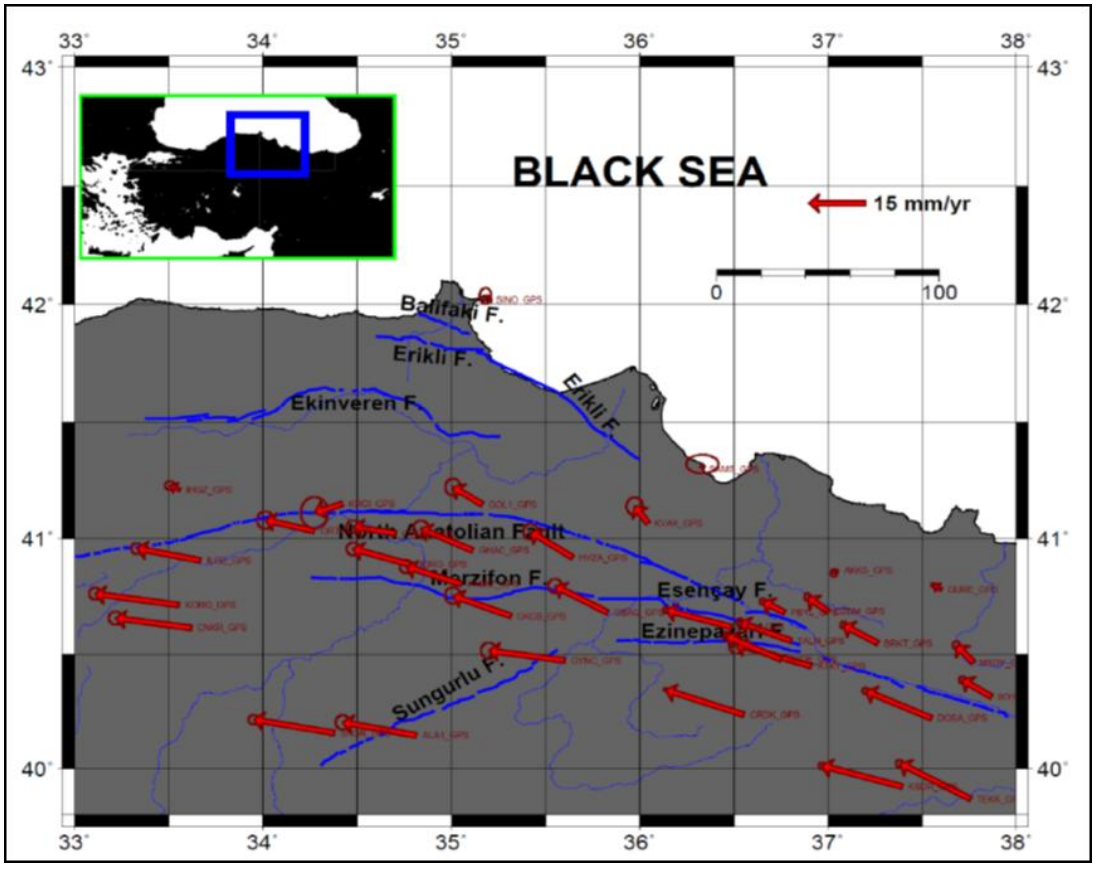

Figure 3.3: Compilation of GPS Velocities from Tatar et al. (2012), Yavaşoğlu et al. (2011) and McClusky et al. (2000)

However, the geological and geomorphological correlations made along the central section of the NAF indicate slip rate of 6.5 mm/y for Neogene and 18±5 mm/y for Holocene periods (Hubert and Ferrari, 2002). Kozacı et al. (2007) proposed the late Holocene slip rate as 20.5 ± 5.5 mm/y and 20.5 ± 8.5 mm/y for the Central North

Anatolian Fault based on cosmogenic radionuclide (^{36}Cl and ^{14}C) studies around the Eksik Village. Later, Kozacı et al. (2009) proposed late Holocene slip rate of 18.6+3.5/-3.3 mm/y for the central segments of NAF around Tahtaköprü based on measurement of a stream offset and cosmogenic nuclides dating. A recent study by Peyret et al. (2012) proposed a similar slip rate of 20 mm/y based on the joint inversion of the GPS and Persistent Scatterer Synthetic Aperture Radar Interferometry and they also proposed mean velocity fields for a locking depth of 15-20 km. In accordance with the geologic and geodetic measurements proposed by aforementioned studies, the slip rate for the whole NAF system has been selected as 18-21 mm/y. However, the main branch of NAF (1942-1943 Earthquake rupture zones) lies parallel to the Esençay-Merzifon and Ezinepazarı branches; therefore the total slip rate should be distributed among these parallel branches (Figure 3.4).

Barka (1996) estimated 1.6 - 2.0 m co-seismic slip for 1942 Niksar-Erbaa rupture zone. Considering the penultimate event, the 1668 Earthquake, the inter-seismic slip rate is calculated as 7 mm/y. Similarly, 1.8 to 2.7 m coseismic slip was proposed by Barka (1996) on Ezinepazarı Fault during the 1939 Erzincan Earthquake and based on this slip, 6.5-10 mm/y slip rate is estimated for Ezinepazarı Segment of 1939 Rupture zone. These values are in agreement with the geologic slip rate calculated for Ezinepazar Fault by Erturaç and Tüysüz (2010) (7-10 mm/y). Similarly, Rojay and Koçyiğit (2011) estimated 2.5 to 6.3 mm/y of geologic slip rate for Merzifon-Suluova-Amasya region.

Based on these interpretations, 6 mm/y slip rate was assigned to the Merzifon-Esençay Branch and 8 mm/y slip rate was assigned to the Ezinepazarı Fault (Figure 3.4). Remaining 7 mm/y is employed in the main branch for 1942 Rupture Zone. Because the Ezinepazarı Fault strikes E-W up to the western end of the Destek segment of the 1943 rupture, the slip rate for the Destek segment was also taken as 7 mm/y. 15 mm/y slip rate is adopted for Köprübaşı, Kamil and Kargı segments since these segments partition the total slip with the Merzifon-Esençay Branch. Finally, 21 mm/y slip rate was assigned to Ilgaz segment at the westernmost end of NAF main branch. Assigned slip rates are in good agreement with the seismic source models of 1944 Bolu-Gerede earthquake rupture zone in the west and 1939 Erzincan earthquake rupture zone in the east (Vakilinezhad et al., 2013; Vakilinezhad, 2014).

3.2.5 Earthquake Catalogue and Source-to-Epicenter Matching

The Integrated Homogeneous Turkish Earthquake Catalogue (KOERI, 2007) including the events with M_w>4 that occurred between 1900 and 2005 in between 30^o-39^o East Longitudes and 39^o-44^o North Latitudes was used for the source-epicenter matching. Web database of Kandilli Observatory and Research Center was used to complete the catalogue for the events occurred between 2005 and 2013. The magnitudes in the catalogue were provided in terms of local magnitude (Ml), body-wave magnitude (Mb), surface wave magnitude (Ms), duration magnitude (Md) and moment magnitude (Mw). When moment magnitude values are not available, magnitude values were converted to moment magnitude using the following conversion formulas proposed by Akkar et al. (2010) (Equation 3.12-3.16). After unifying the magnitudes, the mainshock-aftershock classification of the catalogue was performed and the aftershocks were removed from the dataset using Gardner and Knopoff (1974) method. The remaining database after filtering the aftershocks is composed of 362 events with moment magnitudes between 4.0 and 7.6 (Table 3.4).

$$M_w = 1.104M_b - 0.194, \qquad 3.5 \le M_b \le 6.3 \tag{3.12}$$

$$M_w = 0.571M_s + 2.484, \qquad 3.0 \le M_s \le 5.5 \tag{3.13}$$

$$M_w = 0.817M_s + 1.176, \qquad 5.5 \le M_s \le 7.7 \tag{3.14}$$

$$M_w = 0.953M_L + 0.422, \qquad 3.9 \le M_L \le 6.8 \tag{3.15}$$

$$M_w = 0.764M_d + 1.379, \qquad 3.7 \le M_d \le 6.0 \tag{3.16}$$

In the calculation of b-value, a catalogue with complete earthquake data is essential. The cumulative rates of earthquakes larger than different magnitude levels are plotted vs. years to examine the completeness of the catalogue (Figure 3.5). The breaking points for the linear trends in the cumulative rate of events for different cut-off magnitudes are examined and a significant breaking point is observed around 50 years for magnitudes smaller than 4.5. Similarly, a break point at the cumulative rate of events was observed at 88 years for events for magnitudes smaller than 5.0. Therefore, the earthquake catalogue is assumed to be complete for 50 and 88 years for Mw≤4.5 and Mw≤5.0 earthquakes, respectively. Even though the larger magnitude plots in Figure 3.5 suffers from the lack of data due to the truncation of the catalogue, the catalogue is assumed to be complete for the whole time span (1900-2013) of the catalogue for greater magnitude events.

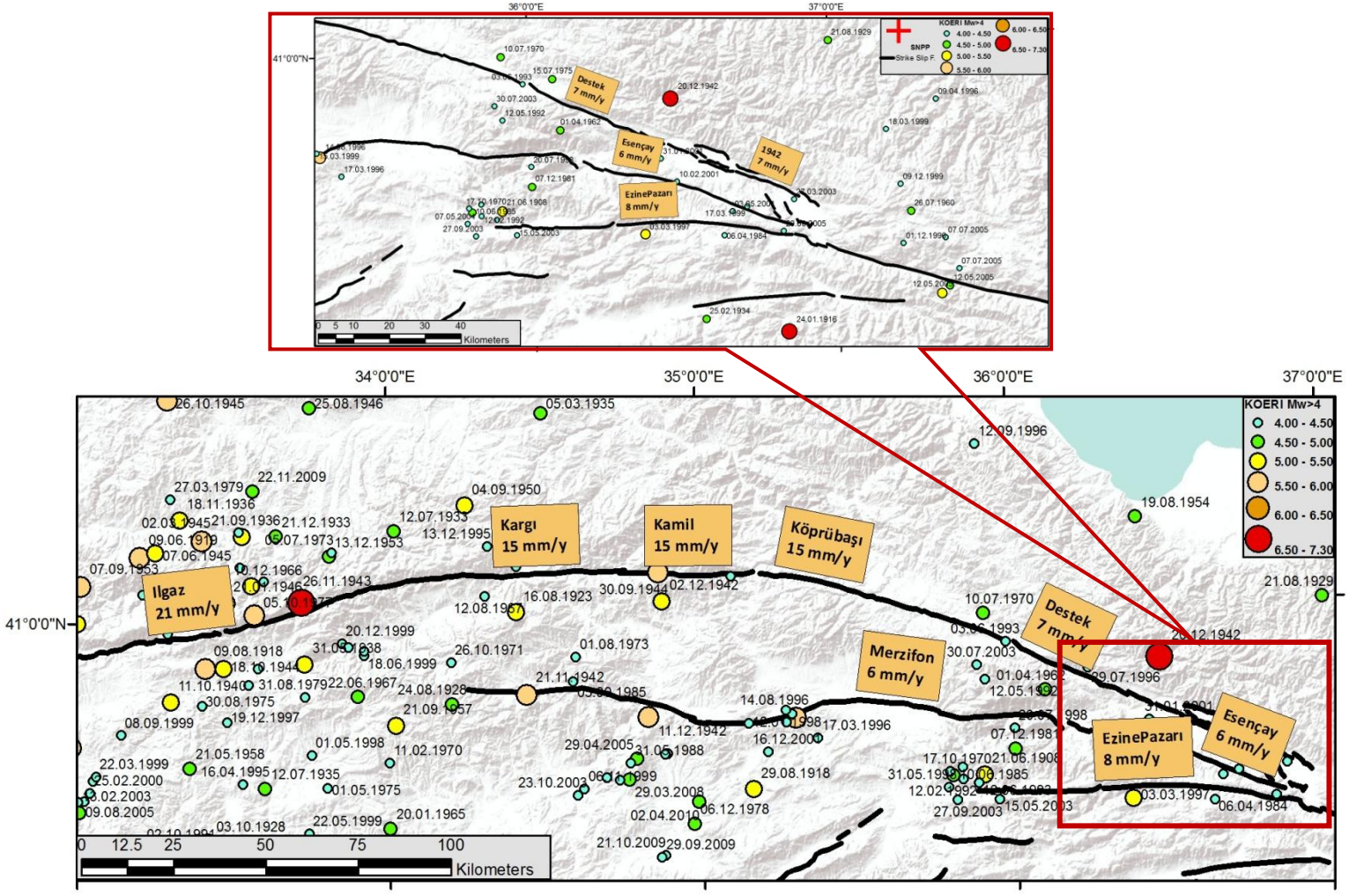

Figure 3.4: a- Closer View to Distribution of Slip Rates at Junction Point, b- Distribution of Slip Rates

Based on the modified maximum likelihood method (Weichert, 1980) that takes into account the variable completeness at the catalogue for different magnitude bins, the b-value is calculated as 0.71 for the region (Table 3.4). Calculated b-value is slightly smaller than the recommended b-value range for shallow crustal and active tectonic regions (0.8-1.2) since the seismicity assigned to the areal source zones is excluded from the database provided in Table 3.4. The regional b-value is employed for all planar seismic sources (NAF and splays, Erikli and Balıfakı Faults).

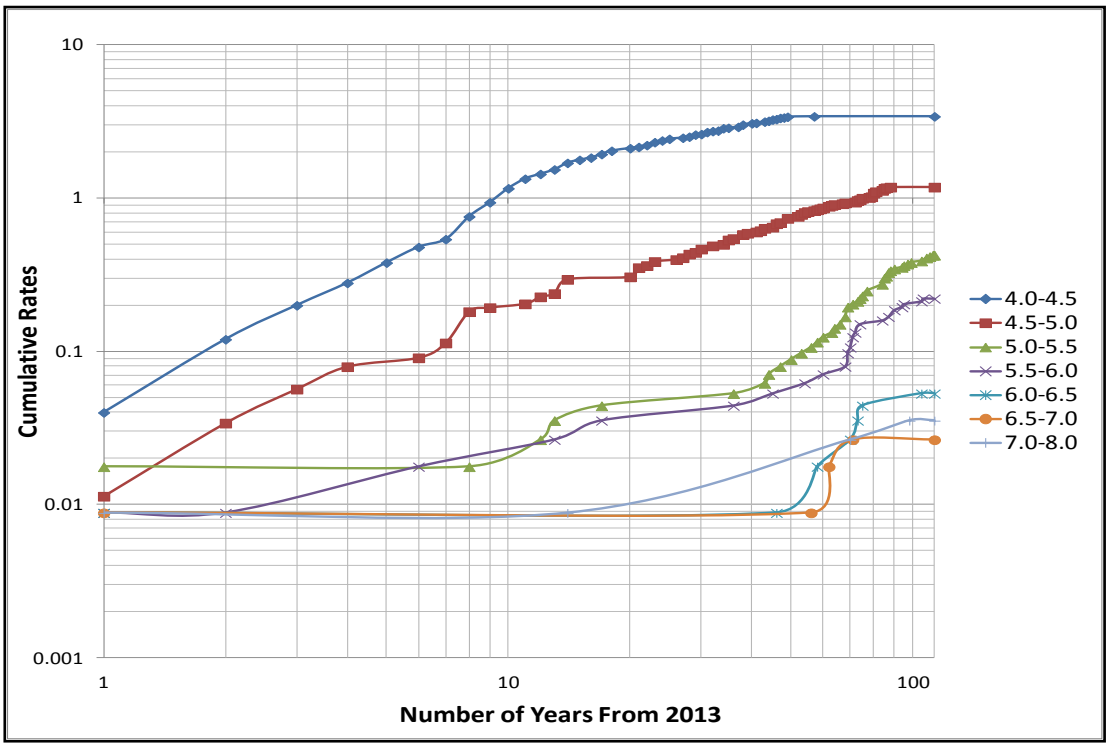

Figure 3.5: The Completeness Intervals for the Earthquake Catalogue

3.2.6 The Rupture Model: USGS Approach

Final step in seismic source characterization is to define the rupture model considering the segmentation model for the rupture zone and seismicity associated with the fault. This study adopts the same approach as the WGCEP-2003 SF Bay Area Model for seismic source characterization, which is primarily based on characterized faults that are divided into non-overlapping segments. WGCEP-2003 approach is based on segment-source-scenario definitions. The shortest fault capable of rupture to produce large earthquakes repeatedly is defined as segment. Change in the strike, occurrence of restraining bends, intersection points (jogs), changes in fault complexity, major changes in lithology along the fault and information about previous earthquakes are major parameters in the deciding the segmentation of a

source. A source is defined as a fault segment or a combination of multiple adjacent fault segments that are possible to rupture and produce an earthquake in the future. Finally, the rupture scenario is defined as any possible combination of sources that describes a possible failure mode (Gülerce and Ocak, 2013). Based on the definitions given above, six non overlapping segments and twenty seven rupture scenarios were produced for the main strand of the NAF as shown in Table 3.5.

Table 3.4: Maximum Likelihood Estimation of the Regional "b-Value"

Lower Bound	Upper Bound	Magnitude	# of events	Complete time intervals (years)	Rate	RxM
4.0	4.2	4.1	45	50	0.90	3.69
4.2	4.4	4.3	74	50	1.48	6.36
4.4	4.6	4.5	62	50	1.24	5.58
4.6	4.8	4.7	38	88	0.43	2.03
4.8	5.0	4.9	51	88	0.58	2.84
5.0	5.2	5.1	10	113	0.09	0.45
5.2	5.4	5.3	26	113	0.23	1.22
5.4	5.6	5.5	18	113	0.16	0.88
5.6	5.8	5.7	11	113	0.10	0.55
5.8	6.0	5.9	10	113	0.09	0.52
6.0	6.2	6.1	5	113	0.04	0.27
6.2	6.4	6.3	3	113	0.03	0.17
6.4	6.6	6.5	2	113	0.02	0.12
6.6	6.8	6.7	4	113	0.04	0.24
6.8	7.6	7.2	3	113	0.03	0.19
Σ		Total:	362	Total:	5.45	25.21
					$\overline{M}$=4.61	
					b Value=0.71	

For a complete rupture model, a weight is assigned to each rupture scenario and the cumulative rates of events attributed to that particular fault are plotted with the weighted average of rupture scenarios to calibrate the assigned weights. By the help of the Geographical Information Software (GIS) Arc-GIS, source-to-epicenter matching for each individual fault strand was performed by creating buffer zones around the fault segments. The buffer zones used for the main strand of NAF (1942-1943 rupture segments) and the parallel Merzifon - Esençay Fault Splay are shown in Figures 3.8 and 3.9, respectively. Different size buffer zones were created to be able to achieve an optimum balance between the accumulated and released seismic

moments. Slip rates attributed to each segment and the weights assigned to different rupture scenarios are validated with the catalogue seismicity that falls into the specified buffer zone. For the 1942-1943 Rupture Zones, the optimum balance is achieved with a buffer zone of R=15 km around the fault line. To improve the balance, slight modifications were made in the shape of the buffer zone by taking into account the possible mislocations of the epicenters. In the west, the buffer zone was extended in the north-south direction to include all the events that are thought to be related to the NAF (Figure 3.8). On the contrary, around the junction where NAF bifurcates into three strands, the buffer zone was restricted within a few kilometers in order not to include the earthquakes related with Esençay and Ezinepazarı Faults.

The cumulative rates of earthquakes for each scenario are calculated and plotted in Figure 3.6 along with the cumulative rate of the events attributed to the NAF master strand. Uncertainty in the rates is represented by the error bars calculated by Weichert (1980) equations. Highest weights were assigned to the scenarios resembling the rupture of individual segments and full rupture of the fault. Main causes and motivation of this kind of weighting is related to the ease of rupture of each segment individually, already observed full rupture of the 5 segments together excluding the 1942 rupture, and the intend to weigh the worst case scenario highly. As seen in Figure 3.6, the weighted average of the rupture scenarios is in good agreement with the associated seismicity (black dots in Figure 3.6).

The buffer zone around the Merzifon-Esençay Fault and the associated seismicity are shown in Figure 3.9. The Merzifon-Esençay Fault zone is modeled by 2 non-overlapping segments (Merzifon and Esençay segments, Table 3.2); therefore 2 sources and 3 rupture scenarios were obtained. The cumulative rate of the events attributed to Merzifon-Esençay Fault and the rupture model for this source is provided in Figure 3.7. Similar to Figure 3.6, Figure 3.7 validates the assigned slip rate and associated seismicity for the Merzifon-Esençay Fault.

3.2.7 1939 Erzincan and 1944 Bolu-Gerede Earthquakes on NAF

The 1939 Erzincan Earthquake (M=7.8) is not only the largest earthquake that occurred in 1939-1967 earthquake sequence but also it was the largest earthquake in Anatolia during the last century (Barka, 1996). The rupture zone of the earthquake is approximately 360 km long with a pure strike-slip motion and the maximum co-

seismic slip is found as 7.5 m (Barka, 1996). Ezinepazarı Fault is the westernmost segment of the 1939 Erzincan Earthquake rupture zone and located within the 320 km radius around the Sinop NPP. Vakilinezhad (2014) included this segment and the ones lying in the east and falling within 320 km radius of Sinop NPP in the rupture model of the 1939 Earthquake, therefore, the proposed model is directly adopted from that study. Detailed segmentation and recurrence models can be found in Vakilinezhad (2014).

The rupture zone of the 1944 Bolu-Gerede Earthquake in the west is approximately 165 km long, extending from North of Kurşunlu to Abant Lake (Barka, 1996). The Ilgaz-Ismetpaşa Segment of 1944 rupture zone lies within the 320 km radius around Sinop NPP, therefore 1944 rupture zone should be included in the PSHA. Similar to the 1939 earthquake rupture zone, the 1944 Bolu-Gerede earthquake rupture zone was modeled by Vakilinezhad et al. (2013) therefore it is directly adopted in this study.

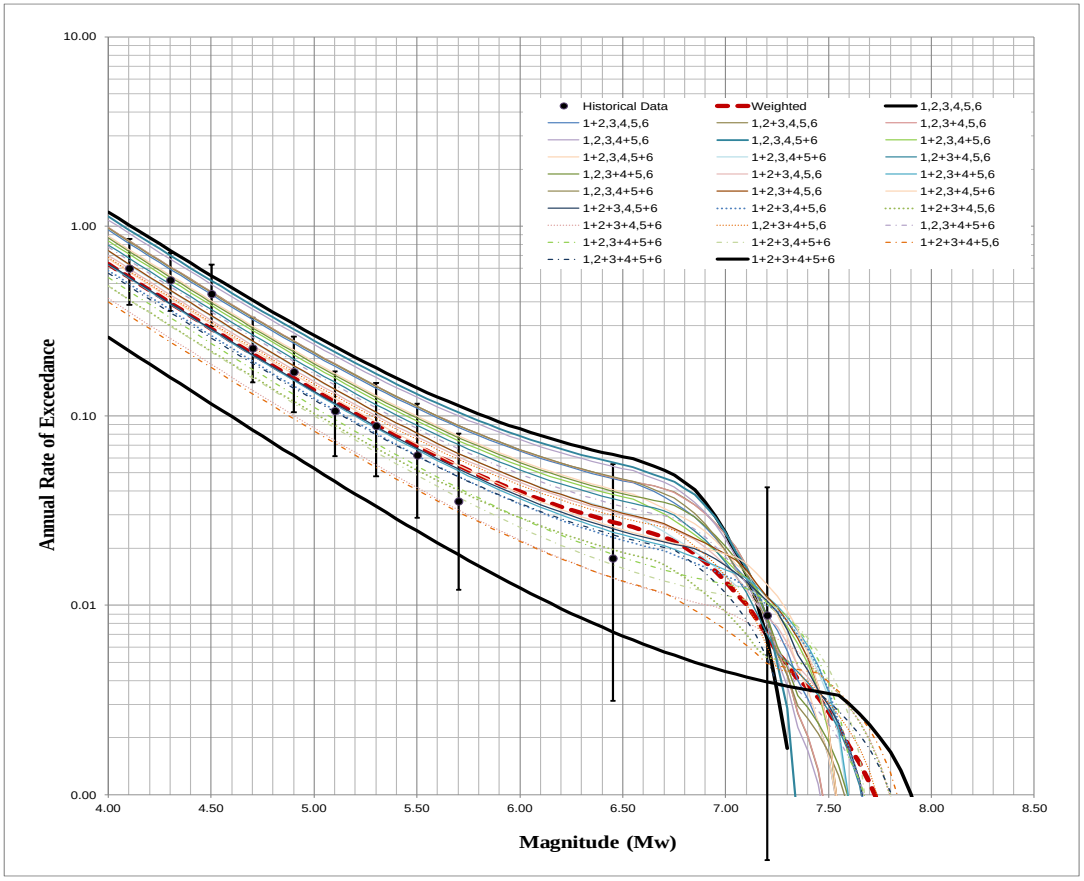

Figure 3.6: Cumulative Rates of Catalogue Events Attributed to 1943 Tosya-Erbaa Earthquake Rupture Zone and its Proposed Rupture Model. (The Black Dots in Figure Stand for the Cumulative Annual Rates of Earthquakes from the Catalogue Assigned to this Source. The Weighted Average of the Rupture Scenarios is shown in Red Broken Line)

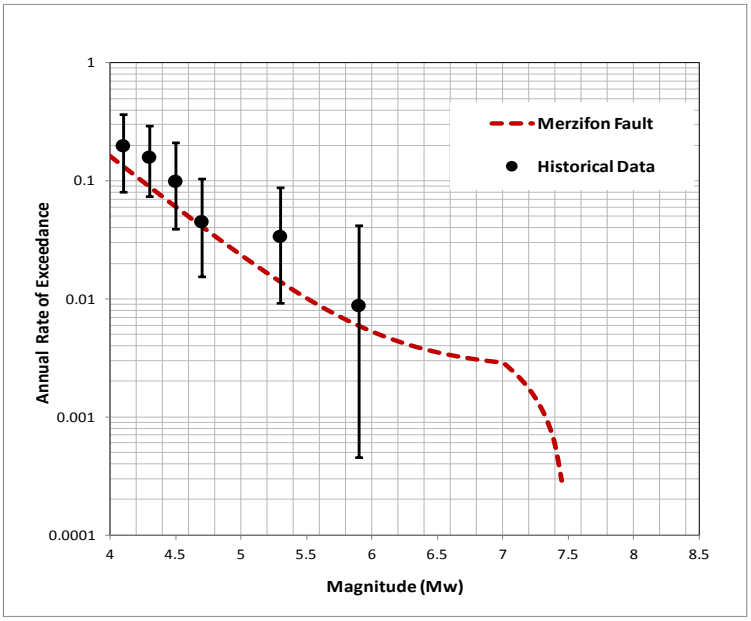

Figure 3.7: Cumulative Rates of Catalogue Events Attributed to Merzifon Fault and its Proposed Rupture Model.
(The Black Dots in Figure Stand for the Cumulative Annual Rates of Earthquakes from the Catalogue Assigned to this Source. The Weighted Average of the Rupture Scenarios is shown in Red Broken Line)

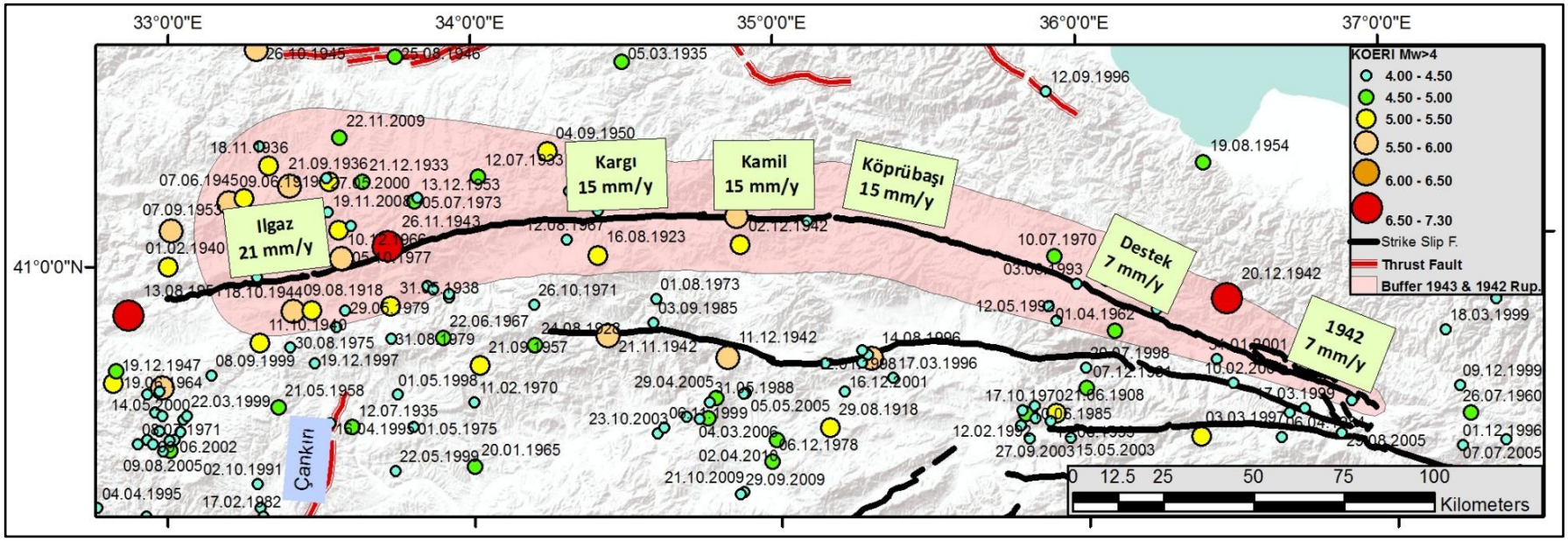

Figure 3.8: Buffer Zone of 1943 and 1942 Ruptures and the Seismicity in the Region

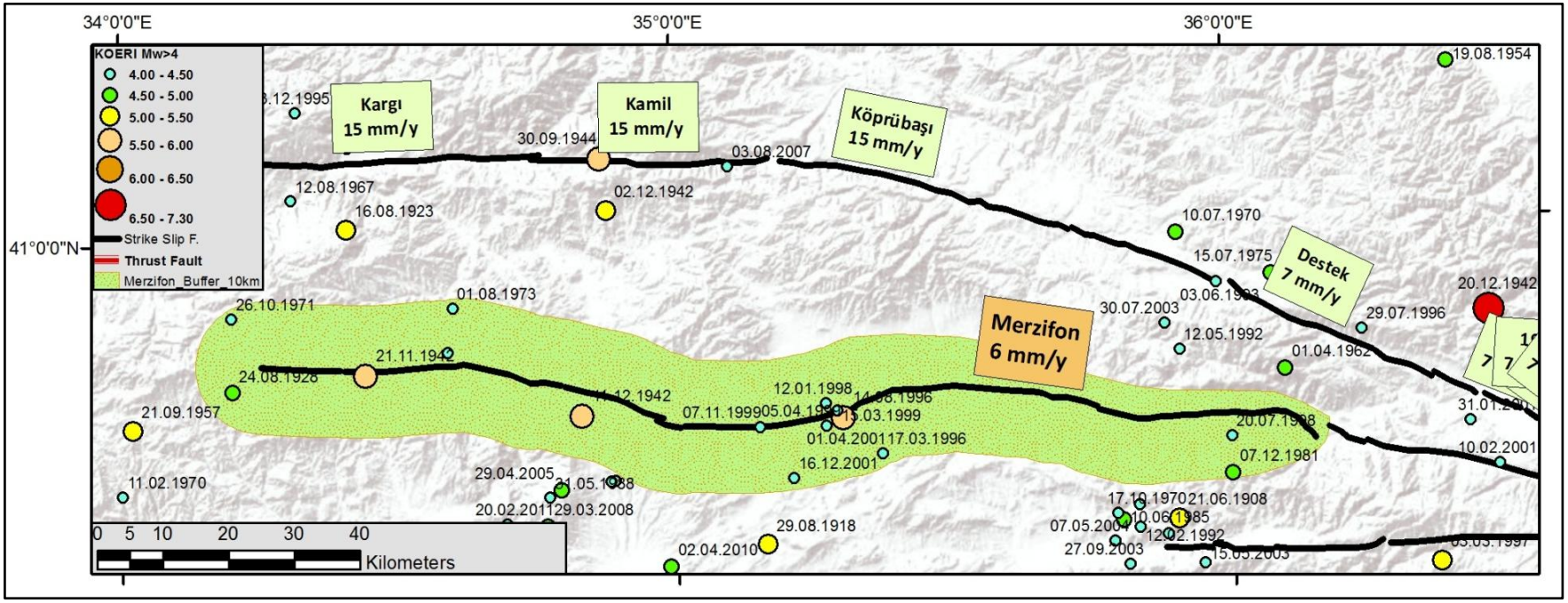

Figure 3.9: Buffer Zone for Merzifon Fault and the Regional Seismicity

Table 3.5: 1943 and 1942 Ruptures with Associated Scenario and Assigned Weights

		1	2	3	4	5	6	7	8	9	10	11	12	13	14	15	16	17	18	19	20	21	
	KAF CENTRAL SEGMENT	*1*	*2*	*3*	*4*	*5*	*6*	*1+2*	*2+3*	*3+4*	*4+5*	*5+6*	*1+2+3*	*2+3+4*	*3+4+5*	*4+5+6*	*1+2+3+4*	*2+3+4+5*	*3+4+5+6*	*1+2+3+4+5*	*2+3+4+5+6*	*1+2+3+4+5+6*	Weights
1	*1,2,3,4,5,6*	1	1	1	1	1	1	0	0	0	0	0	0	0	0	0	0	0	0	0	0	0	**0.09**
2	*1+2,3,4,5,6*	0	0	1	1	1	1	1	0	0	0	0	0	0	0	0	0	0	0	0	0	0	0.02
3	*1,2+3,4,5,6*	1	0	0	1	1	1	0	1	0	0	0	0	0	0	0	0	0	0	0	0	0	**0.02**
4	*1,2,3+4,5,6*	1	1	0	0	1	1	0	0	1	0	0	0	0	0	0	0	0	0	0	0	0	**0.02**
5	*1,2,3,4+5,6*	1	1	1	0	0	0	0	0	0	1	1	0	0	0	0	0	0	0	0	0	0	0.02
6	*1,2,3,4,5+6*	1	1	1	1	0	0	0	0	0	0	1	0	0	0	0	0	0	0	0	0	0	**0.02**
7	*1+2,3,4+5,6*	0	0	1	0	0	1	1	0	0	1	0	0	0	0	0	0	0	0	0	0	0	0.02
8	*1+2,3,4,5+6*	0	0	1	1	0	0	1	0	0	0	1	0	0	0	0	0	0	0	0	0	0	0.02
9	*1+2,3+4+5,6*	0	0	0	0	0	1	1	0	0	0	0	0	0	1	0	0	0	0	0	0	0	**0.02**
10	*1+2,3,4+5+6*	0	0	1	0	0	0	1	0	0	0	0	0	0	0	1	0	0	0	0	0	0	**0.02**
11	*1+2+3,4,5,6*	0	0	0	1	1	1	0	0	0	0	0	1	0	0	0	0	0	0	0	0	0	0.02
12	*1,2+3+4,5,6*	1	0	0	0	1	1	0	0	0	0	0	0	1	0	0	0	0	0	0	0	0	**0.02**
13	*1,2,3+4+5,6*	1	1	0	0	0	1	0	0	0	0	0	0	0	1	0	0	0	0	0	0	0	**0.02**
14	*1,2,3,4+5+6*	1	1	1	0	0	0	0	0	0	0	0	0	0	0	1	0	0	0	0	0	0	0.02
15	*1+2,3+4,5,6*	0	0	0	0	1	1	1	0	1	0	0	0	0	0	0	0	0	0	0	0	0	**0.02**
16	*1+2,3+4,5+6*	0	0	0	0	0	0	1	0	1	0	1	0	0	0	0	0	0	0	0	0	0	**0.02**
17	*1+2+3,4,5+6*	0	0	0	1	0	0	0	0	0	0	1	1	0	0	0	0	0	0	0	0	0	0.02
18	*1+2+3,4+5,6*	0	0	0	0	0	1	0	0	0	1	0	1	0	0	0	0	0	0	0	0	0	**0.02**
19	*1+2+3+4,5,6*	0	0	0	0	1	1	0	0	0	0	0	0	0	0	0	1	0	0	0	0	0	**0.02**
20	*1+2+3+4,5+6*	0	0	0	0	0	0	0	0	0	0	1	0	0	0	0	1	0	0	0	0	0	0.02
21	*1,2+3+4+5,6*	1	0	0	0	0	1	0	0	0	0	0	0	0	0	0	0	1	0	0	0	0	**0.02**
22	*1,2,3+4+5+6*	1	1	0	0	0	0	0	0	0	0	0	0	0	0	0	0	0	1	0	0	0	**0.02**
23	*1+2,3+4+5+6*	0	0	0	0	0	0	1	0	0	0	0	0	0	0	0	0	0	1	0	0	0	0.02
24	*1+2+3,4+5+6*	0	0	0	0	0	0	0	0	0	0	0	1	0	0	1	0	0	0	0	0	0	**0.02**
25	*1+2+3+4+5,6*	0	0	0	0	0	1	0	0	0	0	0	0	0	0	0	0	0	0	1	0	0	**0.2**
26	*1,2+3+4+5+6*	1	0	0	0	0	0	0	0	0	0	0	0	0	0	0	0	0	0	0	1	0	0.10
27	*1+2+3+4+5+6*	0	0	0	0	0	0	0	0	0	0	0	0	0	0	0	0	0	0	0	0	1	**0.15**
Σ																							1

3.2.8 Erikli Fault

Erikli Fault, a thrust fault extending for about 150 km between Yenikonak in the west and Bafra in the east, is the most disputed fault in the region in terms of its nature, extent and activity (Erdik et al. 1990, Doyuran, 1983, Emre et al. 2008, Kaymakçı 2009). Consequently, this fault is the most intensely studied tectonic feature between years 1983 and 2010. According to Emre et al. (2008), Erikli Fault includes four different segments based on the geometry of the bends and changes in its strike and step-overs. Segments from east to west include, Alaçam, Gerze, Erfelek, and Yenikonak Segments (Figure 3.10). The lengths of the segments vary between 17 to 45 km and the nearest segment of the fault is 30 km away from the Sinop NPP site (Emre et al. 2008) (Table 3.6). The average dips of the segments range between 60°-80°. Although Erikli Fault is defined as having listric geometry and shallow characteristic, there isn't any available information about the width of the fault. Therefore, a shallow depth of 5 km is assigned to this fault in the PSHA analysis. Similarly, no information related to the slip rate of the Erikli Fault could be found in the literature. Emre et al. (2008) argued that the GPS data indicates a shortening of 1.2 – 2.2 mm/y between the northern and southern coasts of the Central and Eastern Black Sea based on the findings of Tarı et al. (2000). This range is consistent with the GPS measurements of McClusky et al. (2000), therefore two alternative slip rates: 1.2 mm/y (lower bound) and 2.2 mm/y (upper bound) are considered for Erikli Fault. Effects of the assigned alternative slip rates and assumed depth on the hazard outcome are discussed in Section 3.3. Detailed information related to the segments of Erikli Fault is provided below.

Alaçam Segment: According to Emre et al. (2008), 45 km long Alaçam Segment is the easternmost segment of the Erikli Fault, striking N50ºW and the fault plane is dipping 40°-65º due south. Emre et al. (2008) also argued that while geomorphological findings were interpreted as indirect evidences of the activity of the Alaçam segment in Pliocene and Quaternary, geomorphological and paleoseismological data do not support Holocene activity of the fault. Therefore, this segment is defined as inactive fault by Emre et al. (2008).

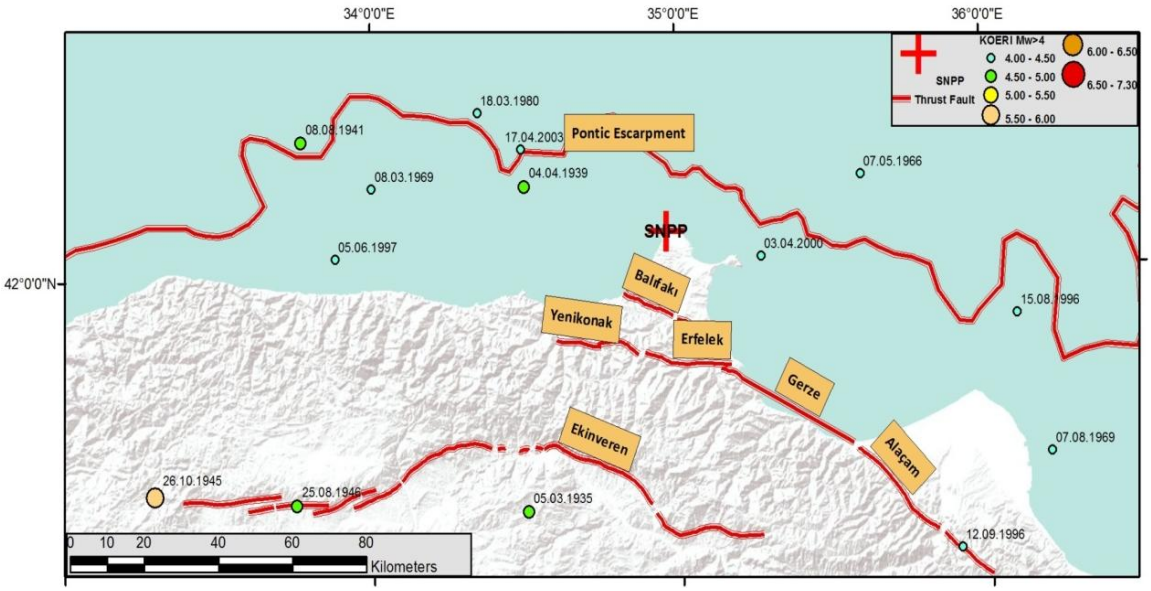

Figure 3.10: Faults in the North of NAF

Gerze Segment: According to Emre et al. (2008) Gerze Segment is the off-shore continuation of the Erikli Fault. It is 30 km long fault line extending from Gerze in the west to Yakakent in the east. It strikes approximately N62ºW. The off-shore shallow seismic profiles acquired along the presumed fault zone and the results indicated that the Holocene cover is undisturbed. Based on this information, the Gerze Segment of the Erikli Fault is also concluded to be inactive by Emre et al. (2008).

Erfelek Segment: The Erfelek Segment is the nearest segment of the Erikli Fault to the Sinop NPP site. It is a 40 km long segment striking approximately N80ºW. Erfelek segment is classified as "capable fault" by Emre et al. (2008) mainly based on the inconclusive paleoseismologic observations along the fault line. The obtained paleoseismological data was inconclusive because the paleoseismological trench which might include some evidence for the fault activity was excavated within a large landslide complex with multiple slide activity. There is possibility that the observed disturbances on the ground could also be related to mass-wasting processes rather than faulting. Besides, 28 trenches out of 29 other trenches did not bear any appreciable ground deformation which could be related fault activity. Therefore, the possible earthquake activity of the Erfelek Segment could not be evaluated. Likewise, it could not also be excluded as a non-seismogenic structure since the origin of the ground deformations along the fault in a paleoseismological trench

could not be determined yet. Accurate information on the mechanism of Erfelek segment is not provided by Emre et al. (2008); while Karapınar Paleoseismological trench site shows a normal faulting mechanism, reverse fault mechanism is observed in Kabanlar site which was concluded to be related to landslide activity rather than faulting. On the other hand, Kaymakçı (2009) reported that lack of a thrust fault at depth, lack of strike-slip activity on the Erikli Fault, presence of widespread landslide activity, and limitation of the activity only to a local area along the full length of the Erikli Fault was implied that the deformation mechanism proposed by Emre et al. (2008) is not justified and misleading.

According to Kaymakçı (2009), presence of small scale normal faults distributed in a large area (also based on TPAO seismic interpretation study, Güney 2008), lack of large scale earthquakes, micro-earthquake activity with extensional solutions, lack of any major movements in the region based on GPS velocities, very minor (negligible) and divergent nature of GPS velocities in the Sinop Peninsula and around Samsun are the indications of relaxation in the region. These information contradicts with Emre et al. (2008)'s thrust mechanism. Therefore, based on these arguments Kaymakçı (2009) argued that Erikli Fault needed to be classified as inactive.

Yenikonak Segment: Yenikonak segment is the westernmost segment of the Erikli Fault. It extends between Yenikonak and Karasu Valleys (Emre et al. 2008). Emre et al. (2008) concludes that no Quaternary units were observed along the fault and due to intensive landslides; it was not possible to collect geomorphological data on the activity of the fault.

Table 3.6: Segments and Characteristic Properties of Erikli Fault

Segment	Length (km)	Width (km)	Slip Rate(mm/y)	Mchar (Mw)
Yenikonak	24	5	1.2-2.2	6.2
Erfelek	24	5	1.2-2.2	6.2
Gerze	40	5	1.2.-2.2	6.4
Alaçam	45	5	1.2-2.2	6.5

Proper modelling of the Erikli Fault for PSHA is quite challenging due to the contrary views of the experts on the activity of the Erikli Fault and very limited seismic activity. Emre et al. (2008) argued that the Erfelek Segment is a tectonically active structure, however did not classify the Yenikonak Segment as "active" due to the widespread landslide activity. Moreover, Holocene term based inactivity definitions of Emre et al. (2008) does not satisfy the activity definitions of TAEK,

US-NRC and IAEA. As mentioned before, Kaymakçı (2009) proposed that the Erikli Fault needed to be classified as inactive normal fault therefore, the mechanism of the fault (normal or thrust) is also a matter of debate. Based on the limited information, Erikli Fault is modeled as a planar source and the Youngs and Coppersmith (1985) composite magnitude distribution model is employed using the regional b-value of 0.71. All 4 segments of the fault are included in the rupture model. However, different scenarios considering the activity of this source are provided and discussed in Chapter 5.

3.2.9 Balıfakı Fault

Balıfakı Fault is the northernmost onshore tectonic structure in the region and approximately 16 km away from the Sinop NPP site (Figure 3.10). It is a south dipping, E-W striking thrust fault parallel to the Erikli Fault. Both the east and the west portions of the fault extend off-shore under the waters of the Black Sea. The only onshore portion is a 30 km long segment passing through the center of the Sinop Peninsula (Emre et al. 2008). Based on the seismic profiles in Ayancık Bay, no faulting was observed on the erosional surfaces of the Last Glacial Period; therefore, Emre et al. (2008) concluded that no earthquakes with surface ruptures were occurred on the Balıfakı Fault in the last 18000 years. Comparison of ages of undisturbed thick terrace deposits with known marine terraces shows that no surface rupture is occurred between late Pleistocene to Recent in the same study. Therefore, the Balıfakı Fault is classified as inactive fault (Emre et al. 2008).

A micro seismicity study conducted in the region between 2006 and 2008 indicated serious seismic activity in the micro scale. As shown in Figure 3.12, best fit of the location of the epicenters coincides with the possible offshore extension of Balıfakı Fault (Ergin et al., 2008). Holocene (10kyear) based inactivity proposal of Emre et al. (2008) in Ayancık Bay falls short to explain the association of this micro seismic activity with Balıfakı Fault. On the other hand, the seismic activity might be associated with the Pontic Escarpment source, therefore a solid opinion is hard to establish.

Even though the inactivity of Balıfakı Fault seems to obey the inactive fault definitions of nuclear regulatory guides in terms of no observed activity in the last several hundred thousand years, it may not satisfy the definition related to the

“association with an active fault” if the Erikli Fault is considered as an active fault. Erikli and Balıfakı Faults resemble each other considering their orientation (strike and dip), low seismicity, and faulting senses are taken into consideration. In this study, Balıfakı Fault was handled as an active tectonic structure only if the Erikli Fault was evaluated as active to satisfy TAEK and US-NRC guidelines. Possible offshore extension of Balıfakı Fault is included in the PSHA as an optional second segment of Balıfakı Fault to explain the off-shore seismicity. The length of this segment is taken as 150 km long, extending northwest linearly by following the best fit of locations of micro seismicity in the region (Figure 3.11, Line B). Focal mechanism solutions of these events given in Figure 3.12 shows normal or strike slip mechanism with normal component. Therefore, it is not logical to extent Balıfakı Fault into Black Sea in scenarios where it is handled as reverse fault. However, to determine the possible effect of this extension in Black Sea, Balıfakı Fault is extended into Black Sea as reverse fault in one alternative scenario provided in Chapter 5. Additionally, different scenarios are considered in terms of the activity of the Erikli and Balıfakı Faults, segmentation of Balıfakı Fault, and the slip rate partitioning between these two parallel structures (see Chapter 5).

Table 3.7: Segments and Characteristic Properties of Balıfakı Fault

Segment	Length (km)	Width (km)	Slip Rate(mm/y)	Mchar (Mw)
Segment-1	30	5	1.2-2.2	6.3
Segment-2	150	5	1.2-2.2	6.9

3.2.10 Ekinveren Fault

Ekinveren Fault is a northwards convex high angle reverse fault, approximately 150 km-long that strikes roughly E-W. The apex of the fault is 60 km away from the Sinop NPP site. Emre et al. (2008) concluded that only the Miocene sequence was cut by the high angle reverse faults in Ekinveren fault zone and Quaternary units were not deformed out of the fault zone although the pre-Miocene sequence was intensely folded and overturned. The Pleistocene and Holocene deposits observed as terrace fills along the fault zone was not cut by the Ekinveren Fault itself. Hence, the Ekinveren Fault was classified as an inactive structure. Inactivity definition of Emre et al. (2008) satisfies the requirements of TAEK, US-NRC and IAEA guidelines; therefore Ekinveren fault was not included in PSHA in this study.

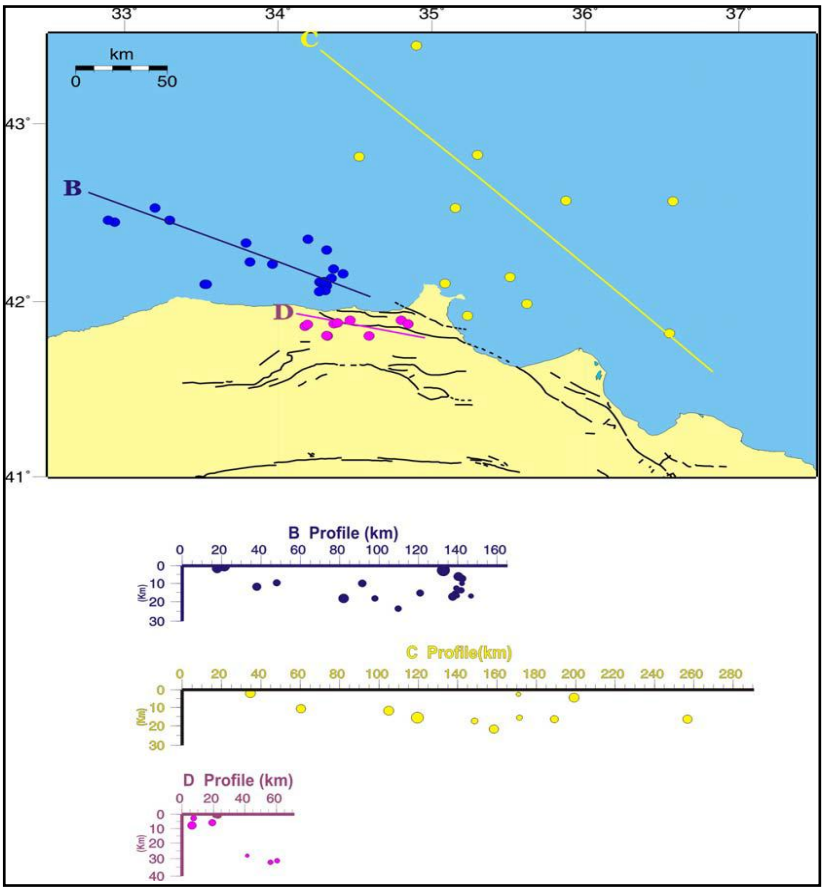

Figure 3.11: Micro Earthquake Study Results Showing Possible Extension of Balıfakı Fault (After Ergin et al. 2008)

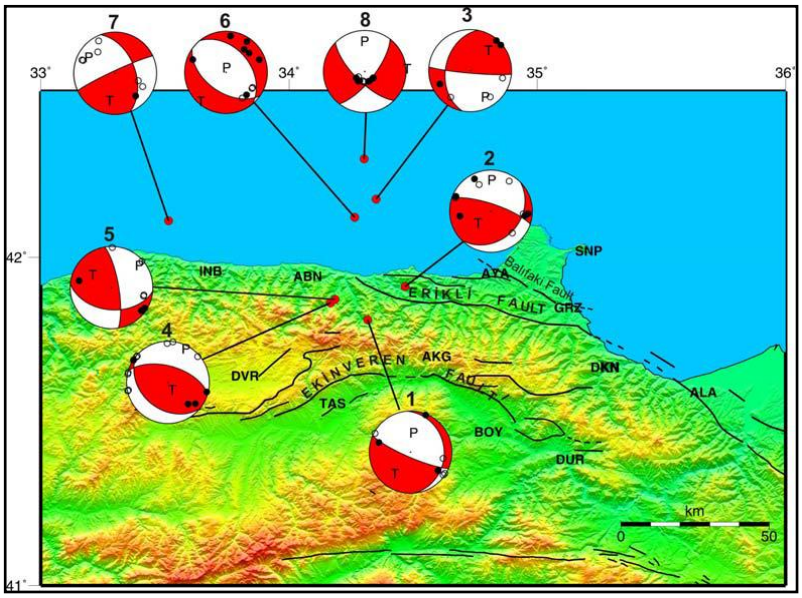

Figure 3.12: First Motion, Lower Hemisphere Focal Mechanism Solutions of Selected Events from P-Wave First Motions (Compressional Quadrant Shaded). (After Ergin et al. 2008)

3.2.11 The Pontic Escarpment

The continental slope delimiting the southern margin of the Black Sea is known as the Pontic Escarpment. Its tectonic importance for the Sinop NPP was first recognized by Doyuran and Erdik (1983) due to its possible connection with the 3 September 1968 Ms=6.8 Bartın Earthquake (Kaymakçı, 2009). The 1968 Bartın Earthquake is the only large event that can be associated to the Pontic Escarpment with recorded strong ground motions. Although there are strike-slip focal mechanism solutions for Bartın Earthquake (Jackson and McKenzi 1984, Kudo 1983, Şengör et al. 1983); Pontic Escarpment is generally regarded as a reverse fault based on the reverse mechanism solutions and the prominent slope of the structure (Doyuran and Erdik 1983, Barka et al. 1985, Erdik et al. 1990).

Profiles that generally indicate quite widespread mass movements in shallow seismic profile surveys conducted by MTA in 2007 (Emre et al., 2008). Emre et al. (2008) underlined that the continental slope of the southern Black Sea may correspond to a north verging thrust zone and may be handled as a major tectonic zone between the Black Sea basin and Pontic uplift based on the interpretations of obtained seismic profiles. The Pontic escarpment corresponding to Black Sea continental slope is evaluated as a capable fault by Emre et al. (2008). On the contrary, Kaymakçı (2009) stated that these thrust zone delineations are misleading and were based on no real data. In addition, seismic reflection studies carried out by Turkish Petroleum Company (Güney, 2008) indicated that the southern continental slope of the Black Sea basin (so called Pontic Escarpment) is dipping northwards in contrary to Emre et al. (2008) and Doyuran and Erdik (1983).

In 2008, a detailed report was prepared for the assessment of seismic activity in the region by an expert from Turkish Petroleum Company (TPAO) submitted to TAEK in 2008. According to Güney (2008), based on seismic reflection studies in the region, two phases are distinguished in Central Black Sea Region; while the Eoecene clastics are highly deformed, Miocene clastics are overlapping the older sequences with a more gentle dip. It is also stated in the report that these compressional deformations were sealed by the Late Miocene deposits. Based on these interpretations, Güney (2008) stated that the thrust faults in the offshore and onshore Central Black Sea - Sinop area are not active, they lost their activity through the geological times, and these paleo thrust faults do not propose a risk of earthquake

affecting the Sinop NPP site. Güney (2008) concluded that recent small scale extensional tectonic structures are active especially in the offshore area and there are many normal faults in character and are oriented in NE-SW direction which could be the only risk to build a Nuclear Power plant in the region.

Similar to the Erikli Fault, experts have different opinions about the activity of the Pontic Escarpment and its mechanism. However, Pontic Escarpment is the closest tectonic structure to the Sinop NPP that may affect the design in many aspects, ground motions, deformations, etc. An areal seismic source is defined for the seismicity around the Pontic Escarpment as shown in Figure 3.13. Because the Pontic Escarpment has not been mapped by MTA (2012) yet, an areal source following the continental slope (-400 m bathymetry) in South Black Sea shore was used to define the source geometry. Considering the 1968 Bartın Earthquake, the maximum magnitude was selected as Mw=6.5 and truncated exponential magnitude distribution model was employed. Again, reverse mechanism was assigned to the areal source to obtain the largest ground motions. However, in sensitivity analyses both the reverse and normal fault mechanism solutions are checked. To calculate the b-value specific to this areal source, a buffer zone was constructed that includes the events in between 30^{o} – 39^{o} north longitudes which can be associated to this structure (Figure 3.12). Previously calculated catalog completeness intervals were used and the area specific b-value was found to be 0.69 (Table 3.8). Different scenarios were considered in terms of the activity of the Pontic Escarpment Zone in Chapter 5.

Table 3.8: "b" Value for Pontic Escarpment Areal Source

Lower Bound	Upper Bound	Magnitude	# of events	Complete time intervals	Rate	RxM
4.0	4.2	4.1	2	50	0.04	0.16
4.2	4.4	4.3	4	50	0.08	0.34
4.4	4.6	4.5	7	50	0.14	0.63
4.6	4.8	4.7	3	88	0.03	0.16
4.8	5.0	4.9	7	88	0.08	0.39
5.0	5.2	5.1	1	113	0.01	0.05
5.2	5.4	5.3	3	113	0.03	0.14
5.4	5.6	5.5	1	113	0.01	0.05
5.6	5.8	5.7	0	113	0.00	0.00
5.8	6.0	5.9	0	113	0.00	0.00
6.0	6.2	6.1	1	113	0.01	0.05
Σ		Total:	38	Total:	0.43	1.98
					$\overline{M}$ =4.63	
					b Value=0.69	

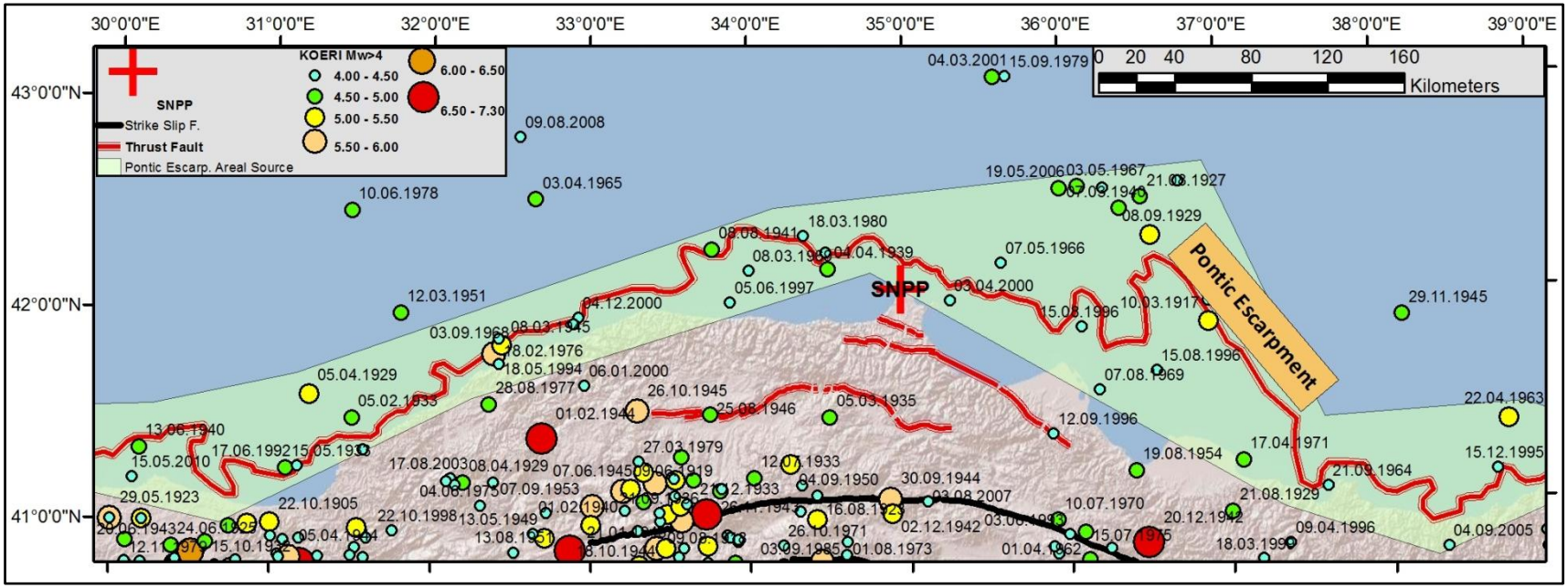

Figure 3.13: Pontic Escarpment Areal Source and the Regional Seismicity

3.3 Sensitivity Analysis

In the PSHA framework, several assumptions and/or simplifications are made to model the complicated nature of seismic source zones. The PSHA analyst has to choose the most realistic and the most appropriate geometry and magnitude recurrence model for each seismic source and then accurately determine the model parameters such as the b-value, slip rate and characteristic earthquake magnitude. These choices may have a great influence on the hazard outcome depending on the sensitivity of the PSHA results to source characterization parameters and the location of the analyzed site with respect to the seismic sources (Vakilinezhad et al., 2013). Determination of the parameters and their uncertainty that contribute to the seismic hazard is the most useful preliminary step for the construction of logic trees. In order to quantify the effect of source characterization parameters on the final hazard outcome, a series of sensitivity analysis are conducted for each source for the annual slip rate, b-value, fault width, dip angle, source mechanism and maximum magnitude and the results were presented in this section.

3.3.1 Sensitivity Analysis for the Pontic Escarpment Source Zone

Being the closest structure to the Sinop NPP site, the Pontic Escarpment Source Zone has the largest effect on the design ground motions. As presented in Section 3.2.11, this source was modeled with an areal zone and the truncated exponential magnitude distribution model was employed. The maximum magnitude was selected as 6.5 and the b-value was calculated as 0.69. The effect of these two important parameters is evaluated by comparing the hazard curves for different M_{max} and b-values as shown in Figure 3.14 (a) and (b). For the sensitivity analysis of this structure, other seismic sources are excluded to isolate the effect of the particular source and all other parameters are held fixed except for the evaluated one. As Figure 3.14(a) depicts, the hazard values increase as the b-value increases, since the rate of small magnitude events decreases. The variation in the b-value changes the peak ground acceleration (PGA) approximately around 0.10 g for 10.000 year return period. The M_{max} for this source was taken as Mw=6.5 to be consistent with the 1968 Bartın Earthquake. Effect of an increase in the M_{max} value on the hazard outcome is observed for all risk levels. Effect of the assigned mechanism to the Pontic Escarpment Source Zone was evaluated by changing the mechanism and the dip angle of the source fault (Figures 3.14 (c) and (d)). If the style of faulting was taken as “normal” instead of “reverse”

(as discussed by Kaymakçı, 2009) the hazard value would have been 0.05 g lower for 10.000 year return period (Figure 3.14(c)). The hazard curve is not sensitive to the dip angle for reverse fault mechanisms as shown in Figure 3.13(d).

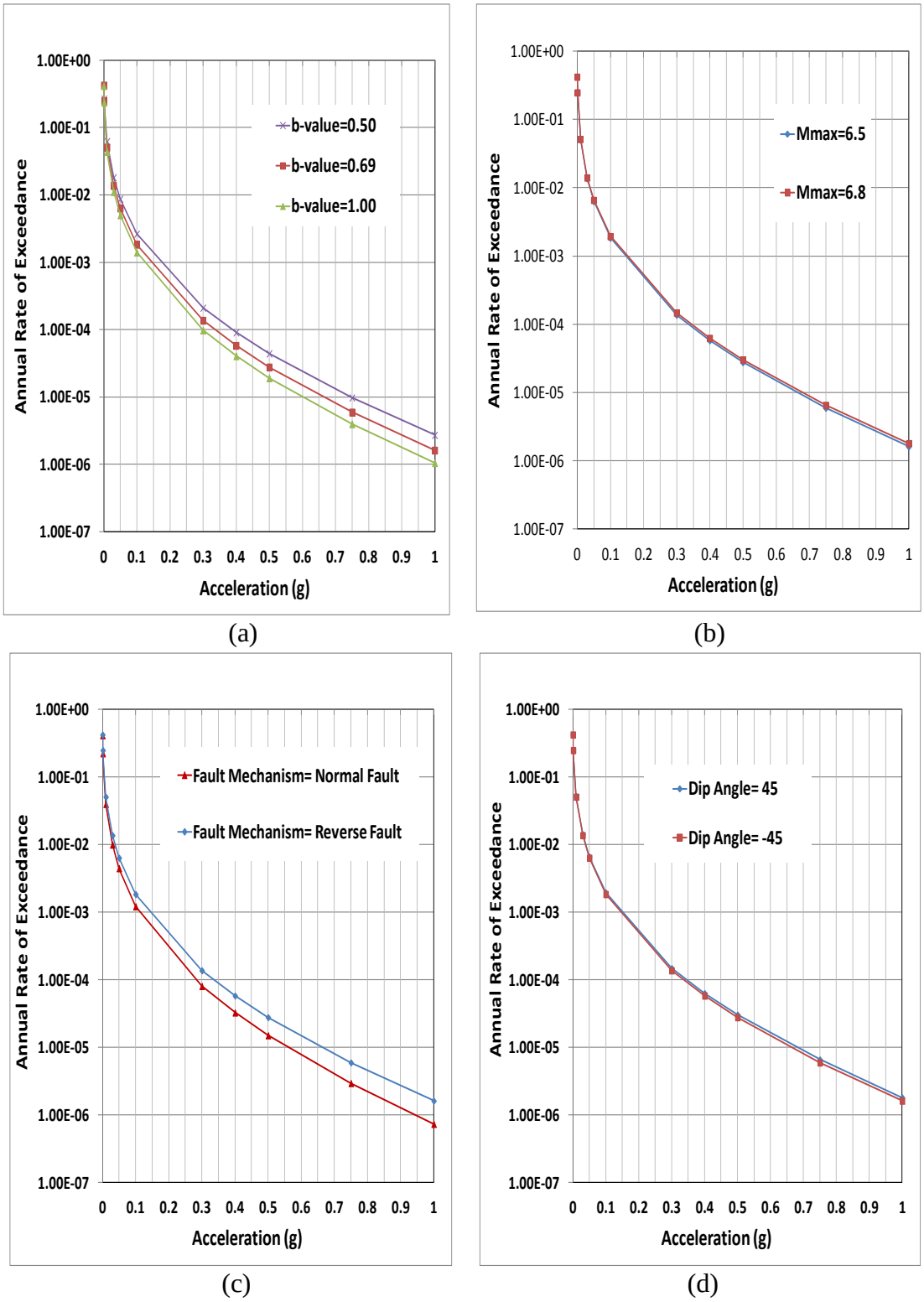

Figure 3.14: Results of Sensitivity Analyses for the Pontic Escarpment Source Zone (all other sources are excluded in these analyses)

3.3.2 Sensitivity Analysis for the Balıfakı and Erikli Faults

The Balıfakı Fault is modeled as a planar source with composite magnitude distribution model. The regional b-value (0.71, Table 3.4) is employed in the magnitude recurrence model. Figure 3.15(a) shows that the effect of the b-value is visible in the small hazard levels. However, the hazard curve is insensitive to the changes in the b-value at the risk levels in engineering interest.

The effect of fault length for Balıfakı Fault is not that effective on the hazard outcome as it is imagined. When the 150 km length of the second segment is taken in to consideration (two-segment rupture model in Figure 3.15b) the difference in the PGA is approximately 10% when compared to one segment scenarios for 10.000 year return period.

If the slip rate is changed from upper bound rate to half of it (1.1 mm/y), PGA decreases around 15 % for 10.000 year return period (Figure 3.15c). This observation indicates that the determination and verification of the slip rate in millimeter sensitivity is of vital importance if Balıfakı and Erikli Faults are active. On the other hand, finding the direction of the movement will also be very useful in determining the regional tectonic regime, which is another important source of uncertainty. For Balıfakı Fault, changing the fault mechanism from "reverse" to "normal" changes the PGA around 20 % for 10.000 year return period.

The effect of dip angle is not significant as shown in Figure 3.15d. They converge to the same value for low rate of exceedance levels. There is no study in the region that claims that the Balıfakı or Erikli fault could be dipping northwards. All the studies in the region argued that these two faults are dipping southwards and the main discussion on these faults is their activity and character (if they are normal or reverse, and what is the component of lateral i.e. strike-slip motion) Therefore, the case for north dipping scenario of the Balıfakı or Erikli faults is not evaluated in this study.

The effect of width of the fault was also observed to be significant. By changing the width of the fault from 5 km to 10 km, 5 % increase in PGA value was observed in the analysis for 10.000 year return period. The variability of width of the fault is less important when compared with other parameters.

The sensitivity analysis for Erikli Fault is presented in Figure 3.16. Similar to Balıfakı Fault, the effect of b-value and dip angle is insignificant (Figure 3.16a&d).

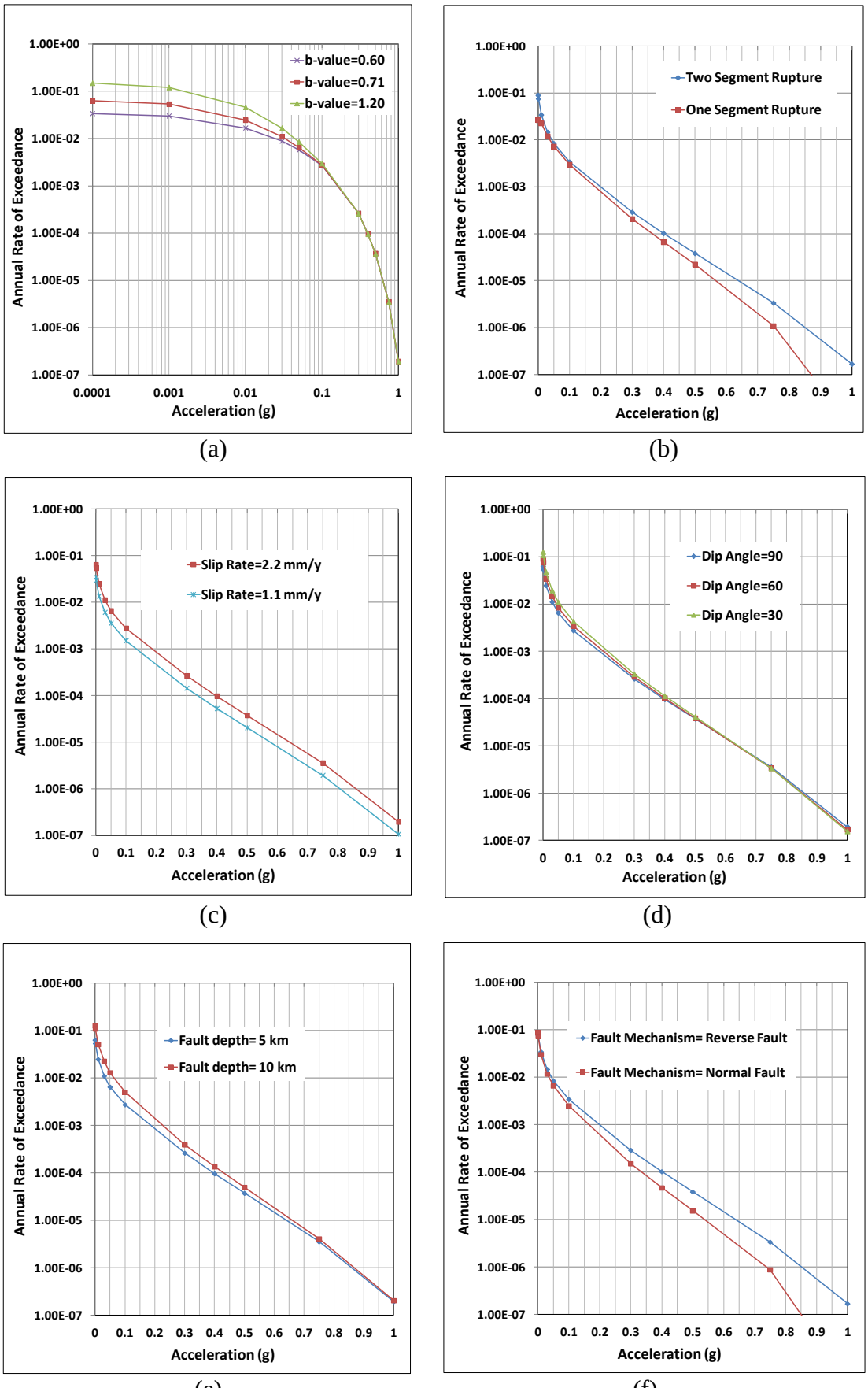

Figure 3.15: Sensitivity Analyses Results of Balıfakı Fault (all other sources are excluded in these analysis)

The effect of slip rate, fault mechanism and fault width is more significant. Figure 3.15c shows that the analyses carried out by using 2.2 mm/y slip rate value results in 10% higher PGA than the case where slip rate is taken as 1.2 mm/y for 10.000 year return period.

Source mechanism is one of the most important parameters for Erikli and Balıfakı Faults in PSHA framework. Although there is a consensus similar to Balıfakı Fault that Erikli Fault is a reverse mechanism source; if the region is under relaxation as proposed by Güney (2008) and Kaymakçı (2009), Erikli Fault may have an inverted character with normal fault mechanism. It is observed that PGA decreases around 17 % for normal fault source mechanism case when compared to the reverse fault mechanism solutions. The effect of the width of the fault is also significant. By changing the width of the fault from 5 km to 10 km, 10 % of increase in the hazard outcome was observed.

3.3.3 North Anatolian Fault and Splays

The first set of sensitivity analysis was conducted to evaluate the effect of the b-value for the source characterization of NAF. In the analysis, b-value was varied within the range of 0.6 and 1.2 and the hazard curves were compared with the base case hazard curve where the b-value is taken as 0.71. The effect of b-value is found to be negligible for all return periods that may be important for engineering interest (Figure 3.17a) for the NAF main strand (Figure 3.18a) and for Merzifon-Esençay Segment.

Secondly, the effect of slip rate is evaluated (Figure 3.17b) by: i) assigning all the slip to the Merzifon-Esençay Segment (green line), ii) assigning all the slip to the NAF-Main strand (blue line), iii) assigning all the slip to the NAF-Main strand and increasing the slip rate to 25 mm/year (dark blue line) and iv) applying the slip rate partitioning defined in Section 3.2.4 (red line). Using a homogenous 21 mm/y slip rate for NAF-main strand increases the PGA for 6 to 7 percent at 10.000 year return period. Increasing it to 25 mm/y slip rate also increases the PGA value around 9-10 % at 10.000 year return period. In addition, if 21 mm/y slip rate is assigned to Merzifon Esençay Fault, which is shorter and further away from the site, the PGA comes out to be 0.09 g (Figure 3.17b). These results show that even if significant uncertainties are involved in assigning slip rates and attributing weights to individual scenarios, the effects of these uncertainties are not that significant when compared to the effect of the sources in the North of NAF.

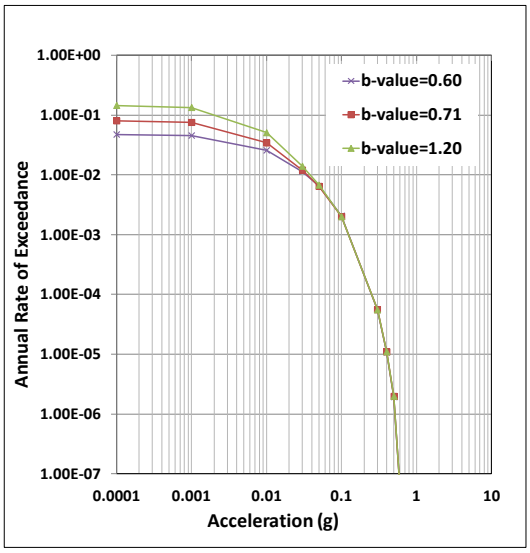

(a)

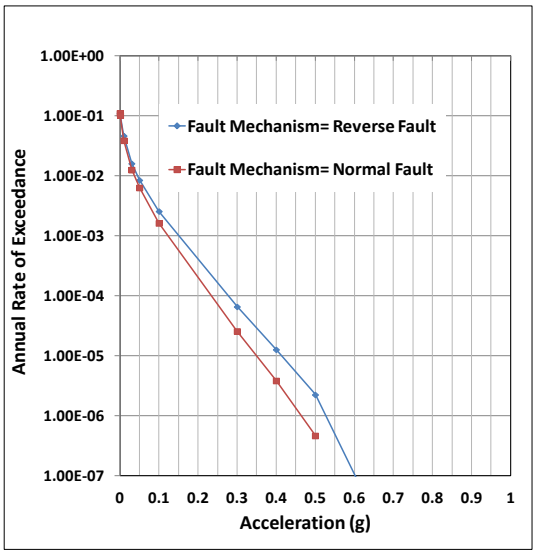

(b)

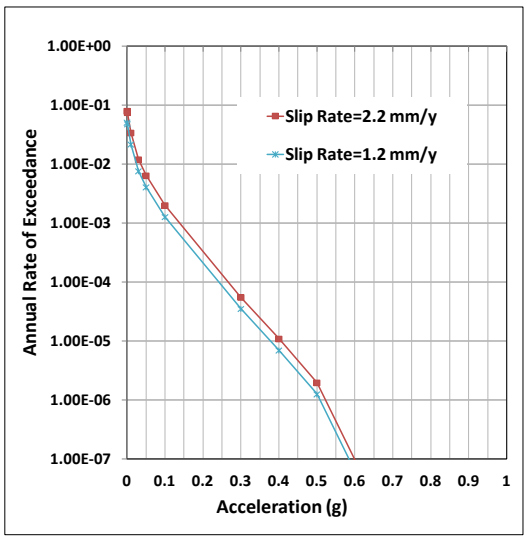

(c)

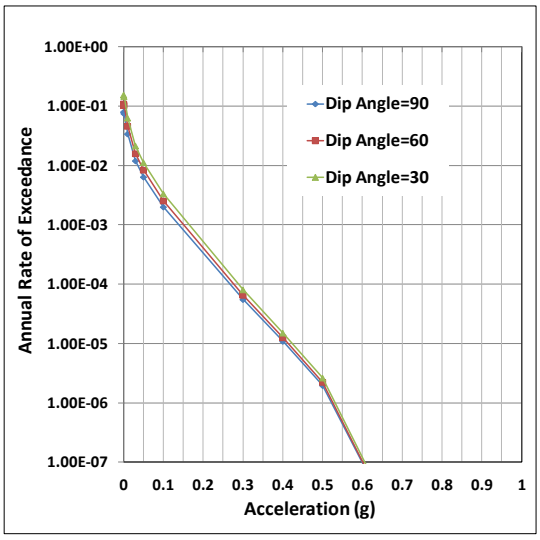

(d)

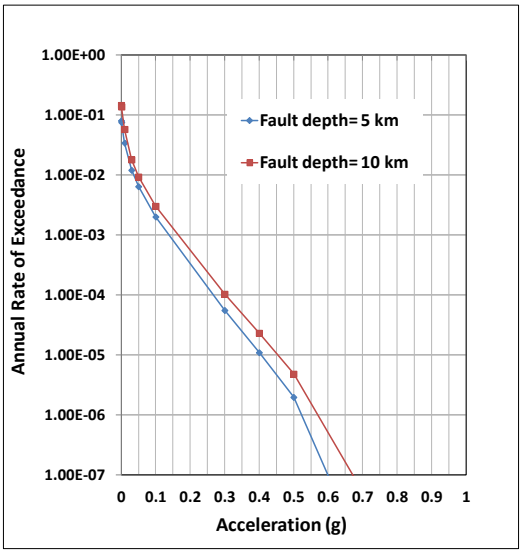

(e)

Figure 3.16: Sensitivity Analyses Results of Erikli Fault (all other sources are excluded in these analysis)

The effect of the slip rate on the hazard curve is investigated by changing the slip rate within reasonable limits for Merzifon Esençay Fault Zone (3 mm/y to 9 mm/year) and the hazard curves are compared with the base case hazard curve. Increasing the slip rate 3 mm/y increases the PGA 10 % and taking slip rate as 3 mm/y instead of 6 mm/y reduces PGA 20 % for 10000 year of return period (Figure 3.18b).

NAF is well studied, it is mature and predictable; and there is very small room for epistemic uncertainty owing to the previously conducted studies. By the help of sensitivity analysis it can be concluded that these epistemic uncertainties do not cause significant amount of change in terms of PGA value. For this reason future site studies should be concentrated on the remaining sources.

3.3.4 Areal Source on the South

Similar to Merzifon-Esençay Fault, the Areal Source defined below this strand is also far away from the Sinop NPP to create a significant impact on the hazard. To investigate the sensitivity of seismic hazard results to the selected maximum magnitude event, the base case is compared with Mmax=6.0 and Mmax=7.0 (Mw) and PGA is observed to change by 50 % for 10000 year of return period (Figure 3.19b). Sensitivity analysis is also conducted to evaluate the effect of the b-value and it is changed within the range of 0.5 and 1.2. The effect of b-value is very prominent and PGA is almost tripled when the tails of the hazard curves are compared.

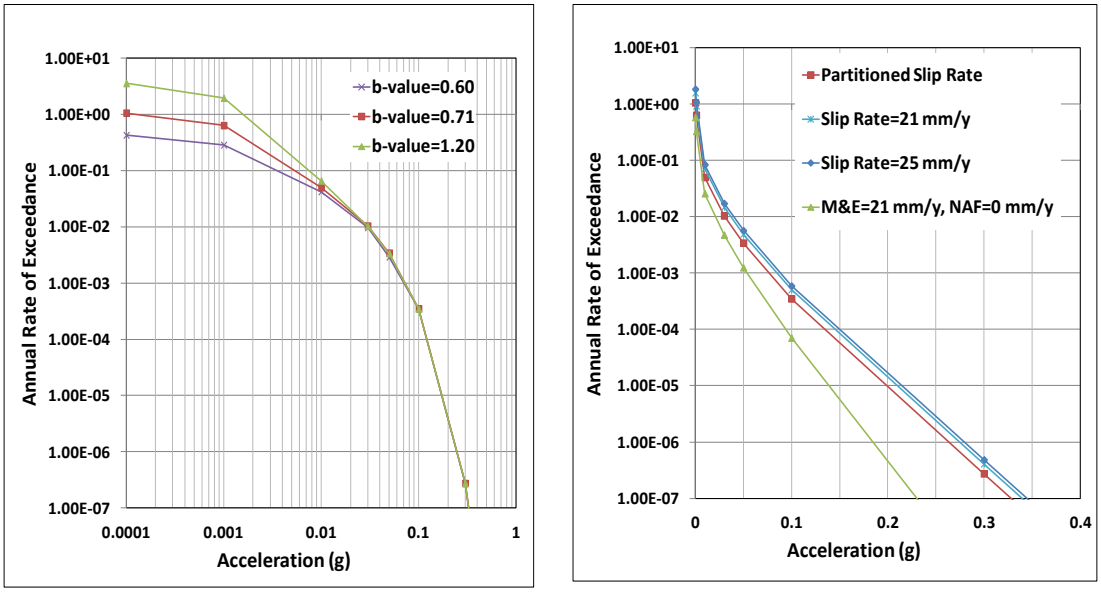

(a) (b)

Figure 3.17: Sensitivity Analyses Results of North Anatolian Fault Main Strand (all other sources are excluded in these analysis)

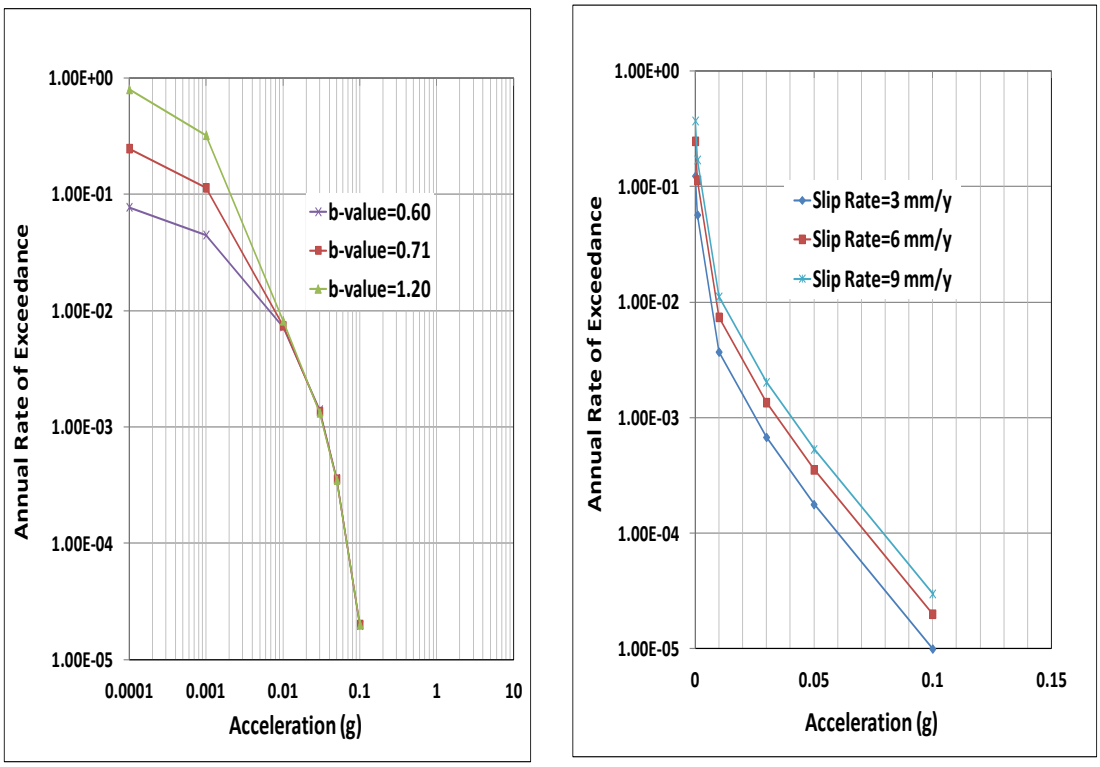

(a) (b)

Figure 3.18: Sensitivity Analyses Results of Merzifon-Esençay Fault (all other sources are excluded in these analysis)

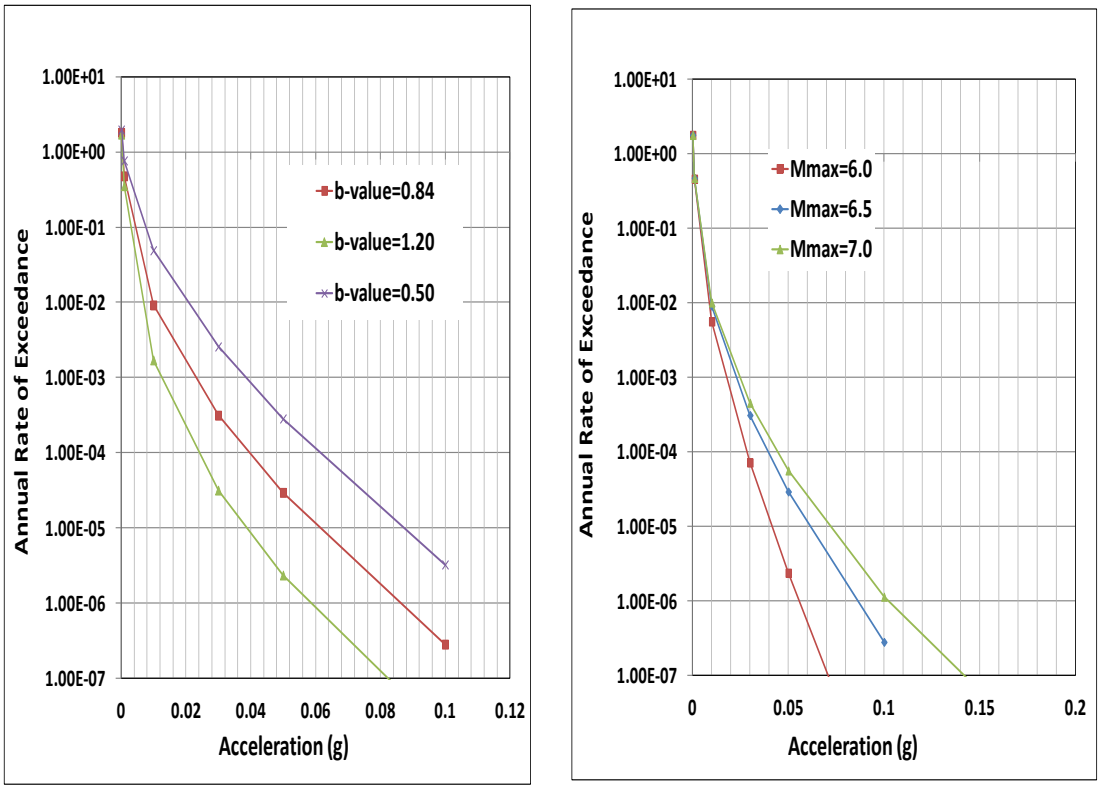

(a) (b)

Figure 3.19: Sensitivity Analyses Results of Areal Source (all other sources are excluded in these analysis)

Chapter 4

4. GROUND MOTION CHARACTERIZATION

Ground Motion Prediction Equations (GMPEs), or commonly known as attenuation relationships, provide a tool for predicting the level of ground shaking and its associated uncertainty at any given site or location based on an earthquake magnitude, source-to-site distance, local soil conditions, fault mechanism, etc. GMPEs are efficiently used to estimate the strong ground motion due to earthquake scenarios from each source in both deterministic and probabilistic seismic hazard analysis for peak ground motion values and elastic response for various spectral ordinates. However, despite their well proven capabilities to predict the level of hazard, GMPEs introduce the biggest uncertainty in the hazard calculations and they have a significant effect on the total hazard at the site (Yılmaz, 2008). As national, regional and global databases of strong-motion records expand, more and more GMPEs are derived, each time better constrained by the available data. Therefore, proper selection of ground motion prediction equations among the global and regional alternatives is one of the important steps in PSHA.

Constructing the GMPE logic tree for PSHA applications is a controversial issue. Sticking only to the global or local models may create a bias on the results since each group has its own advantages and disadvantages. Local GMPEs are developed from the regional databases; therefore, they are expected to reflect the regional differences better than the global models. However, local models generally do not extrapolate well to the larger magnitude events because of their smaller dataset. Due to their smaller data sets when compared to the global GMPEs, regional models may not constrain some important features such as short distance and style of faulting scaling or hanging wall effects that are represented in global models effectively. These models can create illusion of precision while actually adding considerable uncertainty because of the problems associated with extrapolation of magnitude scaling determined mainly from smaller events (Bommer et al., 2010). On the other hand, global models may not represent the regional differences as good as local

models and the applicability of the global models for the target region should be evaluated before implementing them in the PSHA framework.

Stafford et al. (2008) explored the level of agreement between the global pan-European and Next Generation Attenuation (NGA) GMPEs and showed that the NGA models, derived using global data for application in California are applicable for the seismic hazard estimation of shallow crustal active seismic regions in Europe. On the opposite side, Bommer et al. (2010) claimed that there might be considerable differences between the global European and NGA ground motion models for some particular earthquake scenarios. Recent studies by Scasserra et al. (2009), Shoja-Taheri et al. (2010), and Bradley (2013) tested the applicability of the NGA-W1 GMPEs for Italy, Iran, and New Zealand. Findings from these recent studies indicate that the differences between the regional datasets and NGA models exist; however, these differences may be corrected by small adjustments at the NGA models. Akkar and Çağnan (2010) mention that one way of accounting for the epistemic uncertainty in determining the regional seismic hazard levels could be the utilization of both region-specific and global GMPEs.

Gülerce et al. (2014) introduces another alternative to local and global GMPEs by regionalizing the global GMPEs that are developed for the same tectonic region as the target area. The compatibility of the NGA-W1 GMPEs in terms of magnitude, distance and site effects scaling with respect to the Turkish strong ground motions were evaluated by Gülerce et al. (2014) and incompatibilities between the NGA-W1 GMPEs and Turkish strong motion dataset were systematically modified. Based on the modifications, a new set of Turkey-specific versions of the NGA-W1 GMPEs, the TR-Adjusted NGA-W1 models are proposed.

Within the content of this chapter, a brief summary of the candidate GMPES for ground motion characterization of Sinop NPP site is provided. The NGA models, TR-adjusted versions of these models by Gülerce et al. (2014), and the local prediction model developed by Akkar and Çagnan (2010) are included in the list of candidate models. Median spectral values from the candidate models and hazard curves are compared and some of the candidate models are eliminated using the selection criteria proposed by Bommer et al. (2010) and Stewart et al. (2013). Final set of selected GMPEs, and the weights assigned to each model in the logic tree is discussed at the end of this chapter.

4.1 Candidate Ground Motion Prediction Equations

The candidate GMPEs considered for this study are: the NGA models proposed by Abrahamson and Silva (2008), Boore and Atkinson (2008), Campbell and Bozorgnia (2008), Chiou and Youngs (2008) and Idriss (2008), local GMPE prosed by Akkar and Çağnan (2010), and the TR-Adjusted versions of NGA models proposed by Gülerce et al. (2014). A brief summary for each candidate model is provided below.

4.1.1 Akkar and Çağnan (2010) Model (AC10)

The GMPE proposed by Akkar and Çağnan (2010) used the newly compiled Turkish ground-motion database (TSMD) by Akkar et al. (2010). Authors selected 1259 records from 573 earthquakes from the TSMD within the moment magnitude and source-to-site distance ranges of $3.5 \leq M \leq 7.6$ and 0 km $\leq$Rjb $\leq$ 200 km. The majority of the selected ground motions are recorded at Type-C (360 m/s $\leq VS_{30} <$ 760 m/s) and Type-D (180 m/s $\leq VS_{30} <$ 360 m/s) sites according to NEHRP (National Earthquake Hazards Reduction Program) classification. On the other hand, the comfort zone for the proposed model (or range of validity) is 0–200 km and $5 \leq M \leq 7.6$. Therefore, only 433 strong motions from 137 events (consisting of 102 main shocks with 346 recordings and 35 aftershocks with 88 recordings) were utilized in the regression analysis. Authors considered the effects of nonlinear soil behavior and style of faulting in addition to the basic magnitude and distance scaling as given in Equation (4.1).

$$\ln(Y) = a_1 + a_2(M - c_1) + a_4(8.5 - M)^2 + (a_5 + a_6(M - c_1))\ln\sqrt{R_{jb}{}^2 + a_7{}^2} + a_8F_N + a_9F_R + F_S \quad \text{For } M \leq c_1 \tag{4.1}$$

$$\ln(Y) = a_1 + a_3(M - c_1) + a_4(8.5 - M)^2 + (a_5 + a_6(M - c_1))\ln\sqrt{R_{jb}{}^2 + a_7{}^2} + a_8F_N + a_9F_R + F_S \quad \text{For } M > c_1 \tag{4.2}$$

where Y is median spectral acceleration, M is moment magnitude, R_{jb} is Joyner-Boore distance, F_N and F_R are dummy variables used for defining style-of faulting, F_S is site response function and a_1 and a_9 are the model coefficients calculated in regression analysis. The functional form for the base model is adopted from the Abrahamson and Silva (1997) model, but Joyner and Boore distance (R_{jb}) is implemented to define the source-to-site distance. To model the linear and nonlinear site effects (F_S), the functional form of Boore and Atkinson (2008) model is adopted. Authors preferred to disregard magnitude dependency in sigma.

4.1.2 NGA Ground Motion Prediction Models

Pacific Earthquake Engineering Research Center initiated the NGA Project as an effort to develop new ground-motion prediction relations through a comprehensive and highly interactive research program. It was a multidisciplinary research program and performed between 2004 and 2008. Five sets of ground-motion attenuation models were developed for shallow crustal earthquakes in the western United States and similar active tectonic regions by teams working independently but interacting with one another throughout the development process as outputs. All the models were developed based on the updated PEER strong ground motion database. The database composed of 3551 recordings from 173 shallow crustal earthquakes, ranging in magnitude from 4.2 to 7.9 occurred between 1952 and 2003. The NGA models are valid for the moment magnitude ranges of 5.0 to 8.5 for strike-slip earthquakes and 5.0 to 8.0 for reverse and normal earthquakes. All the equations are valid for a distance range of 0 to 200 km. V_{S30}, average shear-wave velocity in the upper 30 meters of sediments, is used in all models as the parameter for characterizing site effects on ground motions. Earthquake magnitude, style of faulting, depth to top of fault rupture, source-to site distance, site location on hanging wall or foot wall of dipping faults are the other predictive parameters used in the models.

4.1.2.1 Abrahamson & Silva (2008) (AS08) Model

Abrahamson and Silva (2008) selected 2754 recordings of 135 earthquakes including the aftershock events among 3551 recordings from 173 earthquakes. As all other NGA models, AS08 model does not over-saturate at short distances through a magnitude dependent distance slope. It includes the style-of-faulting and hanging-wall factors. To define fault-geometric properties, rupture-depth, depth-to-top of rupture, fault dip angle is utilized. AS08 is applicable to both soil and rock sites and includes nonlinear site amplification factors and soil sediment depth effects. VS_{30} and depth to engineering rock $Z_{1.0}$ are used to model the site effects. Magnitude-dependent standard deviations are used in AS08.

The functional form of the AS08 is as follows;

$$\ln S_a(g) = f_1(M, R_{rup}) + a_{12}F_{RV} + a_{13}F_{NM} + a_{15}F_{AS} + f_5(P\hat{G}A_{1100}, VS_{30}) \quad 4.3$$
$$+F_{HW} f_4(R_{jb}, R_{rup}, R_X, W, \delta, Z_{TOR}, M) + f_6(Z_{TOR}) + f_8(R_{rup}) + f_{10}(Z_{1.0}, VS_{30})$$

where Sa is median spectral acceleration, M is moment magnitude, Rrup is rupture distance, F_{RV} and F_{NM} are dummy variables for faulting style, $PGA_{1100,}$ is the rock peak ground acceleration, VS_{30} is the average shear wave velocity in the top 30 meters, R_{jb} is Joyner-Boore distance, R_{rup} is rupture distance, R_x is the horizontal distance from top edge of rupture, W is fault width, δ is dip angle of the fault plane, Z_{TOR} is depth to top of rupture value in kilometer, $Z_{1.0}$ is depth to V_S=1.0 km/s in kilometers, a_{12}, a_{13} and a_{15} are regression coefficients. f_1 is the base model given in Equation 4.3.

4.1.2.2 Boore & Atkinson (2008) (BA08) Model

Authors of BA08 model did not include the aftershocks in their dataset, therefore used only 1574 recordings from 58 earthquakes. The style of faulting factors were included, however rupture-depth and hanging-wall scaling was not incorporated explicitly in the model. BA08 model is applicable to both soil and rock sites. Nonlinear site amplification factors were included, but soil sediment depth effects were not modeled. VS_{30} was used for site characterization and modeling the nonlinear site effects. The functional form of the BA08 model is given in Equation 4.4 as:

$$\ln Y = F_M(M) + F_D(R_{JB}, M) + F_S(VS_{30}, R_{JB}, M) + \varepsilon\sigma_T \qquad 4.4$$

where Y is spectral acceleration, M is moment magnitude, R_{jb} is Joyner-Boore distance, VS_{30} is the average shear wave velocity of upper 30 m of soil strata. FM, FD, and FS represent the magnitude scaling, distance function, and site amplification respectively. The coefficients were estimated by the help of two stage regression method proposed by Joyner and Boore. The BA08 model has magnitude-independent standard deviations.

4.1.2.3 Campbell & Bozorgnia (2008) (CB08) Model

Similar to the BA08 model, the aftershocks were not included in the dataset of CB08 model; therefore, 1561 recordings from 64 events were included. Style-of-faulting, rupture-depth and hanging-wall factors were employed in the model to constrain fault mechanism effects effectively. V_{S30} and $Z_{2.5}$ (depth to 2500 m/s shear wave velocity) were used to characterize the effects of local site conditions. Fault geometric properties such as depth-to-top of rupture and fault dip angle were incorporated. CB08 model is applicable to both soil and rock sites and includes

nonlinear site amplification factors and soil sediment depth effects. The general form of the equation is;

$$\ln \hat{Y} = f_{mag} + f_{dis} + f_{flt} + f_{hng} + f_{site} + f_{sed} \quad 4.5$$

where Y is median spectral acceleration, f_{mag}, f_{dis}, f_{flt}, f_{hng}, f_{site} and f_{sed}, are functional forms for magnitude term, distance term, style-of-faulting term, hanging wall term, site conditions term and basin response term respectively. The CB08 has magnitude-independent standard deviations.

4.1.2.4 Chiou & Youngs (2008) (CY08)

Similar to the AS08 model, the aftershocks were included in the dataset of CY08 model so 1950 recordings from 125 events were utilized. CY08 model includes style-of-faulting, rupture-depth and hanging-wall factors and considered as the most complex model among the NGA models. This model is applicable both to soil and rock sites and nonlinear amplification was directly derived from the NGA data as part of the regression. VS_{30} and $Z_{1.0}$ were used to define local site conditions. Soil sediment depth effects were also included and magnitude-dependent standard deviation was used in the model. The general form of the ground motion prediction equation is;

$$\ln(Y) = \ln(Y_{ref}) + f_{site}(VS_{30}, Y_{ref}) \quad 4.6$$

Where Y_{ref} is the ground motion on the reference site and f_{site} is the site response function.

4.1.2.5 Idriss (2008) (I08)

The ID08 model only includes the earthquakes that occurred on rock sites (450 m/s<VS_{30}<900 m/s) therefore it has the smallest data set 942 recordings from 72 earthquakes. Rather than using a continuous V_{S30} to resemble site effects, V_{S30} bins were preferred in the model. The I08 model includes the style-of-faulting effects, but rupture-depth, hanging-wall and soil sediment depth factors were not incorporated. To model the uncertainties magnitude-dependent standard deviations are used. The functional form of the model is given by Equation 4.7 as:

$$\ln\left(PSA(T)\right) = \alpha_1(T) + \alpha_2(T)M - \left(\beta_1(T) + \beta_2(T)M\right)\ln\left(R_{rup} + 10\right) + \gamma(T)R_{rup} \quad 4.7$$
$$+\varphi(T)F$$

where M is moment magnitude, R_{rup} is rupture distance, T is the period and F is the style of faulting variable.

4.1.3 Turkey-Adjusted NGA-W1 Horizontal Ground Motion Prediction Models

The TR-Adjusted NGA-W1 GMPEs are introduced as alternative to local and global GMPEs by regionalizing the global NGA models that are developed for the same tectonic region as Turkey. It aims to reflect the regional differences by utilizing the local dataset and to reduce the uncertainties by benefiting the well-constrained pieces of NGA models therefore, only the required pieces of the NGA models were modified for applicability in Turkey.

During the regression analysis the dataset including the ground motions recorded from the earthquakes that occurred in Turkey in the last 50 years are used (TSMD, Akkar et al., 2010). The dataset used for comparison includes 1142 recordings from 288 events. By the help of random-effects regression with a constant term, model residuals between the actual strong motion data and NGA model predictions are calculated for a period range of 0.01-10 seconds. The calculated residuals are used to evaluate the differences in the magnitude, distance, and site amplification scaling between the Turkish dataset and the NGA models.

Inter-event residuals indicated that the ground motions in the dataset are overestimated by all five NGA models. Only small-to-moderate magnitude scaling of the NGA GMPEs is changed in order to preserve the well-constrained large magnitude scaling of the global dataset. No trends in the residuals are observed in the intra-event residuals vs. rupture distance plots up to 100 kilometers; therefore, the distance scaling of the NGA-W1 models is not adjusted. The large distance scaling (between 100 and 200 km) of the AS08 and CY08 models with separate gamma terms are modified (Gülerce et al., 2014). An adjustment in the Vs30 scaling was applied to the AS08 and CY08 models in order to modify the overestimation at the stiff soil/rock sites. The TR-Adjusted NGA models are compatible with the regional strong ground motion characteristics and preserve the well-constrained features of the global models; therefore, these models are suitable candidates for ground motion characterization and PSHA studies conducted in Turkey (Gülerce et al., 2014).

4.1.4 Comparison of the Median Predictions of Candidate GMPEs

The average median response spectra of the NGA models (green lines) and TR-Adjusted NGA models (black lines) are compared for different scenarios in Figure 4.1. Median predictions of Akkar and Çağnan (2010) (AC10) model is given by red lines in Figure 4.1 and 4.2. Figures 4.1(a) and 4.1 (b) show the median predictions

for magnitude 5 and magnitude 7 strike-slip earthquakes at the rupture distance of 10 kilometers for average rock (V_{S30}=760 m/s) conditions, respectively. For the small magnitude scenario provided in Figure 4.1(a), predictions of the TR-adjusted models and AC10 model are very similar indicating that the small-to-moderate magnitude scaling of the Turkish ground motions are captured by the magnitude adjustment function. However, the TR-Adjusted NGA models are significantly lower than the NGA models. The median predictions of the TR-Adjusted models are only slightly different from the NGA models, however a significant difference between the other models and AC10 is observed in Figure 4.1(b); predictions of the TR-adjusted NGA models are very close to the predictions of global models for large magnitudes, but significantly higher than the predictions AC10 model.

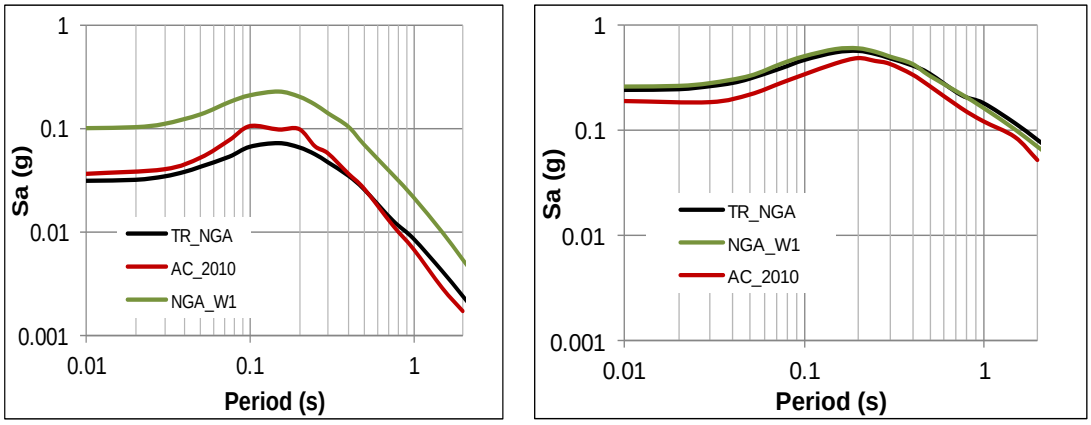

(a) **(b)**

Figure 4.1: Median Predictions of NGA-W1, TR-Adjusted NGA_W1 and Akkar and Çağnan (2010) Models for; (a) M=5, D=10km, V_{S30}=760 m/s, (b) M=7, D=10km, V_{S30}=760 m/s.

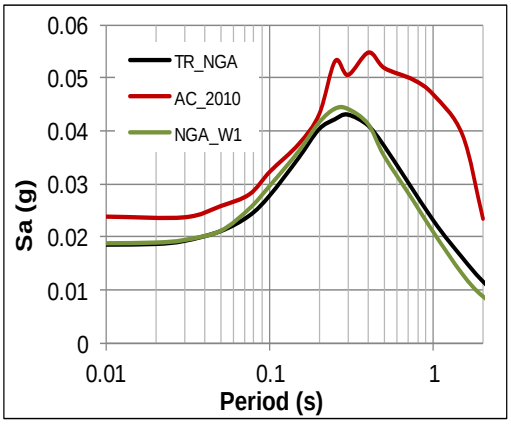

Figure 4.2: Median Predictions of NGA-W1, TR-Adjusted NGA_W1 and Akkar and Çağnan (2010) Models for M=7, D=150km, V_{S30}=760 m/s.

For large magnitude events at long distances (M7, D150 km rock conditions provided in Figure 4.2) the TR-adjusted NGA model predictions are quite similar to NGA models in the short period range. Prediction of AC10 model for large magnitudes at large distances are quite different. This difference is related to the constraints in the magnitude scaling from small to large magnitudes; in the TR-Adjusted models the large magnitude scaling is constrained by the global data, whereas in the AC10 model the large magnitude scaling is estimated from the sparse Turkish dataset (Gülerce et al. 2014).

For the Sinop NPP site, all sources within the radius of 320 km should be included in the PSHA analysis and the dominating source, the NAF Zone, is more than 100 km away from the site. Based on the discrepancy in the large distance scaling, the AC10 model is excluded from the GMPE logic tree for the Sinop NPP site.

4.2 Sensitivity Analysis for the Selection of Most Applicable GMPEs

To evaluate the effect of used GMPEs on the hazard outcome, all candidate GMPEs except for the AC10 model, are implemented individually in the PSHA framework and the hazard curves are compared through Figures 4.3 to 4.5. For these analyses, all seismic sources defined in Chapter 3 including the NAF Zone, the areal source in the south of NAF, Pontic Escarpment Areal Source Zone, Erikli and Balıfakı Faults (sharing the slip rate of 2.2 mm/y equally) are incorporated. Figure 4.3 compares the hazard curves for T=2.5 sec using the original versions of AS08, BA08, CB08, CY08, and ID08 models (the original versions). Similarly, Figure 4.4 shows the hazard curves for PGA using the TR-adjusted versions of the NGA models. In these analyses, the V_{S30} value of the analyzed site is assumed to be equal to 760 m/s to represent the average rock site conditions (NEHRP B/C boundary).

Figure 4.3 indicates that the hazard curve using the ID08 model is significantly different than the others at long periods. Based on this significant difference, the selection criteria proposed by Bommer et al. (2010), and the necessity of using GMPEs with the equations explicitly include V_{S30} as a predictor variable, the ID08 model is excluded from the ground motion logic tree. Gülerce et al. (2014) pointed out that the mean bias in the median predictions of TR-adjusted ID08 model remains for the long periods even after the adjustment; therefore, the TR-adjusted version of the ID08 model is excluded from the candidate GMPE list along with the original version.

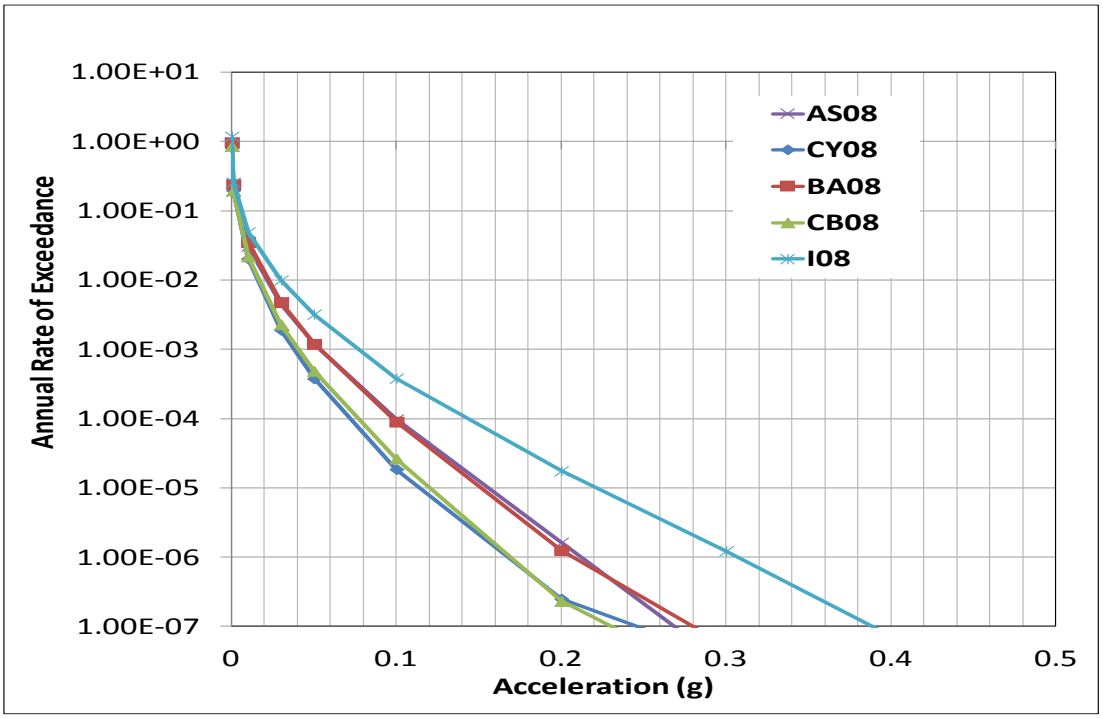

Figure 4.3: Hazard Curves Gives Spectral Acceleration at T=2.5 Sec Based on Original NGA-2008 Models

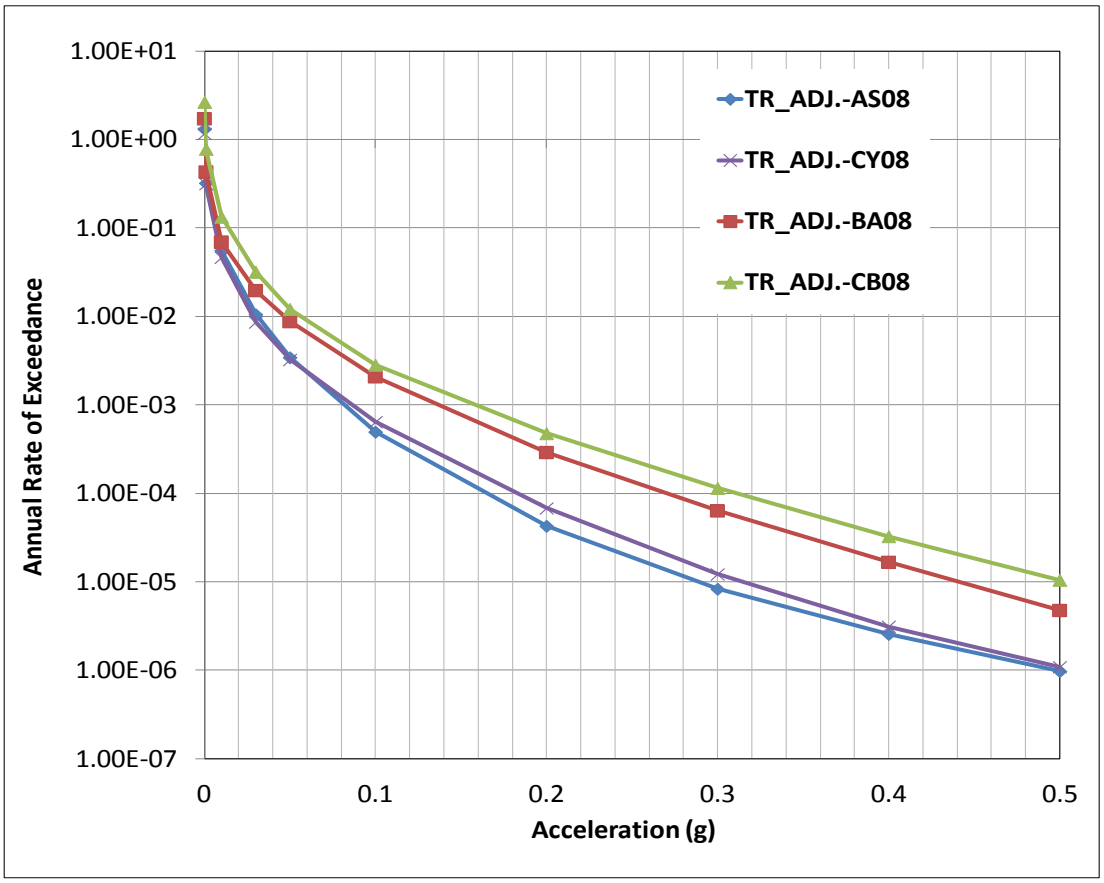

Figure 4.4: Hazard Curves for PGA Using TR_Adjusted NGA Models for Rock Site Conditions (V_{S30}=760 m/s)

When the hazard curves based on the TR-Adjusted NGA models (Figure 4.4) are compared, it is observed that the TR-Adjusted AS08 and TR-Adjusted CY08 models result in very low hazard estimates for rock site conditions (V_{S30}=760 m/s). However for soil site conditions (V_{S30}=270 m/s), this significant difference in hazard curves is not observed (Figure 4.5). For the initial versions of the TR-adjusted NGA models which are implemented in the hazard code HAZ43 (PG&E, 2010), AS08 and CY08 models were adjusted for the trends observed in V_{S30} residuals plots using the solid black line in Figure 4.6(a) (Kargıoğlu, 2012). The adjustment model proposed by Kargıoğlu (2012) results in a significant change in the model predictions for the stiff soil/engineering rock sites based on the overestimation trend for these site conditions. The trends in the residuals for BA08 and CB08 models were negligible so no V_{S30} scaling adjustment was applied to these models. This feature of the TR-Adjusted NGA models was later re-evaluated by Gülerce et al. (2014) and a new adjustment function shown in Figure 4.6(b) was proposed. In the new adjustment function a smooth scaling with V_{S30} is maintained, which does not accommodate the bias in the higher velocity range. Hazard curves based on the final versions of the TR-Adjusted AS08 and TR-Adjusted CY08 models are expected to be higher than the versions shown in Figure 4.4.

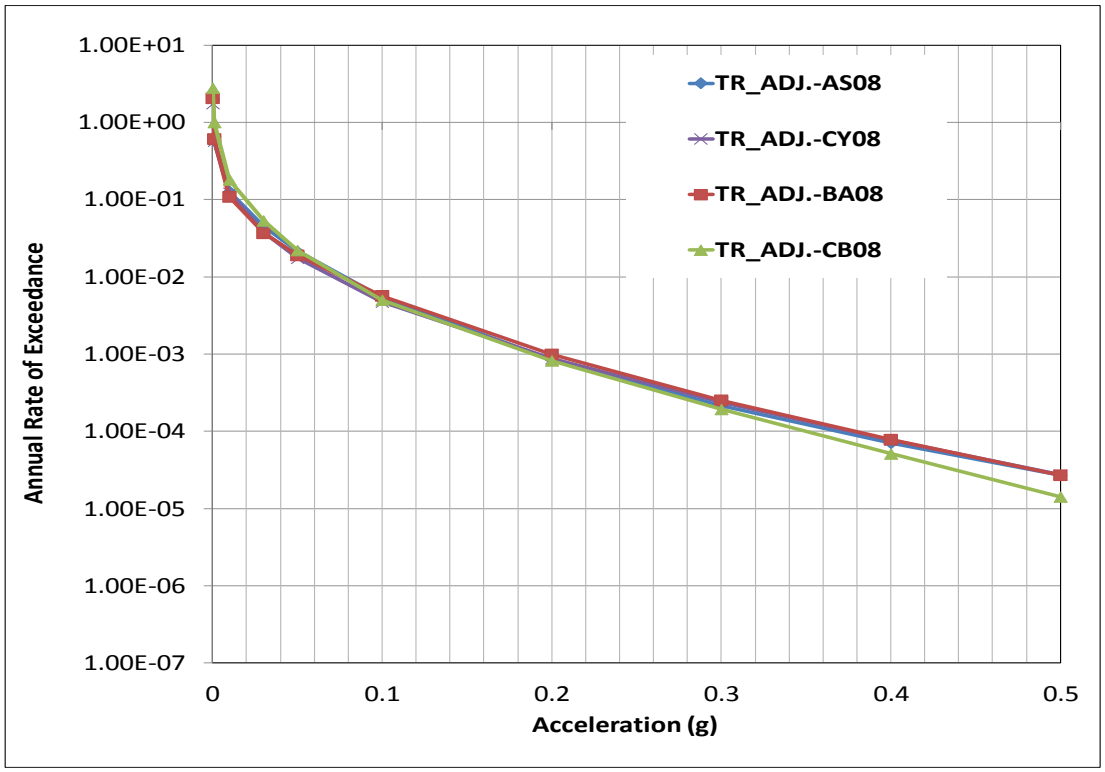

Figure 4.5: Hazard Curves at PGA Using TR_Adjusted NGA Models for Soil Site Conditions (V_{S30}=270 m/s)

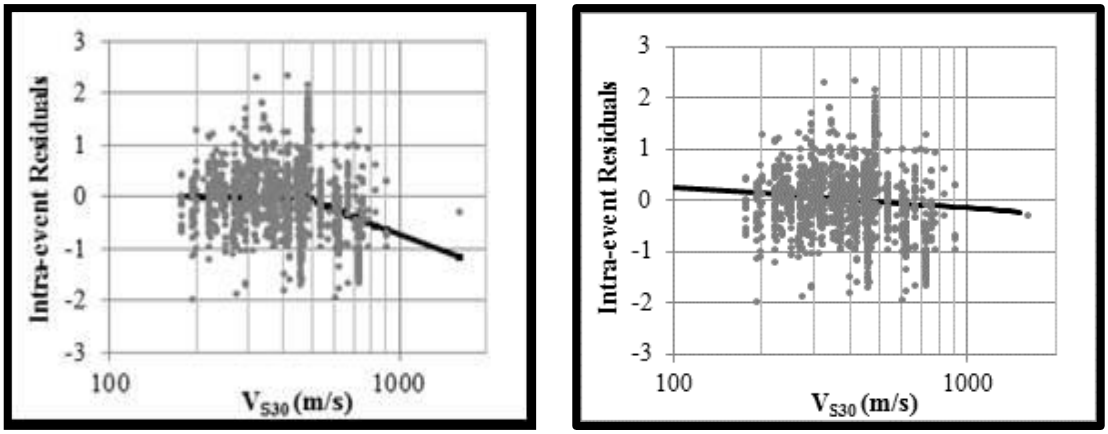

(a) **(b)**

Figure 4.6: Comparison of VS30 Adjustment Functions to the AS08 and CY08 Models by (a) Kargıoğlu (2012) and (b) Gülerce et al. (2014)

Currently, the recent versions of TR-Adjusted NGA models are being implemented into HAZ43, however due to time limitations the TR-Adjusted AS08 and TR-Adjusted CY08 models are excluded from the GMPE logic tree for this study. Remaining four NGA models (AS08, BA08, CB08, and CY08) and two TR-adjusted NGA models (TR-Adjusted BA08 and TR-Adjusted CB08) were used for the ground motion characterization of the Sinop NPP site. Equal weights are assigned to the global models for the first 50 % (12.5% each) and regionalized NGA models shared the remaining 50% equally (25% each).

CHAPTER 5

5. PROBABILISTIC SEISMIC HAZARD ANALYSIS RESULTS AND CONCLUSIONS

5.1 PSHA Methodology and Software

Earthquakes are very complicated natural events that may be predicted by the help of probabilistic approaches. The estimations on the effects of future earthquakes on the structures are mainly used in loss estimation, earthquake resistant design practices, insurance and credit risk premium calculations. For the assessment of design ground motions for a region or a specific site, there are two widely used approaches; deterministic (DSHA) and probabilistic (PSHA). While the PSHA takes into account the effects of all future earthquakes of all possible magnitudes, at all significant distances from the site, DSHA is based on a single earthquake scenario (Yılmaz, 2008). Because earthquakes are random in terms of magnitude and mainly cluster in both space and time, probabilistic approaches are more appropriate for critical structures where decision makers need to compare the taken and allocated risk levels with other natural and human induced phenomenon.

Cornell (1968) proposed a model formulating the probabilistic approach for the computation of the seismic hazard at a site. The basic advantage of this model is the capability of giving the ground motion levels for the corresponding exceedance probabilities. After the pioneering work of Cornell (1968), many other models were proposed to define the temporal, spatial and magnitude distributions of earthquakes which are the basis of current PSHA methodology. In this study, the probabilistic seismic hazard assessment methodology defined by Cornell (1968) and McGuire (2004) is used. In Cornell-McGuire approach, the hazard integral for a single point source is given by:

$$\nu(A>z) = N_{\min} \cdot \int_M \int_R \int_R f_M(M)\, f_R(M,R)\, f_\varepsilon(\varepsilon) P(A>z|M,R,\varepsilon) \times dM \times dR \times d\varepsilon \quad 5.1$$

where R is the distance from the source to the site, M is the earthquake magnitude; N_{min} is the annual rate of earthquakes with magnitude greater than or equal to the

minimum magnitude, $f_M(M)$ and $f_R(M, R)$ are the probability density functions for the magnitude and distance, ε is the number of standard deviations above or below the median, $f_\varepsilon(\varepsilon)$ is the probability density function for the epsilon (given by a standard normal distribution), and $P(A > z \mid M, R, \varepsilon)$ is either 0 or 1. In this formulation, $P(A > z|M, R, \varepsilon)$ selects those scenarios and ground motion combinations that lead to ground motions greater than the test level z. The numerical integration of the hazard integral is performed by the computer code HAZ43 developed by N. Abrahamson (PG&E, 2010). HAZ43 treats the epistemic uncertainties in the source characterization and the GMPEs through use of logic trees. For each source, all combinations of the logic tree branches are evaluated. For the total hazard, Monte Carlo sampling of source characterization uncertainty is used to combine the epistemic uncertainty for each source and full sampling of the GMPEs is used to develop fractals on the total hazard.

5.2 Logic Trees for Seismic Source and Ground Motion Characterization Models

An improved probabilistic seismic hazard assessment was intended to be accomplished by utilization of advanced seismic source models in terms of source geometry and recurrence relationships and application of new ground motion prediction models for this very important structure. The seismic source models were developed for all the sources that lie within the 320 km radius of the Sinop NPP and the details of source characterization models are discussed in Chapter 3. In summary:

- Nearly all faults that are mapped in the latest active fault map of MTA (2012) are adopted in the PSHA analysis with the exception of the Ekinveren Fault. This fault is disregarded in the analysis because the Ekinveren Fault was classified as an inactive structure by both Emre et al. (2008) and Kaymakçı (2009).
- Planar fault segments are defined and composite magnitude distribution model (Youngs and Coppersmith, 1985) is used for the NAF main strand (1942-1943 earthquake rupture zones) and the Merzifon-Esençay Splay to properly represent the characteristic behavior of NAF without an additional background zone. Fault segments, rupture sources, rupture scenarios and fault rupture models are determined using the WGCEP-2003 terminology and multi-segment rupture scenarios are considered. Events in the earthquake

catalogue are attributed to the parallel fault lines and scenario weights are determined by releasing the accumulated seismic energy by the catalogue seismicity on each source.

- The seismic sources on the south of Ezinepazarı Fault, including the splays of NAF Shear Zone and the other small faults (Çankırı, Turhal, Kazankaya, Çekerek and Gökçe Faults) are modelled by a large areal source zone. The areal source model is preferred since the slip rate for the EzSF splay is unknown and the sources are far away from the Sinop NPP site.
- Balıfakı and Erikli Faults are modeled as planar sources based on the interpretations from recent site surveys for the Sinop NPP site (mainly from Emre et al., 2008). Since the site investigations for these tectonic structures are not yet completed, alternative models are considered in terms of fault activity, fault geometry, mechanism and slip rate.
- In addition to the sources mapped by MTA (2012), the Pontic Escarpment Zone, is modeled as an areal source with the help of a buffer zone that follows the -400 m bathymetry line at South Black Sea coast.

Sensitivity of the hazard outcome to the source characterization models is evaluated through series of PSHA analysis with varying source parameters. Analysis results implied that:

- The Areal Source defined below the Merzifon-Esençay Strand is so far away from the Sinop NPP site to create a significant impact on the hazard.
- Even if significant uncertainties are involved in assigning slip rates and attributing weights to individual scenarios for the parallel segments of NAF, the effects of these uncertainties are not that significant on the ground motion levels. NAF is well studied, mature and predictable; there is a small room for epistemic uncertainties but these uncertainties do not turn into a significant change in terms of design ground motions.
- The regional b-value is used for all planar sources and the effect of this parameter is found to be negligible for all return periods that may be important for engineering interest.
- Based on the above interpretations, no uncertainties related to the fault parameters (length, depth, dip, width, maximum magnitude, b-value and slip

rates) are included in the logic tree for the NAF source zone (main strand and Merzifon-Esençay Splay) and the areal source on the south.

- The effect of the fault length for Balıfakı Fault is not that significant on the ground motion levels. If the 150 km long second segment is taken into consideration, the PGA for 10.000 year return period increases around only 10% due to the low slip rate of the fault.
- The fault mechanism has a significant effect on the hazard outcome for the Balıfakı and Erikli Faults. For example, changing the fault mechanism from "reverse" to "normal" decreases the PGA around 20 % for 10.000 year return period for Balıfakı Fault.
- If the slip rate is changed from upper bound rate (2.2 mm/y) to the half of it (1.1 mm/y), 15% decrease in design PGA levels is observed for 10.000 year return period for Erikli and Balıfakı faults. This observation indicates that the determination and verification of the slip rate is of vital importance if Balıfakı and Erikli Faults are considered as active tectonic structures.
- The Pontic Escarpment Source Zone is very close to the candidate site; therefore any changes in the source model (geometry, b-value, etc.) will have a significant impact on the design ground motions.

Based on the sensitivity analysis results, six alternative source models were considered in PSHA. It is notable that the Balıfakı Fault should only be considered as active if the Erikli Fault is active as explained in Section 3.2.9. The main differences among these alternative models are: i) activity of Erikli and Balıfakı Faults, ii) the slip rate partitioning between Balıfakı and Erikli Faults, iii) mechanism of Erikli, Balıfakı and Pontic Escarpment zones, and iv) geometry of the Balıfakı Fault. Details of alternative source characterization models are provided below.

- **Alternative 1:** In this model, Erikli Fault, Balıfakı Fault, and Pontic Escarpment are accepted as inactive structures based on the conclusions of Kaymakçı (2009). Only the NAF main strand, Merzifon-Esençay Fault and the Areal Source on the south are included in the PSHA analysis. No uncertainties related to the model parameters are considered.
- **Alternative 2:** For this model, the NAF main strand, Merzifon-Esençay Fault, the Areal Source on the south, and Erikli Fault are considered as active tectonic structures. On the contrary, Balıfakı Fault and Pontic Escarpment

Zone are disregarded. Based on the sensitivity analysis, variability in the fault mechanism, dip angle, and fault width are considered; therefore three different sub-models are created and provided in Table 5.1.

Table 5.1: Source Model Parameters for Alternative 2

R. Scenario	Source	Slip R.	b-value	Fault M.	Dip A.	Fault D.	Mmax
Alternative 2 (A)	Erikli F.	2.2	0.71	R	60	5	NA
	NAF	Partitioned	0.71	SS	90	16	NA
	Mer.-Esen.	6	0.71	SS	90	9	NA
	Areal S.	NA	0.84	R	60	12	6.5
Alternative 2 (B)	Erikli F.	2.2	0.71	R	45	10	NA
	NAF	Partitioned	0.71	SS	90	16	NA
	Mer.-Esen.	6	0.71	SS	90	9	NA
	Areal S.	NA	0.84	R	60	12	6.5
Alternative 2 (C)	Erikli F.	1.2	0.71	N	60	5	NA
	NAF	Partitioned	0.71	SS	90	16	NA
	Mer.-Esen.	6	0.71	SS	90	9	NA
	Areal S.	NA	0.84	R	60	12	6.5

- **Alternative 3:** Alternative #3 is similar to the Alternative #2. For this model, the Erikli Fault is discarded, however, the Pontic Escarpment Zone is considered as active. To account for the uncertainty in the model parameters, three sub-models listed in Table 5.2 are incorporated.

Table 5.2: Source Model Parameters for Alternative 3

R. Scenario	Source	Slip R.	b-value	Fault M.	Dip A.	Fault D.	Mmax
Alternative 3 (A)	Pontic Esc.	NA	0.69	R	60	15	6.5
	NAF	Partitioned	0.71	SS	90	16	NA
	Mer.-Esen.	6	0.71	SS	90	9	NA
	Areal S.	NA	0.84	R	60	12	6.5
Alternative 3 (B)	Pontic Esc.	NA	0.50	R	45	15	6.8
	NAF	Partitioned	0.71	SS	90	16	NA
	Mer.-Esen.	6	0.71	SS	90	9	NA
	Areal S.	NA	0.84	R	60	12	6.5
Alternative 3 (C)	Pontic Esc.	NA	1.00	N	60	15	6.5
	NAF	Partitioned	0.71	SS	90	16	NA
	Mer.-Esen.	6	0.71	SS	90	9	NA
	Areal S.	NA	0.84	R	60	12	6.5

- **Alternative 4:** In this model, both Erikli Fault and Pontic Escarpment Zone is considered as active structures together with the NAF main strand, Merzifon-Esençay Fault zone, and the Areal Source on the south. To account for the uncertainty in the fault mechanism, dip angle and fault width, three sub-models listed in Table 5.3 are incorporated.

Table 5.3: Source Model Parameters for Alternative 4

R. Scenario	Source	Slip R.	b-value	Fault M.	Dip A.	Fault D.	Mmax
Alternative 4 (A)	Pontic Esc.	NA	0.69	R	60	15	6.5
	Erikli F.	2.2	0.71	R	60	5	NA
	NAF	Partitioned	0.71	SS	90	16	NA
	Mer.-Esen.	6	0.71	SS	90	9	NA
	Areal S.	NA	0.84	R	60	12	6.5
Alternative 4 (B)	Pontic Esc.	NA	0.50	R	45	15	6.8
	Erikli F.	2.2	0.60	R	45	10	NA
	NAF	Partitioned	0.71	SS	90	16	NA
	Mer.-Esen.	6	0.71	SS	90	9	NA
	Areal S.	NA	0.84	R	60	12	6.5
Alternative 4 (C)	Pontic Esc.	NA	1.00	N	60	15	6.5
	Erikli F.	1.2	1.20	N	60	5	NA
	NAF	Partitioned	0.71	SS	90	16	NA
	Mer.-Esen.	6	0.71	SS	90	9	NA
	Areal S.	NA	0.84	R	60	12	6.5

- **Alternative 5:** In this alternative model, the Erikli and Balıfakı Faults are both considered as the active tectonic structures sharing the slip rate equally, in addition to the NAF main strand, Merzifon-Esençay Fault zone, and the Areal Source. The Balıfakı Fault is modeled in two segments: the 30 km long segment on the land and the 150 km off-shore segment. Variations in the source mechanism and the dip angle are considered as shown in Table 5.4.
- **Alternative 6:** This alternative considers all sources defined in Chapter 3 as active tectonic structures. The total slip rate is equally distributed in between Erikli and Balıfakı Faults. Since the Pontic Escarpment is taken as an active structure and the second segment of Balıfakı Fault which is extended offshore in the northwest direction coincides with Pontic Escarpment, the Balıfakı Fault is modeled as one segment (segment on the land).

Table 5.4: Source Model Parameters for Alternative 5

R. Scenario	Source	Slip R.	b-value	Fault M.	Dip A.	Fault D.	Mmax
Alternative 5 (A)	Balıfakı	1.1	0.71	R	60	5	NA
	Erikli F.	1.1	0.71	R	60	5	NA
	NAF	Partitioned	0.71	SS	90	16	NA
	Mer.-Esen.	6	0.71	SS	90	9	NA
	Areal S.	NA	0.84	R	60	12	6.5
Alternative 5 (B)	Balıfakı	1.1	0.60	R	45	10	NA
	Erikli F.	1.1	0.60	R	45	10	NA
	NAF	Partitioned	0.71	SS	90	16	NA
	Mer.-Esen.	6	0.71	SS	90	9	NA
	Areal S.	NA	0.84	R	60	12	6.5
Alternative 5 (C)	Balıfakı	1.1	0.71	N	60	5	NA
	Erikli F.	1.1	0.71	N	60	5	NA
	NAF	Partitioned	0.71	SS	90	16	NA
	Mer.-Esen.	6	0.71	SS	90	9	NA
	Areal S.	NA	0.84	R	60	12	6.5
Alternative 5 (D)	Balıfakı	0.6	1.20	N	60	5	NA
	Erikli F.	0.6	1.20	N	60	5	NA
	NAF	Partitioned	0.71	SS	90	16	NA
	Mer.-Esen.	6	0.71	SS	90	9	NA
	Areal S.	NA	0.84	R	60	12	6.5

Tables 5.1 to 5.5 show that seventeen alternative source characterization models are proposed to cover the uncertainties involved in the fault activity, fault geometry, style of faulting, dip angle and direction, maximum magnitude, b-value and slip rate. Hazard curves for each alternative are presented through Figures 5.1 to 5.7 for PGA and for average rock site conditions (V_{S30}= 760 m/s). Currently, the recent versions of TR-Adjusted NGA models are being implemented into HAZ43, however due to time limitations; the TR-Adjusted AS08 and TR-Adjusted CY08 models are excluded from the GMPE logic tree for this study. Remaining 4 NGA models (AS08, BA08, CB08, and CY08) and 2 TR-adjusted NGA models (TR-Adjusted BA08 and TR-Adjusted CB08) were used for the ground motion characterization of the Sinop NPP site. Equal weights are assigned to the global models for the first 50 % (12.5%

for each model) and regionalized NGA models shared the remaining 50% equally (25% for each model).

Table 5.5: Source Model Parameters for Alternative 6

R. Scenario	Source	Slip R.	b-value	Fault M.	Dip A.	Fault D.	Mmax
Alternative 6 (A)	Balıfakı	1.1	0.71	R	60	5	NA
	Erikli F.	1.1	0.71	R	60	5	NA
	Pontic Esc.	NA	0.69	R	60	15	6.5
	NAF	Partitioned	0.71	SS	90	16	NA
	Mer.-Esen.	6	0.71	SS	90	9	NA
	Areal S.	NA	0.84	R	60	12	6.5
Alternative 6 (B)	Balıfakı	1.1	0.60	R	45	10	NA
	Erikli F.	1.1	0.60	R	45	10	NA
	Pontic Esc.	NA	0.50	R	45	15	6.8
	NAF	Partitioned	0.71	SS	90	16	NA
	Mer.-Esen.	6	0.71	SS	90	9	NA
	Areal S.	NA	0.84	R	60	12	6.5
Alternative 6 (C)	Balıfakı	1.1	0.71	N	60	5	NA
	Erikli F.	1.1	0.71	N	60	5	NA
	Pontic Esc.	NA	0.69	N	60	15	6.5
	NAF	Partitioned	0.71	SS	90	16	NA
	Mer.-Esen.	6	0.71	SS	90	9	NA
	Areal S.	NA	0.84	R	60	12	6.5
Alternative 6 (D)	Balıfakı	0.6	1.20	N	60	5	NA
	Erikli F.	0.6	1.20	N	60	5	NA
	Pontic Esc.	NA	1.00	N	60	15	6.5
	NAF	Partitioned	0.71	SS	90	16	NA
	Mer.-Esen.	6	0.71	SS	90	9	NA
	Areal S.	NA	0.84	R	60	12	6.5

The analysis is performed only for the candidate Sinop NPP site located at 42.096 N and 34.965 E. The exact location of the site may be changed however the effect of this change would be negligible since almost all the seismic sources lie parallel all the way through the south coast of Black Sea. Based on the hazard results, following interpretations can be made:

- Alternative 1 results in the lowest PGA values as expected. In this alternative source model, the faults in the north of NAF zone are considered as inactive

structures. Since the NAF Zone and the sources lying on the south of it are quite far from the Sinop NPP site, their effect on the design ground motion levels are limited. NAF Zone is almost the only contributor to the hazard.

- Activity of the Erikli Fault is one of the most controversial issues on the site license investigations for this structure and Alternative 2 points out the possible effect of Erikli Fault on the design ground motions. When the hazard curves in Figure 5.1 and Figure 5.2 are compared, the PGA for 10.000 year of return period is almost doubled with the inclusion of Erikli Fault to the PSHA.
- Figure 5.2 indicates that the properties of Erikli Fault may have a significant effect on the design ground motion levels. The effect of source parameters on the PGA for the same return period is around 60%, therefore site surveys should be continued to be able to evaluate the mechanism of the fault, the dip angle and direction accurately to decrease the uncertainty in the future.
- Pontic Escarpment is the other seismic source that experts are not yet agreed on, different opinions by Emre et al. (2008), Güney (2008) and Kaymakçı (2009) were summarized in Chapter 3. Figure 5.3 shows that inclusion of the Pontic Escarpment Zone into the PSHA results in quite similar design ground motion levels with the second alternative presented in Figure 5.2 that includes the Erikli Fault. The effect of selection of source parameters is prominent when maximum and minimum cases in Figure 5.3 are considered; the difference in the hazard curves for Alternative 3(b) and Alternative 3(c) is 0.16 g for 10.000 years return period.
- Alternative models that incorporate the Pontic Escarpment Zone (Alternatives 3, 4 and 6) converge to the same hazard levels for very low probability of exceedance ($>10^5$ years). One possible explanation for this observation is the selected magnitude recurrence model for the Pontic Escarpment Zone; the large magnitude tail of truncated exponential distribution governs the seismic hazard estimates for long return periods.
- Figure 5.5 shows the effect of another controversial issue; the off-shore extension of Balıfakı Fault proposed. Ergin et al. (2008) discussed that the single and combined fault plane solutions of earthquakes that occur in the North of Abana Station shows normal or strike-slip/normal (oblique)

deformations. On the other hand, if the segment of Balıfakı Fault on the land shows "reverse" sense of slip, the off-shore section should also be considered as a fault with reverse mechanism. Both combinations are considered in Alternative 5(a) and 5(d). Figure 5.5 indicated that the mechanism of this source has a significant effect on the design ground motion levels.

- Alternative 6 results in the highest PGA values for all return period as expected. The design PGA level of Alternative 6(a) is almost three times higher than that of Alternative 1(a) for 10000 years return period.
- Figures 5.1 to 5.6 indicate that the selection of source parameters affects the corresponding PGA level for 50 to 80% for 10.000 years return period. Therefore, proper determinations of source parameters are very crucial in the accurate assessment of design ground motions.
- Figure 5.7 compares the hazard curves for each alternative. The most significant observation from this comparison is the significant contribution of the seismic sources on the north of NAF Zone to the design ground motion level. Off-shore extension of Balıfakı Fault does not result in the maximum PGA values, inclusion of this segment increases the PGA level but the value is still smaller that the PGA values from Alternatives 4 and 6. This result can be explained by the low slip rate assigned to Balıfakı Fault and indicated that the assigned slip rate is as important as the geometric properties of the fault.
- The highest PGA values are obtained from the Alternative 6(b). For 10.000 years return period the design PGA is found to be 0.42 g (Figure 5.7). This value is comparable with the previous seismic hazards studies, Erdik et al., (1990) and Kalkan and Gülkan (2010) proposed 0.35 g and 0.41 g for the same return period.

5.3 Effect of V_{S30} of the Site on the Hazard Outcome

For the analysis presented in Figures 5.1 to 5.7, the V_{S30} value of the site is assumed to be 760 m/s (NEHRP B/C boundary). For an arbitrarily chosen source model (Alternative 6(a)), 3 more analysis are conducted with V_{S30}= 900 m/s, V_{S30}= 1100 m/s and V_{S30}= 1500 m/s to evaluate the effect of this assumption. Hazard curves of these analyses are presented in Figure 5.8. According to this figure, the analysis results are sensitive to the V_{S30}; change in this parameter results in 17% change in the

PGA for 10000 years return period. It is notable that taking V_{S30}= 760 m/s results in larger ground motion levels.

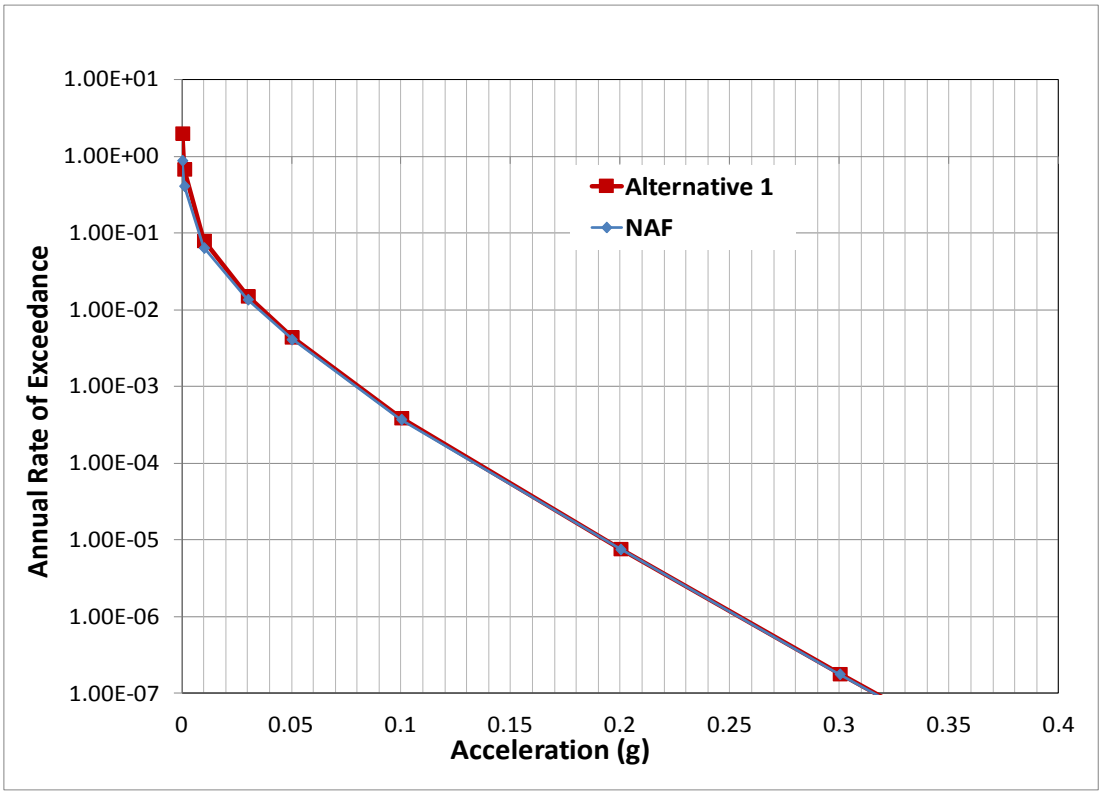

Figure 5.1: Hazard Curves for Alternative 1

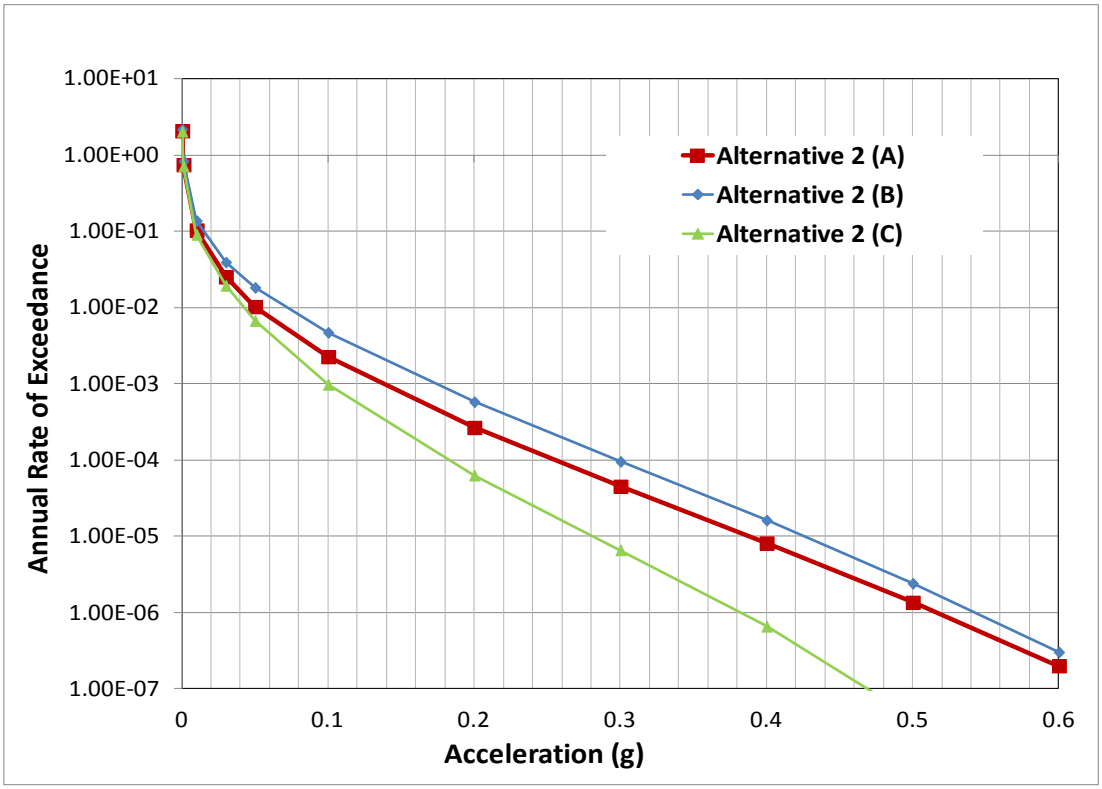

Figure 5.2: Hazard Curves for Alternative 2

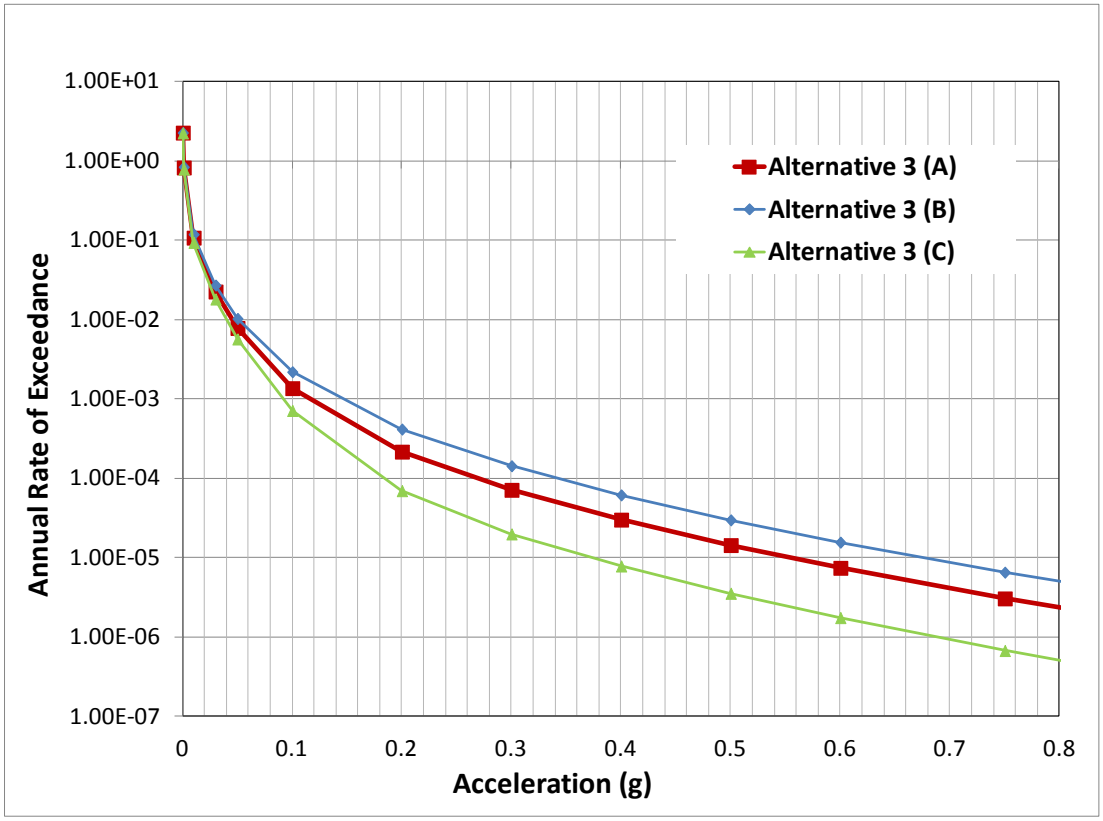

Figure 5.3: Hazard Curves for Alternative 3

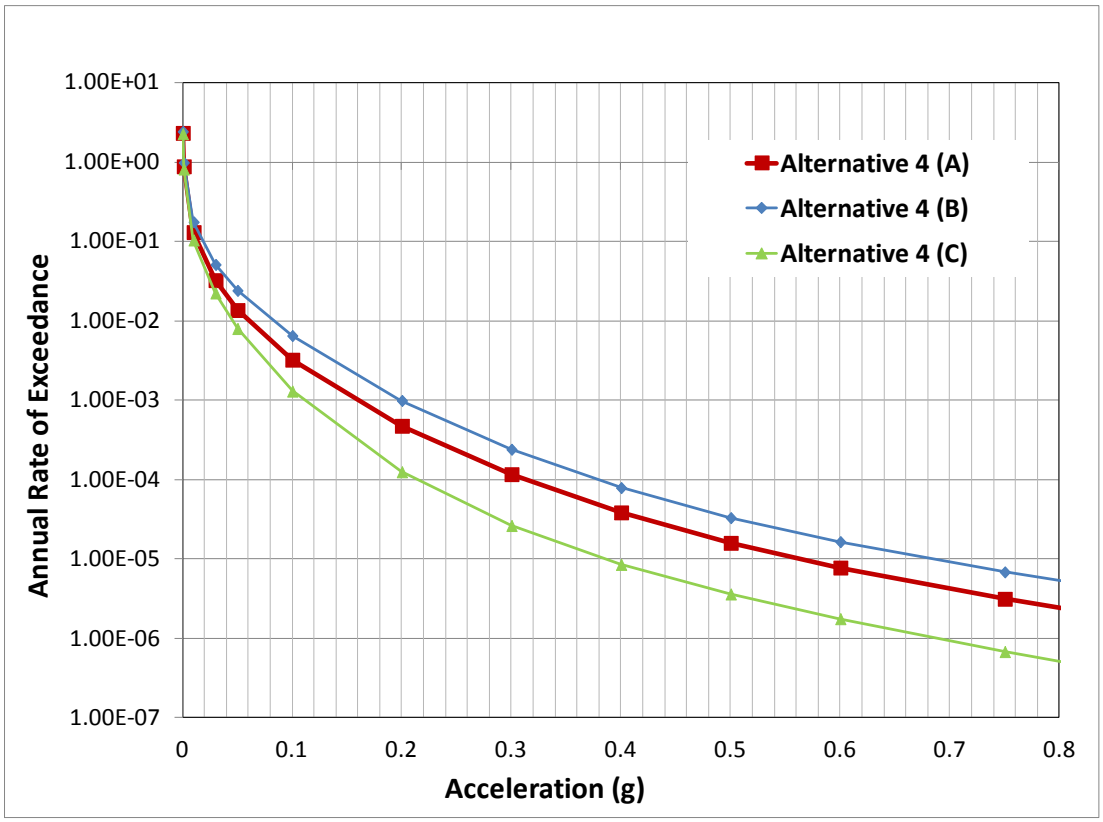

Figure 5.4: Hazard Curves for Alternative 4

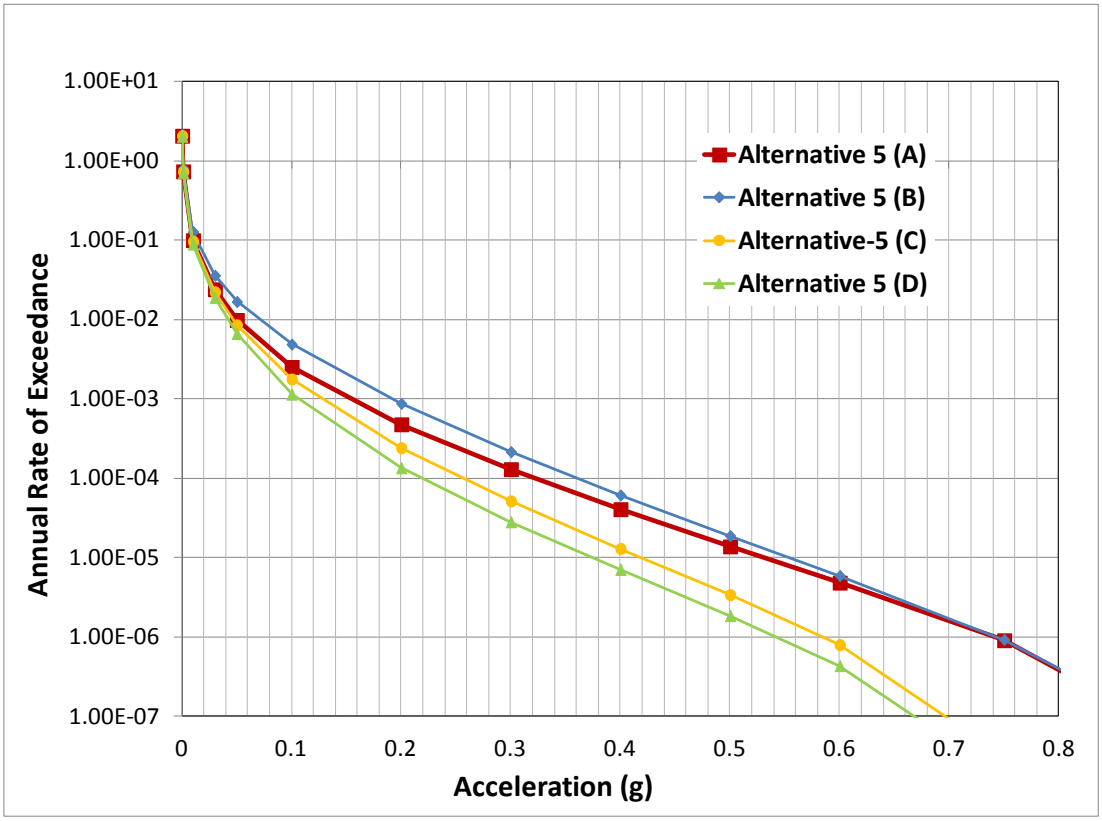

Figure 5.5: Hazard Curves for Alternative 5

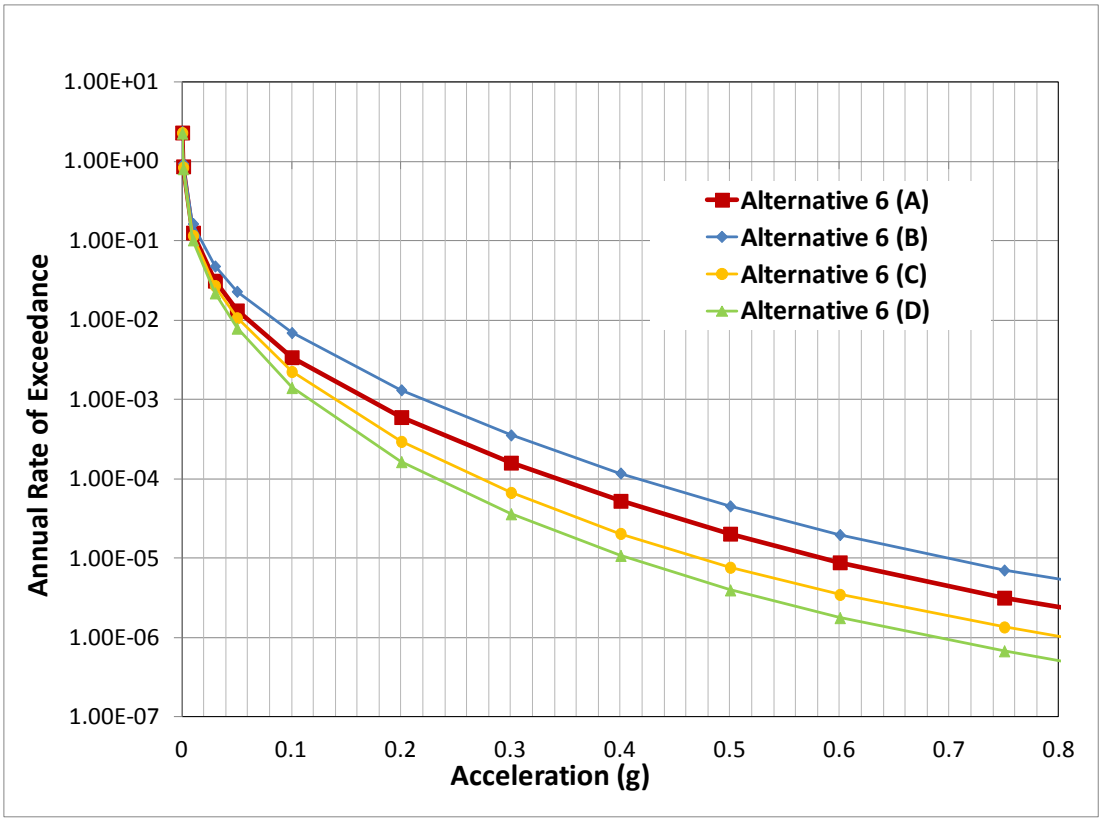

Figure 5.6: Hazard Curves for Alternative 6

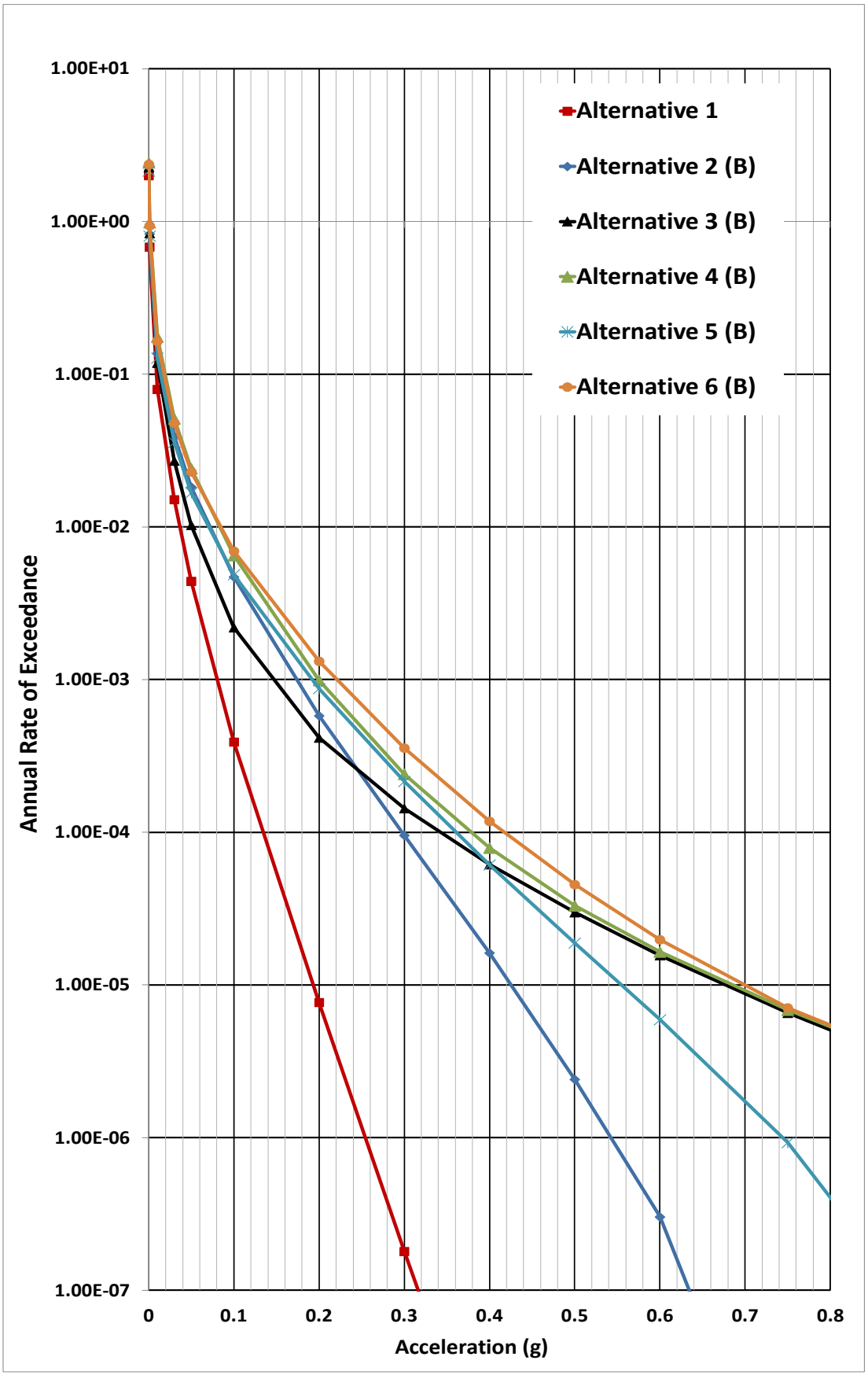

Figure 5.7: Hazard Curves from Each Alternative Model with the Maximum Design Ground Motions

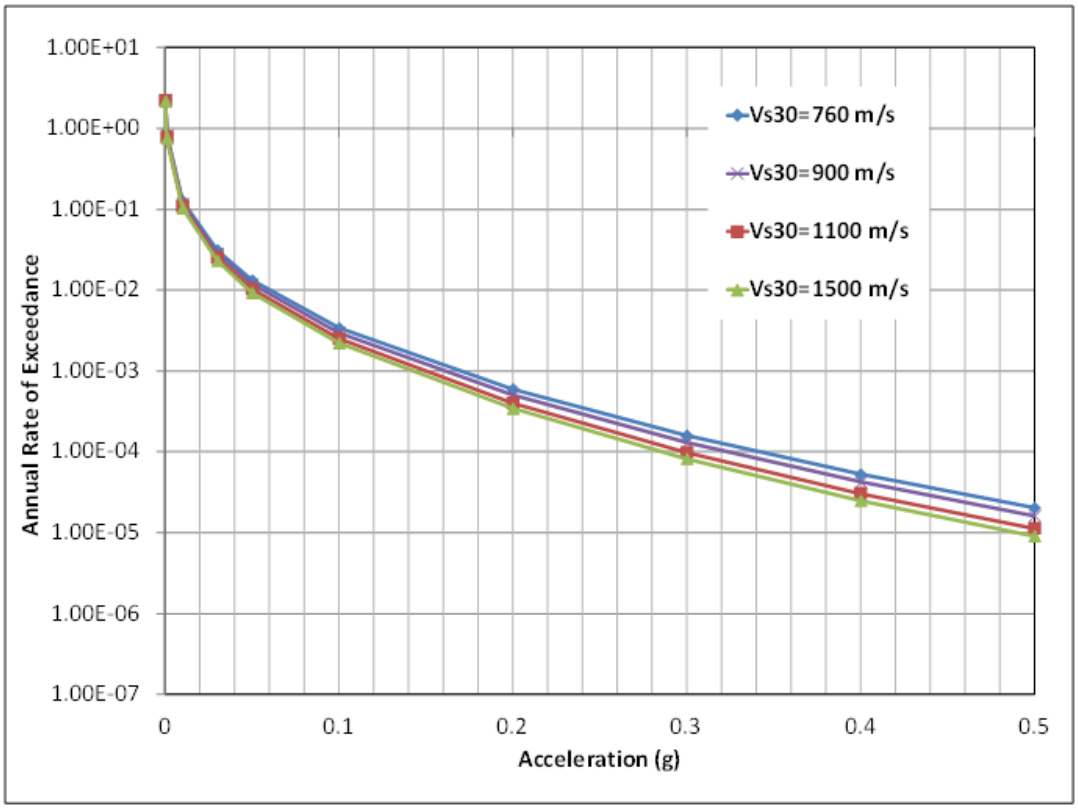

Figure 5.8: Sensitivity Analysis for Different Rock Site Conditions Based on V_{S30} (Alternative 6a)

5.4 Conclusions and Recommendations

Based on the studies conducted for more than 40 years, Sinop is chosen as one of the three most convenient places in Turkey to construct a Nuclear Power Plant (NPP). In this study the preliminary probabilistic seismic hazard assessment of Sinop Nuclear Power Plant site was performed with the application of improved seismic source models and updated ground motion models.

This study introduces significant improvements over the previous seismic hazard studies conducted for the Sinop NPP in terms of seismic source characterization models. Based on the regulations of Turkey, United States and International Atomic Authority, the seismic sources located within the 320 km radius around the Sinop NPP site were investigated. To develop the planar source characterization models, geometries of the fault segments were determined with the help of previously conducted site studies, new fault maps and previous studies in the literature. Fault segments, rupture sources, rupture scenarios and fault rupture models were determined using the USGS Working Group (2003) terminology. To properly

represent the characteristic behavior, planar fault segments were defined with composite magnitude distribution model and multi-segment ruptures were considered. The Pontic Escarpment Zone and Sungurlu Fault were modeled as areal sources using truncated exponential magnitude distribution model. The sensitivity of the hazard results to the parameters of seismic source models was analyzed for each source to illustrate the needs for further site studies for Sinop NPP.

This study makes the first attempt to characterize the ground motions and its variability for Sinop NPP site. Several local, global and regionalized candidate ground motion prediction models (GMPEs) were proposed and evaluated. After a detailed evaluation of median predictions and resulting hazard curves, four NGA models and two TR-adjusted NGA models were used for the ground motion characterization of the Sinop NPP site. Equal weights are assigned to the global and regionalized NGA models. Results of the study are presented in terms of a range of hazard curves for the peak ground acceleration since the site surveys and ground motion characterization efforts are not yet finalized. Following issues have to be revisited in future before the final PSHA analysis is completed:

- Due to the proximity of the sources in the north of NAF to the site, activities of these sources are the governing parameters in the determination of hazard level. Future site studies concentrating on the determination of the activity of these sources is necessary for the reduction of uncertainty. Association of Pontic Escarpment with 1968 Bartın Earthquake and constructing the logic tree for the maximum magnitude parameter for this source are one of the important tasks to be completed. Also segmentation and fault geometries for the Erikli and Balıfakı Faults, their association with each other and extension of Balıfakı Fault in Black Sea are the other issues to be investigated in the new site studies.
- The results of the sensitivity analysis showed that determined peak ground acceleration levels for the same return period are both dependent on the activity or inactivity of the sources and selection of source parameters. However, it is not possible to have a perfect agreement of experts on the source parameters and geometric properties of sources. For these cases, application of logic trees to represent the all accountable proposals by assigning weights should be used as a solution. Several alternative source models are proposed in this study, however, weights for these alternatives to use in logic tree has not been offered.

- The lower and upper bound slip rates based on the GPS velocities are used to model the activity of Erikli and Balıfakı Faults. Proper evaluation of associated slip rates on these faults by state of the art GPS measurements will reduce the uncertainty in these parameters and will lead to more accurate estimation of design ground motion levels.
- The catalogue completeness and recurrence parameters (b and a value) are found by the help of earthquake database of KOERI. Sensitivity analysis results showed that the effect of these parameters for fault sources are negligible, however, for areal sources their effects are significant. Therefore, inclusion of the new micro seismicity database by TUBİTAK MAM and compilation of available international catalogues will improve the estimates for these parameters.
- The recurrence interval for the characteristic event for NAF zone is not yet properly estimated, therefore, time dependent hazard methodologies are not employed in this study. Determination of penultimate event and recurrence period will help the hazard analyst to utilize the time dependent methods and eventually will lead to a decrease in the hazard estimates.
- In probabilistic seismic hazard analysis ground motion prediction models introduce the biggest uncertainty in the hazard calculations. Hence, unbiased selections of ground motion models are necessary. In this study AS08, CY08, AB08, CB08 NGA models are used together with Turkey Adjusted BA08, CB08 models in the light of the sensitivity analysis results of Chapter 4. In terms ground motion characterization the results of this study can be improved by the help of newly implemented ground motion prediction motions with the increased number ground motion recordings, such as; NGA_W2 models.
- Deaggregation of seismic hazard will give a chance for the future site studies to concentrate on the specific seismic sources, selection of dominating earthquake scenarios and time series for site response analysis.
- For Nuclear Power Plants vertical design ground motions are also necessary. Therefore, design ground motions for the vertical component should be estimated using the horizontal uniform hazard spectrum and V/H prediction models.
- Establishment of new regulations and amendment of old guides with current state of the art by TAEK will determine the frame of the site studies. Proper definition of extent of site studies will decrease the uncertainty in hazard assessment studies.

REFERENCES

A Performance-Based Approach to Define the Site-Specific Earthquake Ground Motion, 2007. (USNRC Regulatory Guide RG 1.208)

Abrahamson, N.A. and J.J. Litehiser., 1989. Attenuation of Vertical Peak Acceleration, Bull. Seism. Soc. Am., v.79-3, pp 549-580.

Abrahamson, N. A., and W. J. Silva., 1997. Empirical response spectral attenuation relations for shallow crustal earthquakes, Seismol. Res. Lett. 68, 94–127.

Abrahamson, N. A. and Silva, W., 2008. Summary of the Abrahamson & Silva NGA Ground-Motion Relations, Earthquake Spectra, Volume 24, No. 1, 67 – 97.

Abrahamson, N. A., Atkinson, G. M., Boore, D. M., Bozorgnia, Y., Campbell, K. W., Chiou, B., Idriss, I. M., Silva, W., and Youngs, R., 2008. Comparisons of the NGA ground-motion relations, Earthquake Spectra, 24:45–66.

Akkar, S. and Cagnan,Z., 2010. A local ground-motion predictive model for Turkey and its comparison with other regional and global ground-motion Models. Bulletin of the Seismological Society of America 100, 2978-2995.

Akkar, S., Cagnan, Z., Yenier, E., Erdogan, E., Sandikkaya, M.A., Gulkan, P., 2010. The recently compiled Turkish strong-motion database: preliminary investigation for seismological parameters, *Journal of Seismology*, 14, 457-479.

Akyüz, H. S., Hartleb, R., Barka, A.A., Altunel, E. & Sunal, G., 2002. Surface Rupture and slip Distribution of the 12 November 1999 Düzce Earthquake (M 7.1), North Anatolian Fault, Bolu, Turkey. Bulletin of Seismological Society of America 92, 61-66.

Alptekin, Ö., J. L. Nabelek and M. N. Toksöz., 1986. Source Mechanism of the Bartın Earthquake of September 3, 1968 in Northwestern Turkey: Evidence for Active Thrust Faulting at the Southern Black Sea Margin. Tectonophysics, 122, 73-88.

Barani S., Spallarossa D., Bazzurro P., Eva C. (2007). Sensitivity Analysis of Seismic Hazard for Western Liguria (North Western Italy): A First Attempt towards the Understanding and Quantification of Hazard Uncertainty, Tectonophysics, Vol. 435, pp. 13-35.

Barka, A., Sütçü, Y.F., Gedik, A., Tekin, T.F., Arel, E., Özdemir, M., and Erkal, T., 1985, Final Report Of The Geological Investigation Of The Sinop Nuclear Power Plant, General Directorate of Mineral Research and Exploration (MTA) Report No: 7963, Ankara.

Barka, A. A., 1992. The North Anatolian fault, *Anneles Tectonicae* VI, 164-195.

Barka, A.A., 1996. Slip distribution along the North Anatolian Fault associated with the large earthquakes of the period 1939–1967. Bulletin of Seismic Society of America 86, 1238–1254.

Barka, A.A., Akyüz, H.S., Altunel, E., Sunal, G. & Çakır, Z., 2002. The Surface Rupture and Slip Distribution of the 17 August 1999 İzmit Earthquake (M 7.4), North Anatolian Fault. Bulletin of Seismological Society of America 92, 43–60.

Bradley, B. A., 2013. A New Zealand-Specific pseudospectral acceleration ground-motion prediction equation for active shallow crustal earthquakes based on foreign models, Bull. Seismol. Soc. Am. 103, 1801–1822.

Bommer, J. J., Stafford P., and Akkar S., 2010. Current empirical ground motion prediction equations for Europe and their application to Eurocode 8, Bull. Earthq. Eng. 8, 5–26.

Bommer, J.J., J. Douglas, F. Scherbaum, F. Cotton, H. Bungum & D. Fäh., 2010. On the selection of ground-motion prediction equations for seismic hazard analysis. Seismological Research Letters, 81(5), 794-801.

Boore, D. M., Atkinson, G. M., 2008. Ground-Motion Prediction Equations for the Average Horizontal Component of PGA, PGV, and 5%-Damped PSA at Spectral Periods between 0.01 s and 10.0 s, Earthquake Spectra, Volume 24, No. 1, 99 – 138.

Campbell, K.W., 1981. Near-source Attenuation of the Peak Horizontal Acceleration, Bull. Seism. Soc. Am., 68, 828-843.

Campbell, K. W. and Bozorgnia, Y., 2008. NGA Ground Motion Model for the Geometric Mean Horizontal Component of PGA, PGV, PGD and 5% Damped Linear Elastic Response Spectra for Periods Ranging from 0.01 to 10 s, Earthquake Spectra, Volume 24, No. 1, 139 – 171.

Chiou, B. S. J. and Youngs, R. R., 2008. An NGA Model for the Average Horizontal Component of Peak Ground Motion and Response Spectra, Earthquake Spectra, Volume 24, No. 1, 173 – 215.

Doyuran, V. and M. Erdik., 1983. Geotectonics and Seismicity of the Black Sea: Site Selection Investigations for the second NPP. Middle-East Technical University, Earthquake Engineering Research Center, Ankara.

Emre, Ö., 2008. Geological investigations for the Sinop NuclearTechnology Center. MTA Report No: 11044.

Erdik, M., Üçer, B. and Barka, A., 1990. Sinop Nuclear Power Plant Design Basis Ground Motion. Dep. of Earthquake Eng., Kandilli Observatory and Earthquake Res. Ins., Boğaziçi Univ.

Ergin, M., 2008. Microseismic ctivity of Sinop Nuclear Technology Center TUBITAK MAM Report No. 5057106.

Erturaç, M.K., Tüysüz, O., 2010. Kinematics and basin formation along the Ezinepazar - Sungurlu Fault Zone, NE Anatolia, Turkey. Turkish Journal of Earth Sciences.

Fukushima, Y., T. Tanaka, and S. Kataoka., 1988. A New Attenuation Relationship for Peak Ground Acceleration Derived from Strong Motion Accelerograms., Proc. of the 9th World Conf. On Earthquake Engineering, Tokyo, Japan.

Gardner, J. K., and L. Knopoff (1974), Is the Sequence of Earthquakes in Southern California, with Aftershocks Removed, Poissonian?, Bull. Seis. Soc. Am., 64(5), 1363–1367.

Gülerce, Z., Kargıoğlu, B., Abrahamson, N., 2014. Turkey Adjusted NGA W-1 Horizontal Ground Motion Prediction Models. Earthquake Spectra (under review).

Gülerce, Z., Ocak S., 2013. Probabilistic seismic hazard assessment of Eastern Marmara Region. Bulletin of Earthquake Engineering, doi: 10.1007/s10518-013-9443-6.

Gülkan, P., Kalkan, E., 2010. An Assessment of Seismic Hazard For the Sinop Nuclear Technology Center. Middle East Technical University Earthquake Engineering Research Center.

Güney, H., 2008. Tectonic activity in offshore central Black Sea area evaluation report. Unpublished TPAO Report.

Hanks, T. and Kanamori, H., 1979. A moment magnitude scale, Journal of Geophysical Research, 84, No. B5, 2348-2350.

Hubert-Ferrari, A., Armijo, R., King, G., Meyer, B., Barka, A.A., 2002. Morphology, displacement, and slip rates along the North Anatolian Fault, Turkey. Journal of Geophysical Research 107 (B10), 9/1–9/33.

Jackson J. and McKenzie D., 1984, Active tectonics of the Alpine-Himalayan Belt between Western Turkey and Pakistan, Geophy. J. Royal Astr. Soc. 7, 185-264.

Joyner, W.B., and Boore D.M.,1981. Peak Horizontal Acceleration and Velocity from strong-Motion Records Including Records from the 1979 Imperial Valley, California, Earthquake, Bull. Seism. SOC. Am., 73, 1479-1480.

Kalkan, E. and Gülkan, P., 2004. Site-Dependent Spectra Derived from Ground Motion Records in Turkey, Earthquake Spectra, Volume 20, No. 4, 1111 – 1138.

Kargıoğlu, B. 2012. Turkey-Adjuested Next Generation Attenuation Models. MS Thesis Dissertation, Middle East Technical University.

Kawashima K., K.Aizawa and K.Takahashi. 1984. Attenuation of Peak Ground Motion and Absolute acceleration Response Spectra, Proc. 8th WCEE, v.2, pp.257-264, San Francisco, California, USA.

Kaymakçı, N., 2009. "Tectonic Framework And Seismic Potential of Sinop Peninsula in Relation to Sinop Nuclear Research Center (SNTC)," Department of Geological Engineering, Middle East Technical University, December.

Ketin, İ., 1948. Ober Die Tektonisch-Mechanischen Folgerungen Aus Den Grossen Anatolischen Erdbeben Des Letzten Dezenniums, *Geol. Rudsch.* 36, 77-83.

Kozacı, O., Dolan, J.F., Finkel, R., Hartleb, R., 2007. Late Holocene slip rate for the North Anatolian Fault, Turkey, from cosmogenic 36Cl geochronology: Implications for the constancy of fault loading and strain release rates. Geology 35, 867– 870.

Kozacı, O., Dolan, J. F., Finkel R. C., 2009. A late Holocene slip rate for the central North Anatolian fault, at Tahtaköprü, Turkey, from Cosmogenic 10Be

Geochronology: Implications for Fault Loading and Strain Release Rates. 114, B01405, doi:10.1029/2008JB005760.

Kudo, K., 1983, Seismic source characteristics of recent major earthquakes in Turkey, In: A comprehensive study on earthquake disaster in Turkey in view of seismic risk reduction. Hokkaido Univeristy, Sapporo.

McClusky, S. et al., 2000. Global Positioning System constraints on plate kinematics and dynamics in the eastern Mediterranean and Caucasus. Journal of Geophysical Research, 105(B3): 5695-5719.

Nükleer Tesislere Yer Lisansi Ve Sinirli Çalisma izninin Verilmesinde Aranacak Depremle Ilgili Konular Hakkinda Klavuz (Turkish Atomic Authority Regulatory Guide) (1989).

M. Peyret, F. Masson, H. Yavasoglu, S. Ergintav and R. Reilinger (2012) Present-day strain distribution across a segment of the central bend of the North Anatolian Fault Zone from a Persistent-Scatterers InSAR analysis of the ERS and Envisat archives. Geophysical Journal International. 192, 929-945.

Pacific Gas & Electric Company (2010) Verification of PSHA code Haz39. GEO.DCPP.10.03 Rev 0.

Reilinger, R., McClusky, S., Vernant, P., Lawrence, S., Ergintav, S., Cakmak, R., Ozener, H., Kadirov, F., Guliev, I., Stepanyan, R., Nadariya, M., Hahubia, G., Mahmoud, S., Sakr, K., ArRajehi, A., Paradissis, D., Al-Aydrus, A., Prilepin, M., Guseva, T., Evren, E., Dmitrotsa, A., Filikov, S.V., Gomez, F., Al-Ghazzi, R., Karam, G., 2006. GPS constraints on continental deformation in the Africa–Arabia, Eurasia continental collision zone and implications for the dynamics of plate interactions. Journal of Geophysical Research—Solid Earth 111, B05411.

Rojay, B., Koçyiğit, A., 2011. An Active Composite Pull-apart Basin Within the Central Part of the North Anatolian Fault System the Merzifon-Suluova Basin, Turkey. Turkish Journal of Earth Sciences. 21, 473-496.

Scasserra, G., Stewart, J. P., Bazzurro, P. Lanzo, G. and Mollaioli, F., 2009. A comparison of NGA ground-motion prediction equations to Italian data, Bull. of the Seis. Soc. of Am. 99, 2961-2978.

Schwartz, D. P. and Coppersmith, K. J., 1984. Fault behavior and characteristic earthquakes: examples from the Wasatch and San Andreas faults, J. Geophys. Res. 89, 5681-5698.

Seismic Hazards in Site Evaluation for Nuclear Installations (IAEA Regulatory Guide SSG-9).

Shoja–Taheri, J., Naserieh, S., and Hadi, G., 2010. A test of the applicability of NGA models to the strong ground-motion data in the Iranian plateau, J. Earthquake. Engineering 14, 278–292.

Stafford, P. J., F. O. Strasser, and Bommer J. J., 2008. An evaluation of the applicability of the NGA models to ground motion prediction in the Euro-Mediterranean region, Bull. Earthq. Eng. 6, 149–177.

Şengör, A. M. C., & Yılmaz, Y. (1981). Tethyan evolution of Turkey: A plate tectonic approach. Tectonophysics, 75, 181–241.

Şengör, A.M.C, Gorur, N. & Şaroğlu, F., 1985. Strike slip faulting and related basin formation in zones of tectonic escape: Turkey as a case study. *In*: Christie-Blick, N. & Biddle, K. (eds), *Strike-slip Deformation, Basin Formation, and Sedimentation*. Society of Economic Paleontologists and Mineralogists, Special Publications 37, 227–64.

Şengör, A.M.C., Tüysüz, O., İmren, C., Sakınc, M., Eyidoğan, H., Görür, N., Le Pichon X. & Rangin, C., 2005. The North Anatolian Fault: a new look. Annual Review Earth Planetary Sciences 33, 1–75.

Tarı, E., Sahin, M., Barka, A., Reilinger, R., King, R.W., McClusky, S. and Prilepin, M., 2000, Active tectonics of the Black Sea with GPS, Earth Planets Space, 52, 747–751.

Vakilinezhad, M., Levendoğlu, M., Gülerce, Z. and Şaroğlu F., 2013, Effect of Fault Characteristics on the Probabilistic Seismic Hazard Assessment Results, Proceedings of International Conference on Earthquake Engineering, 29-31 May 2013, Skopje.

Vakilinezhad, M. 2014, Influence of Seismic Source Parameters on the Probabilistic Seismic Hazard Assessment Results, MS Thesis Dissertation, Middle East Technical University (expected to be completed in 2014).

Weichert, D. H. (1980), Estimation Of The Earthquake Recurrence Parameters For Unequal Observation Periods For Different Magnitudes, Bull. Seismol. Soc. Am. 70, no. 4, 1337–1346.

Wells, D. L., and Coppersmith K. J., 1994. New empirical relationships among magnitude, rupture length, rupture width, rupture area, and surface displacement, Bull. Seismol. Soc. Am. 84, no. 4, 974–1002.

Working Group for Earthquake Probabilities (USGS Working Group) (2003). Earthquake Probabilities in the San Francisco Bay Region: 2002–2031, U.S. Geological Society Open File Report 03-214.

Yavaşoğlu, H., Tarı, E., Tüysüz, O., Çakır, Z., Ergintav, S., 2011. Determining And Modeling Tectonic Movements Along the Central Part of the North Anatolian Fault (Turkey) Using Geodetic Measurements. Journal of Geodynamics 51, 339–343.

Yılmaz, N., 2008. Probabilistic Seismic Hazard Analysis: A Sensitivity Study With Respect To Different Models. Phd. Thesis Dissertation, Middle East Technical University.

Youngs, R. R., and Coppersmith K. J., 1985. Implications of fault slip rates and earthquake recurrence models to probabilistic seismic hazard estimates, Bull. Seismol. Soc. Am. 75, no. 4, 939–964.